# Molecular Insight into the Regulation of Cell Differentiation by A Master Regulator Spo0A in Starving *Bacillus subtilis* Cells

By

**Anuradha Marathe**

A Dissertation submitted to the Department of Biology and Biochemistry,

College of Natural Science and Mathematics

In Partial Fulfillment of the Requirements for the Degree of

Doctor of Philosophy

In Biochemistry

Chair of Committee: Masaya Fujita

Committee Member: William Widger

Committee Member: Debora Rodrigues

Committee Member: Hye-Jeong Yeo

University of Houston

August 2020

## ACKNOWLEDGEMENTS

This academic journey towards obtaining a doctoral degree has been incredibly rewarding, and I would like to thank so many wonderful people, for supporting me throughout the years. With their help and encouragement, I complete my graduate program as the world faces a global crisis triggered by the Covid-19 pandemic.

First and foremost, I would like to express my deepest gratitude towards my advisor, Dr. Masaya Fujita, for his thorough guidance and support. His passion for research and dedication towards his lab and his students make him an excellent mentor. I am grateful for the intensive training he provided me under his supervision. This dissertation work would not have been possible without his consistent encouragement.

I wish to express my sincere thanks to my dissertation committee members, Dr. William Widger, Dr. Hye-Jeong Yeo, and Dr. Debora Rodrigues for their expert advice and valuable inputs. I am immensely thankful to have all of them on my dissertation committee and support me besides monitoring my progress.

My sincere thanks to my former advisors Dr. Toivo Kallas (University of Wisconsin, Oshkosh), Dr. Colleen McDermott (University of Wisconsin, Oshkosh) and my professors of my bachelor's and master's education at University of Mumbai, Maharashtra, India. I would like to thank Dr. George Fox for giving me a chance to do a lab rotation in his lab and work with RNA biology. Thanks to Madhan, for his helpful guidance and cheerful conversations in the hallway.

I would like to express my deep appreciation to all the past Fujita lab members- Drs. Brittany, Lindsey, Archna, and Priyanka for sharing their skills and knowledge

and collaborating on different projects. Thanks to Dr. Prahathees, for providing the opportunity to present my work online during the pandemic. Special thanks to Priyanka for being an elder sister to me and guiding me from my first day in the lab. I would like to thank Brenda for her help in the ongoing projects and wish her good luck for all her future endeavors.

Thanks to Nilu, Berra, Abi, Shreesti, and Dimple for being great friends. My best wishes for all your future endeavors. Thanks to Sujina for being an awesome roommate. Thanks to Oshin, Burak, and other friends who made living in Houston a memorable and fun experience. I will miss you all and I hope we'll stay in touch.

I would like to thank my wonderful family, without whom this journey would not have been possible. I am grateful to my parents, Meenakshi and Anant, for their unconditional love, thorough motivation, and absolute support. My heartfelt thanks to my brother, Hrishikesh, father in law, Arun, mother in law, Chhaya and, sister in law, Dr. Deepika for their strong support, care, and affection. Thanks to Malu aunty, Surendra uncle, and Kedar for sweet memories and good times in Houston.

Above all, I am eternally thankful and indebted to my dear husband, Tejas, for his unwavering support, unconditional love, and complete faith in me. I am truly so blessed to have you by my side as my best friend, a strong supporter, and a caring life partner. Your patience, kindness, and appreciation of my efforts warm my heart and soul.

## ABSTRACT

Gram-positive soil bacterium *Bacillus subtilis* can activate cellular differentiation pathways such as biofilm formation and sporulation, in response to starvation. Spo0A, the master regulator of these cellular differentiation processes is activated (phosphorylated) via a multi-component phosphorelay signaling cascade comprising of histidine kinases (KinA, KinB, KinC) and phosphotransferases (Spo0F and Spo0B). A gradual increase in the Spo0A~P levels is crucial for proper initiation of these cellular differentiation processes and cell survival under starvation conditions. Despite decades of intensive research on these cellular processes, certain questions, such as how the cell fate decisions to sporulate or form biofilms are made, remain unanswered. However, when the cell decides to undergo the energy-consuming sporulation process, it forms a septum near one of the poles, resulting in two unequal compartments, larger mother cell, and a smaller forespore. After this asymmetric septation, Spo0A activity is found in the larger mother cell compartment, but its function and importance in sporulation remain unknown.

Through this dissertation, I attempted to answer some of these fundamental questions connected to the master regulator Spo0A, such as the transcriptional control of *spo0A* and the mother cell-specific activity of Spo0A. Using EMSA, I provided the first of its kind direct evidence of Spo0A~P binding to three regulatory 0A boxes in the *spo0A* promoter region. Through transcriptional studies, I presented a revised model involving the role of 0A boxes in the *spo0A* transcription. I further found two previously undiscovered 0A boxes in the promoter

region of *spoIID*, a mother cell-specific 0A-controlled gene. Transcriptional studies showed that *spoIID* expression is positively regulated by Spo0A~P binding to 0A1 and 0A2 boxes and repressed by Spo0A~P binding to 0A3 box. Through microscopy and immunoblot studies, I provided evidence that Spo0A~P regulation of *spoIID* expression is important for the completion of the engulfment process and SpoIID levels maintained by Spo0A~P regulation are crucial for proper sporulation. Based on these results, I propose a new model for *spoIID* expression governed by a triple-input AND gate consisting of $\sigma^E$-RNAP, SpoIIID, and Spo0A~P.

# TABLE OF CONTENTS

# List of Tables

# List of Figures

# Chapter I: Introduction, *Bacillus subtilis* sporulation as a model for differentiation

*"By decomposition of the Bacillus filaments, single members become isolated which contain only single spores. When these have completely separated from their mother cell, they show a delicate, jelly-like enclosure (spore membrane) and a strongly refracting interior……With the maturation, release and settling out of the spores, the development of the Bacillus is ended, and no further changes take place in the hay infusion……The spores are viable however".*

-spore formation in *Bacillus subtilis* explained by Ferdinand Cohn (1876) in Studies on the biology of the *Bacilli*, Translated by Thomas Brock (Brock,1961; Cohn 1876)

## I.i A short history on *Bacillus subtilis* discovery and research

*Bacillus subtilis*, a gram-positive, rod-shaped bacterium was discovered and termed as *Vibrio subtilis* in 1835 by Christian Gottfried Ehrenberg. It was later renamed as *Bacillus subtilis* by Ferdinand Cohn in 1872, referring to the rod shape of the bacteria (Figure I-1). *Bacillus subtilis* is an endospore-forming bacterium and an obligate aerobe belonging to the phylum firmicutes and naturally dwelling in soil and vegetation.

The endospore formation in *Bacillus subtilis* was first discovered by Ferdinand Cohn in 1876 while disproving the theory of spontaneous generation. Cohn described the *Bacillus subtilis* motile rods and the spore formation process, by observing boiled hay infusions under a microscope (Brock, 1961). In his observations, Cohn also described biofilm formation by *Bacillus subtilis*, although the official term "Biofilm" was coined much later. In the year 1880, Robert Koch, discovered another gram-positive, spore-former, *Bacillus anthracis*, to be the causative agent for anthrax, a lethal disease. This work also indicated the medical importance of spore-forming micro-organisms (Brock, 1961).

For more than 500 years before its discovery, *Bacillus subtilis subsp. natto*, a strain of *Bacillus subtilis*, has been consumed in east Asian countries like Japan, China, Thailand, and Korea. A fermented soybean product called Natto is produced using this *B. subtilis* strain, and, is consumed for its health benefits (Sun, Wang, & Zhang, 2010). The ancestor of the most common *B. subtilis* laboratory strain was isolated in 1899 at the University of Marburg by Meyer and Gottheil (Cohn, 1930). This strain, popularly known as “Marburg strain” was used for laboratory experiments after it was shown to be competent for genetic manipulation (McLoon, Guttenplan, Kearns, Kolter, & Losick, 2011). The genetic competency of this strain facilitated the way for innumerable molecular genetic experiments that helped in understanding the biology of *B. subtilis* and related Gram-positive bacterial species (McLoon et al., 2011).

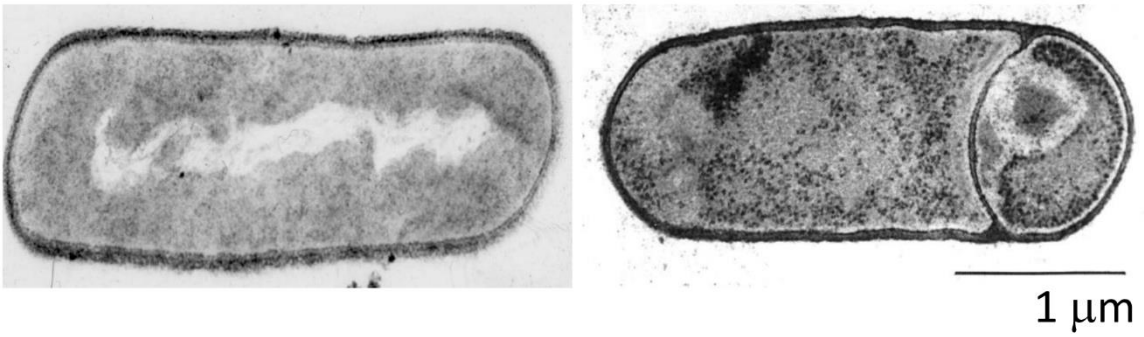


**Figure I-1. Electron Micrographs of a *Bacillus subtilis* cell.**
Images of *Bacillus subtilis* during the vegetative growth phase (left) and after asymmetric septation during sporulation (right) provided graciously by Dr. David Rudner (Harvard Medical School).

1n 1997, *Bacillus subtilis* 168, the most popular *B. subtilis* laboratory strain, was the first gram-positive species to have its entire genome sequenced over in ten years (Kunst et al., 1997). This genome sequencing paved a way for genome-

wide analysis, gene identification, and characterization which proved important in the field of fundamental research.

Among numerous applications of *Bacillus subtilis* some far-reaching ones are production of industrial enzymes such as amylases, lipases and proteases, production of insecticides, antibiotics, purine nucleotides, polyglutamic acid, D-Ribose and Poly hydroxy butyrate (PHB) (Shahcheraghi, Ayatollahi, & Lotfi, 2015). All these products are important in both the medical and industrial fields.

In recent years, *Bacillus subtilis* has been found to act successfully as a vaccine vehicle, by expressing antigenic factors fused to the spore coat proteins (Rosales-Mendoza & Angulo, 2015). When studied as a potential probiotic, *Bacillus subtilis* has shown to inhibit the growth of pathogens like *Salmonella enteritidis* and *Vibrio spp.* in the intestinal epithelial cells (Vaseeharan & Ramasamy, 2003). Another unique industrial application of *Bacillus subtilis* includes use as a biological indicator determining the effectiveness of the low steam sterilization process (Rogers, 2012). This ubiquitous micro-organism has been found in the GI (Gastro-Intestinal) tract of both animals and humans, in the marine habitats, and holds the record for surviving in space for 6 years on a NASA satellite (Horneck, Bucker, & Reitz, 1994; Nicholson, Munakata, Horneck, Melosh, & Setlow, 2000).

### I.ii *Bacillus subtilis* as a model organism for studying differentiation

Differentiation is an important process in eukaryotes as well as prokaryotes, even though the purpose of differentiation is discrete in multicellular organisms versus unicellular organisms. In the eukaryotes, cell differentiation occurs as a result of development, when the cell changes from a simple zygote to complex

tissues. This is a normally occurring process that is a part of both animal and plant kingdom. Whereas, unicellular organisms such as bacteria can experience cell differentiation under environmental stress conditions.

Since the invention of the single-lens microscope by Antonie Van Leeuwenhoek in the 17$^{th}$ century, scientists have been studying microbes and using them as models to enhance their understanding of complex eukaryotes. Some well-studied examples of differentiation include heterocyst formation in some filamentous cyanobacteria such as *Nostoc sp.* and *Anabaena sp.* (Golden & Yoon, 1998), myxospore formation in *Myxococcus sp.* (Kroos, Kuspa, & Kaiser, 1986), 'swarmer' daughter cells and 'stalked' daughter cells arising from a single *Caulobacter cresentus* (Gober & Marques, 1995), *Streptomyces sp.* sporulation by forming a multinucleate sporogenic cell at the leading tip of an aerial hyphal filament (Jakimowicz & van Wezel, 2012), swarming and swimming motile cells in *Bacillus subtilis* (Aguilar, Vlamakis, Losick, & Kolter, 2007) and sporulation in *Bacillus subtilis*(Stragier & Losick, 1996).

Sporulation in *Bacillus subtilis* (Figure I-2), a non-pathogenic gram-positive endospore former, is the best-studied model for understanding bacterial differentiation as a stress response. Since the endospore formation discovery, studies have shown that these *Bacillus* spores are highly heat-resistant, and survive harsh conditions (UV, desiccation, and γ-radiation) and predation by micro-organisms and macro-organisms (P. Setlow, 2006). Bacterial spores pose a serious concern for the food industry, due to their ability to survive industrial processing and decreasing the shelf life of food products (Daelman et al., 2013;

Soni, Oey, Silcock, & Bremer, 2016). Especially, the spore-forming pathogens like *Bacillus cereus* are of particular concern. The non-pathogenic *Bacillus subtilis* shares many similarities with the pathogenic spore-formers and hence has been a model organism for sporulation research since its discovery. As mentioned before, it is the first gram-positive spore former to have its entire genome sequenced, making it easier to study. *Bacillus subtilis* also provides the flexibility for genetic engineering and differentiates into several cell types (competent, cannibalistic, motile, biofilm-forming or spore-forming cells) under environmental stress conditions. All these properties make *B. subtilis* a model organism to study differentiation under laboratory settings.

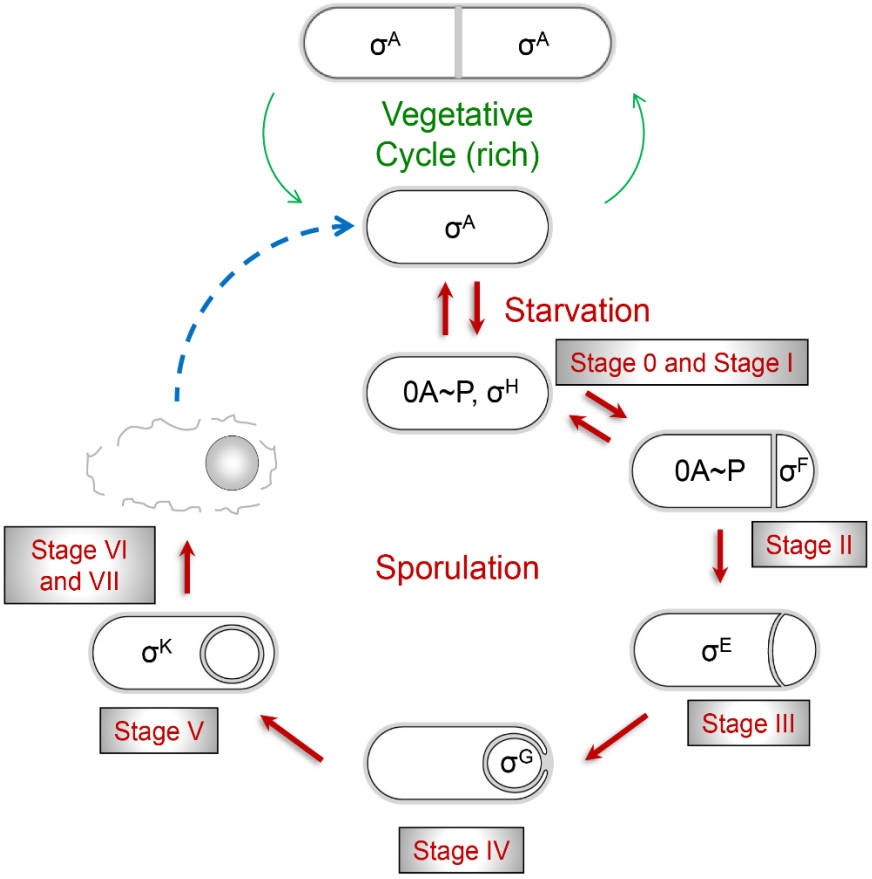


**Figure I-2. Schematic diagram of the sporulation life cycle of *B. subtilis* under starvation conditions.**
The vegetative life cycle is shown on the top, under vegetative growth, the bacterium divides medially giving rise to two daughter cells. Under stress conditions such as starvation, *B. subtilis* undergoes a sporulation cycle to form a stress-resistant endospore. This cycle is divided into several stages, governed by different compartment-specific sigma (σ) factors indicated above. At the end of the sporulation cycle, the mother cell lyses and releases a mature spore into the environment. This spore is stress-resistant and survives for long periods without nutrients. Upon availability of nutrients, the spore germinates (indicated by the dotted blue arrow) into a vegetative *B. subtilis* cell.

### I.iii Differentiation in *Bacillus subtilis* under starvation

*Bacillus subtilis* can activate or adopt several cell differentiation pathways mainly due to environmental stress. Upon onset of the stationary phase, some *B. subtilis* can differentiate into competent cells which can uptake exogenous DNA from the environment (Dubnau, 1991; Lopez & Kolter, 2010). Most of the cell

differentiation pathways are triggered upon nutrient limitation, however, a fraction of exponentially growing *B. subtilis* cells can also differentiate. These exponentially growing *Bacillus* cells can transform into motile cells upon expressing *sigD* ($\sigma^D$), a sigma factor necessary for the production of *flagellin* (a motility gene) (Kearns, Chu, Branda, Kolter, & Losick, 2005; Lopez, Vlamakis, Losick, & Kolter, 2009). The cell differentiation pathways triggered in *Bacillus subtilis* due to nutrient limitation include biofilm formation (Vlamakis, Aguilar, Losick, & Kolter, 2008), Cannibalism (Gonzalez-Pastor, 2011) and sporulation (Sonenshein, 2000) (Figure I-3). These differentiation pathways are regulated by a master transcriptional regulator, Spo0A, which is activated upon phosphorylation via a multi-component phosphorelay.

I.iii.1 Biofilm formation

Biofilm formation is exhibited in almost all bacterial species, where the bacterial cells co-exist by attaching to surfaces and each other, embedded in an extracellular matrix composed of exopolysaccharides, proteins, lipids, and extracellular DNA (eDNA) (Cairns, Hobley, & Stanley-Wall, 2014). These biofilms have complex architecture, display wrinkles on the surface, and are highly hydrophobic (Vlamakis et al., 2008). In nature, multi-species biofilms are a common phenomenon, although pathogenic biofilms often involve single species. Predominantly, *B. subtilis* colonizes at the rhizosphere of plant roots (Beauregard, Chai, Vlamakis, Losick, & Kolter, 2013). Interestingly, according to recent reports, *B. subtilis* can colonize fungal hyphae (Holscher et al., 2015).

The bacterial biofilms are an important topic of research, not only because of the nuisance they cause in man-made environments but also because of the positive impacts in certain industries. Examples of harmful biofilms include biofilm-associated infections by *P. aeruginosa*, and *S. Pneumoniae*, food-borne infections caused by *Salmonella spp.* in dairy, seafood, and on poultry farms, and biofilm formation on biomedical devices resulting in 60 – 70% nosocomial infections (Bryers, 2008). Biofilms can be beneficiary in certain avenues such as microbial leaching for extraction of copper from ore deposits, bioremediation of contaminated soil, and underground water (Morikawa, 2006).

Biofilms formed by *Bacillus subtilis* have been studied in laboratories as a means to understand the social behavior such as quorum-sensing of the micro-organisms in a natural environment (Kalamara, Spacapan, Mandic-Mulec, & Stanley-Wall, 2018). The laboratory strain of *Bacillus subtilis*, PY79, is unable to form biofilms due to loss of 84 kb endogenous plasmid pBS32 and is considered to be biofilm deficient, with no effect on other cellular processes (Konkol, Blair, & Kearns, 2013; Zeigler et al., 2008). Another strain of *Bacillus subtilis* (undomesticated) which retains the extrachromosomal plasmid (pBS32) is used for studying biofilms in laboratories. Initially, it was difficult to genetically manipulate the undomesticated strain because of its poor competence. This problem was solved by the introduction of a mutation in the *comI* gene of pBS32, which increased the competency of the undomesticated strain 100-fold (Konkol et al., 2013).

Under laboratory settings, the undomesticated strain of *Bacillus subtilis* forms biofilms in the form of pellicles at the air-liquid interface in the liquid media and architectural colonies with wrinkles on solid media. Different media can produce architecturally different biofilms, for example using LB (Luria-Bertani) media supplemented with glycerol and manganese (LBGM) can enhance biofilm production and make large and robust biofilms as compared to MSgg media which also promotes biofilm formation (Shemesh & Chai, 2013).

Biofilm formation in *Bacillus subtilis* is regulated by the master regulator Spo0A, which activates upon phosphorylation (Spo0A~P). During starvation, when the Spo0A~P levels are low, *B. subtilis* cells can undergo biofilm formation which begins with the expression of extracellular matrix genes. Biofilm formation is regulated via Spo0A~P, which indirectly regulates another transcriptional regulator SinR through SinI (the anti-repressor of SinR). SinR is the repressor for matrix producing operon *epsA-O*, amyloid synthesis operon *tapA-sipW-tasA,* and another regulatory gene *slrR*. SinI, the anti-repressor for SinR, is under the direct control of Spo0A~P. When *sinI* is expressed, SinR is repressed causing de-repression of matrix genes, and matrix production is switched on (Branda, Chu, Kearns, Losick, & Kolter, 2006; Chai, Chu, Kolter, & Losick, 2008). Amyloid synthesis operon *tapA-sipW-tasA* is also repressed by AbrB, a transition state regulator, controlling ~500 genes. Spo0A~P represses AbrB, which in turn de-represses the amyloid synthesis operon. Once the matrix production is switched on, the cells start attaching and producing extracellular matrix. This cell chaining is an essential step in the biofilm formation (Vlamakis, Chai, Beauregard, Losick, & Kolter, 2013). Once

the biofilm matures, some cells can differentiate into spore-forming cells. As the biofilm becomes old, some cells secrete D-amino acids and polyamines that detach the biofilm and the biofilm contents are scattered in the environment (Vlamakis et al., 2013).

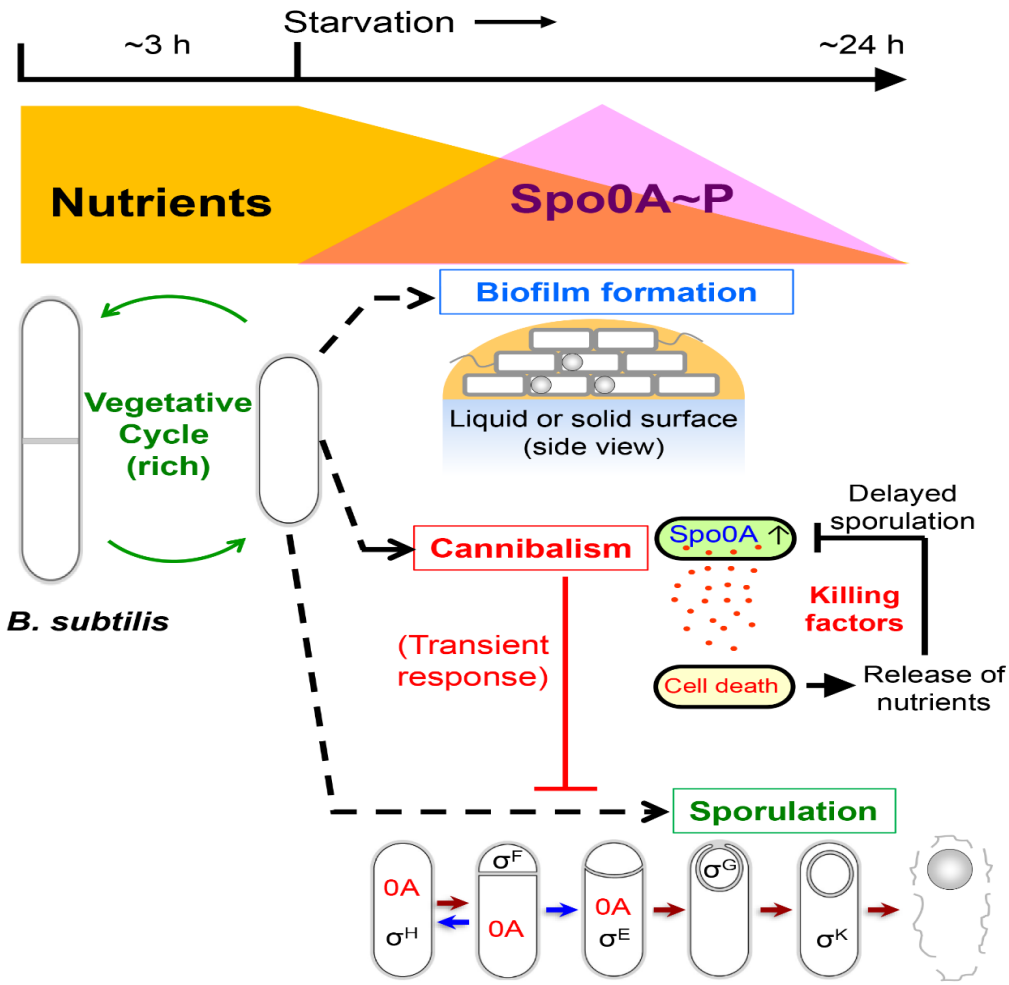


**Figure I-3. Differentiation pathways adopted by *Bacillus subtilis* under starvation conditions.**
When the nutrients are readily available, *B. subtilis* undergoes vegetative cycle, by dividing medially to give rise to two daughter cells. Under starvation conditions, the *B. subtilis* cells can choose three pathways. When Spo0A~P levels are low, cells can switch on the matrix production and become encased in an extracellular matrix, forming biofilms at the air-liquid interface and on solid media. Some cells can produce killing factors, which kill the surrounding cells and provide nutrients to the killing factor producing cannibalistic cells. Cannibalism is a transient response, and upon prolonged starvation, *B. subtilis* cells have to undergo an energy-consuming sporulation process driven by compartment-specific sigma factor regulated gene expression to form stress-resistant endospore.

I.iii.2 Cannibalism

Cannibalism is a social behavior and a transient response seen in some *B. subtilis* cells to postpone sporulation, an energy-consuming process for the cell. Cannibalism is also regulated by the master regulator, Spo0A. Heterogeneity is one of the key features of the *Bacillus subtilis* population (Figure I-4). Hence, in a population, some cells might be sporulating, while others non-sporulating, and few exhibiting some other differentiation pathway like biofilm formation. Cannibalism is displayed by some cells with substantial levels of Spo0A~P, to delay the initiation of sporulation. In these cells, Spo0A~P activates the gene expression of *skf* and *sdp* operons, which produce killing factors or toxins. Along with the toxin production, these operons contain immunity genes, which provide immunity against the killing factors to these cannibalistic cells. The killing factors secreted by the cannibalistic cells kill the neighboring non-immune sibling cells in the population. The nutrients released upon the cell death are then consumed by the cannibalistic cells, to postpone the initiation of sporulation (Gonzalez-Pastor, 2011).

Cannibalism is also a social behavior portrayed by *B. subtilis* in natural environments, against other bacterial species. The killing factors secreted by *skf* (sporulation killing factor) and *sdp* operons (sporulation delaying protein) can act as bacteriocins to kill other soil-inhabiting bacteria such as *Xanthomonas oryzae*, a gram-positive plant pathogen(Lin, Qu, Gu, & Chen, 2001). Thus sporulating cells might be using cannibalism in order to remove all the competition for nutrients required to complete the complex sporulation process (Claverys & Havarstein,

2007). One study reported that SDP (Sporulation Delaying Protein) secreted by *Bacillus subtilis* displayed inhibitory activity against two variants of *Staphylococcus aureus* and other pathogens, suggesting its potential use as an active antibiotic lead compound with few modifications (Liu et al., 2010).

Another bacterial species that display similar behavior is the gram-negative, pathogenic *S. pneumoniae*. In *S. pneumoniae*, “fratricide” is observed in mixed populations of competent and non-competent pneumococci. Competent pneumococci secrete toxins that lyse their non-competent siblings, releasing DNA and other cell components. Fratricide is believed to increase the virulence of pneumococci during human infections, as it also releases the important virulence factor, pneumolysin (Claverys & Havarstein, 2007).

### I.iii.3 Sporulation

Upon prolonged starvation, cells of *Bacillus subtilis* undergo sporulation, an energy-consuming process that results in the production of a highly refractive, stress-resistant endospore. The sporulation process in *B. subtilis* is the “last resort” mechanism governed by the master regulator Spo0A and important for cell survival under environmental stress. Active Spo0A is responsible for triggering transcription of certain sporulation-specific sigma (σ) factors, which govern the gene regulation in a compartment-specific and timely manner, throughout the entire sporulation process.

Spo0A is activated (Phosphorylated) via a multi-component phosphorelay, at the initial stage (stage 0) of sporulation. As the active Spo0A (0A~P, hereafter)

concentration increases in the cell, it activates an alternative sigma factor $\sigma^H$, which further enhances the transcription of certain phosphorelay genes such as *kinA*, *spo0F* and *spo0A* (Fujita & Sadaie, 1998). During the stage I of sporulation, duplicated chromosomes are segregated to two poles of the cell, and the chromosome number is controlled by Spo0A~P, by direct binding to sites near the origin of replication (Boonstra et al., 2013). The stage II of sporulation is marked by asymmetric division near one of the poles, and formation of a larger compartment (mother cell hereafter) and a smaller compartment (forespore hereafter).

The switch from vegetative division to asymmetric septation is the morphological hallmark feature of sporulation. After asymmetric septation, the cell is committed to this energy-consuming process and has to undergo sporulation governed by activation of compartment-specific sigma factors at each stage. These sporulation-specific sigma factors are not essential for the survival of a vegetative cell, but the loss of any of these sigma factors has shown arrest in the sporulation process at that particular stage (Haldenwang, 1995; Kroos, Zhang, Ichikawa, & Yu, 1999). The first sporulation-specific sigma factor, $\sigma^F$, is activated in the forespore, shortly after asymmetric septation. The sigma factor $\sigma^F$, present in an inactive form held by an anti-sigma factor, is activated by the SpoIIE protein under 0A~P regulation in a Spatio-temporal manner (Decatur & Losick, 1996; Kroos et al., 1999).

In stage III of sporulation, the mother cell extends its membrane across the forespore, to engulf the forespore. This stage III, also known as engulfment, is

driven by the mother cell-specific sigma factor $\sigma^E$. The sigma factor $\sigma^E$ is present in an inactive form (pro- $\sigma^E$) and is activated by a protein SpoIIR, regulated by $\sigma^F$ in the forespore. SpoIIR crosses the membrane from the forespore to intermembrane space between the forespore and mother cell, and it signals the protease SpoIIGA for the activation of the mother cell-specific sigma factor $\sigma^E$ (Karow, Glaser, & Piggot, 1995; LaBell, Trempy, & Haldenwang, 1987). The genes controlled by $\sigma^E$, help in the engulfment process and activation of the next sporulation-specific sigma factor $\sigma^G$ in forespore.

After the engulfment of the forespore by the mother cell, cortex formation occurs at stage IV, which is governed by the forespore specific sigma factor, $\sigma^G$ (Kellner, Decatur, & Moran, 1996). In stage V, inner and outer spore coat proteins are added to the forespore under the control of the mother cell-specific sigma factor, $\sigma^K$ (Cutting, Roels, & Losick, 1991; Eichenberger et al., 2003). In stage VI, the spore matures and is ready to survive the starved environment. Eventually, the mother cell lyses, releasing the mature spore into the environment at stage VII or final stage of sporulation. This spore is resistant to heat, UV, desiccation, and can survive indefinitely without nutrients(P. Setlow, 2006).

The cortex of the spore, made of specialized peptidoglycan, maintains its dehydrated state and thus protects the spore from high heat. Additionally, mineralization and the presence of the small molecule dipicolinic acid (DPA) also help in heat resistance and reduction in spore water content (Atrih & Foster, 2001; B. Setlow & Setlow, 1993b; P. Setlow, 2006). The coat proteins protect the spore from enzymatic attacks such as lysozyme. Furthermore, the spore's DNA is bound

by small acid-soluble proteins (SASPs) that protect the DNA from exposure to UV irradiation and hydrogen peroxide (B. Setlow & Setlow, 1987, 1993a). Upon the availability of nutrients in the environment, the spore can germinate to a vegetative *Bacillus* cell.

*Bacillus subtilis* is a well-studied model system, especially because of its relative simplicity and genetic tractability. Over the years, *Bacillus* sporulation research has helped us understanding basic biological processes such as differential gene expression, membrane remodeling, intercellular communication, subcellular protein localization, and morphogenesis (Tan & Ramamurthi, 2014). However, despite decades of research, certain questions remain unexplained. The mystery behind the cell fate decision to sporulate or form biofilms still needs to be deciphered. Similarly, even after finding out the individual contributing factors, the basic biological mechanism underlying the switch from medial to asymmetric division remains largely unexplained. Thus continued research in *Bacillus* sporulation, along with developing new tools and strategies may provide answers to fundamental biology questions.

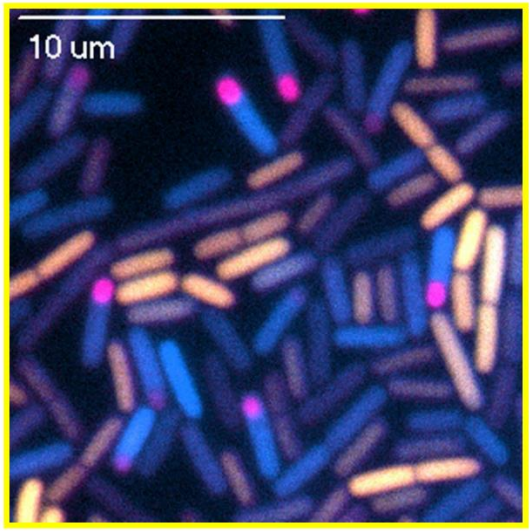


**Figure I-4. Heterogeneity in the *Bacillus subtilis* population.**
Cells from the same genetic background can undergo different gene regulation and cell differentiation programs. Cells in yellow are in a vegetative growth state and expressing yellow fluorescent protein (YFP) fused to an *abrB* promoter. Cells in cyan are in the early stages of sporulation and are expressing cyan fluorescent protein (CFP) fused to the *spoIIA* promoter expressed before asymmetric septation. Cells advanced in sporulation, are expressing mCherry (pink) fused to forespore-specific promoter *spoIIQ*. Scale bar 10 μm.

## I.iv Spo0A and the multi-component phosphorelay

Spo0A is the master regulator of the post-exponential cell differentiation in *Bacillus* and *Clostridia species* (Brown et al., 1994). In *Bacillus subtilis*, Spo0A, a DNA binding protein, is activated via a multi-component signaling cascade, known as phosphorelay (Burbulys, Trach, & Hoch, 1991). Unlike many two-component bacterial systems, involving a “receiver” kinase and a response regulator protein, *Bacillus subtilis* phosphorelay system is composed of four components (Figure I-5). At the top of this cascade are histidine kinases, five (KinA, KinB, KinC, KinD, and KinE) present in *Bacillus subtilis* (Jiang, Shao, Perego, & Hoch, 2000). The histidine kinases respond to various extracellular or intracellular signals and

autophosphorylate on a conserved histidine residue. Studies have shown that KinA and KinB play a role in the initiation of sporulation via the phosphorelay (Hoch, 1993) (Perego, Cole, Burbulys, Trach, & Hoch, 1989), whereas KinC and KinD are involved in biofilm formation (Chen et al., 2012; Devi, Vishnoi, Kiehler, Haggett, & Fujita, 2015). It is also known that KinE does not play any specific role in the phosphorelay (Jiang et al., 2000).

The histidine kinases autophosphorylate and transfer the phosphoryl group to two consecutive phosphotransferases, Spo0F and Spo0B respectively. This transfer of the phosphoryl group occurs in a his-asp-his-asp manner in the signaling cascade. Ultimately, Spo0B transfers the phosphoryl group to the N-terminal aspartyl residue of Spo0A, leading to the activation of the C-terminal DNA binding domain of this master regulator (0A~P) (Stephenson & Hoch, 2002). As shown in figure I-5; activation of Spo0A (0A~P) leads to further gene regulation leading to downstream cellular differentiation events.

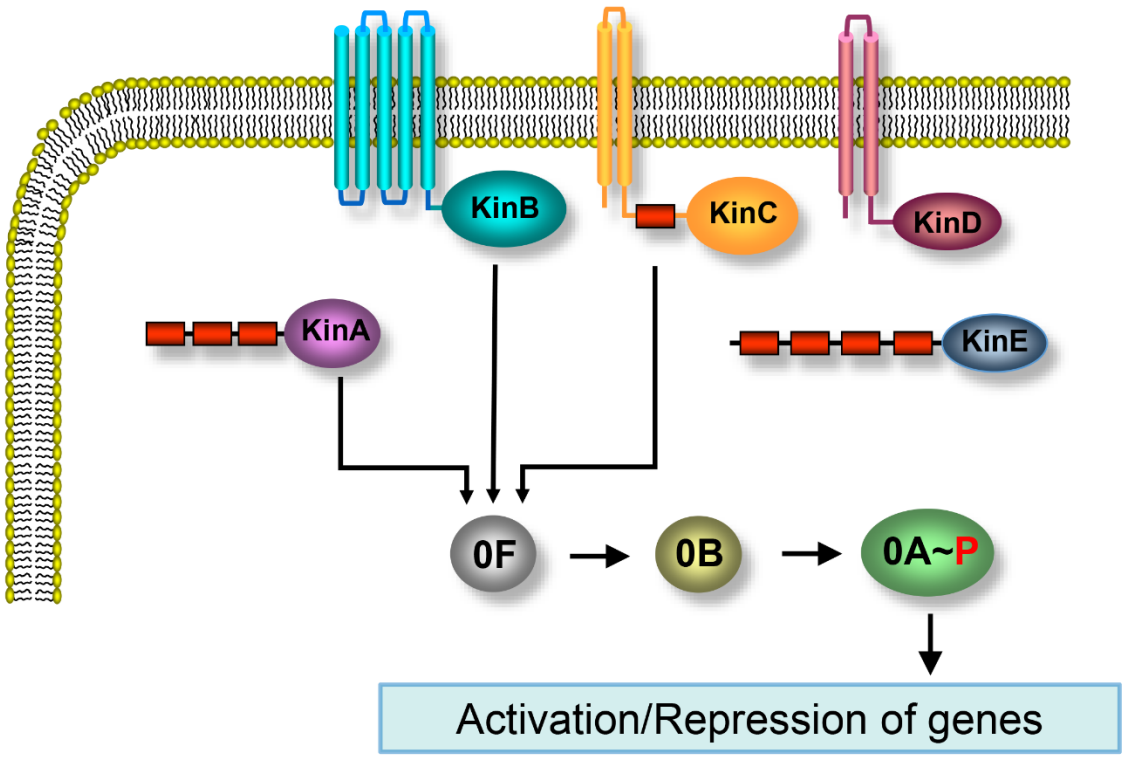


**Figure I-5. Illustration of the multi-component phosphorelay in *Bacillus subtilis*.** All five histidine kinases (KinA, KinB, KinC, KinD and KinE) are shown. KinA, KinB and KinC are known to auto-phosphorylate and transfer the phosphoryl group to Spo0F (0F), a phosphotransferase. 0F passes the phosphoryl group to another phosphotransferase, Spo0B (0B), which then transfers it to Spo0A (0A). Phosphorylation of 0A (0A~P) activates it and this master regulator regulates several genes involved in cell differentiation in *Bacillus subtilis*.

There are two proposed models explaining the entry into sporulation by *Bacillus subtilis*. The first, traditional model is widely accepted as “Signal Model” in the field, according to which, the histidine kinase senses an extracellular, undetermined starvation signal that causes the autophosphorylation on the conserved histidine residue and the phosphoryl group transfer through the signaling cascade (Grossman, 1995; Hoch, 1993). Even though this model is widely accepted, there is no evidence of an external “starvation” signal, despite numerous studies aimed towards proving its authority.

Another newly proposed “Threshold Model” suggests that, a threshold level of KinA, the major sporulation kinase governs the entry of the *Bacillus* cells into sporulation. According to this model, KinA, a major sporulation kinase, is constitutively produced throughout the *Bacillus subtilis* life cycle. This KinA concentration is not high enough to generate threshold levels of Spo0A~P through the phosphorelay in the growing *Bacillus* cells. As the cells begin to starve due to nutrient limitation, the cell growth decreases resulting in accumulation of the constantly produced KinA. This higher concentration of KinA in the starved cells is responsible for generating higher levels of Spo0A~P through the phosphorelay, causing the entry of starved *Bacillus* cells into sporulation (Eswaramoorthy et al., 2010; Narula, Fujita, & Igoshin, 2016).

According to the traditional model, the autophosphorylation of histidine kinase is triggered when the N-terminal “sensor” domain of KinA, containing three PAS domains (PAS-ABC), receives an unidentified starvation signal, similar to other bacterial two-component systems. However, studies supporting the threshold model have shown that, instead of an external “starvation” signal, the autophosphorylation of KinA depends on its tetramer formation, mediated by its PAS-B and PAS-C domains (Kiehler, Haggett, & Fujita, 2017).

Thus, according to the threshold model, rather than sensing an unidentified external “starvation” signal, the cell senses the slowdown in growth and the accumulation of KinA to threshold levels, which initiates the phosphorelay and production of 0A~P to threshold levels controlling the downstream differentiation events necessary for cell survival in adverse conditions.

I.iv.1 Spo0A regulon

Upon activation through the phosphorelay, this DNA-binding, master regulator Spo0A~P, forms dimers (Lewis et al., 2002) and binds to the target sequences situated in the promoters of the 0A-controlled genes. By performing a genome wide "ChIP-on-Chip" analysis of Spo0A binding sites, 121 genes were detected to be directly under the Spo0A control. These genes have a seven nucleotide consensus binding sequence, 5'-TGTCGAA-3' often referred to as a "0A box" (Molle et al., 2003). Binding of 0A~P to these 0A boxes results in either the activation or repression of the transcription. The variations in this 0A consensus sequence are commonly found and can alter the 0A~P binding affinity resulting in differential expression of the 0A-controlled (0A regulon) genes.

Depending on the binding affinity of the 0A~P, 0A regulon genes can be distinguished further into two categories: Low-threshold and high-threshold genes (Figure I-6). The genes that require lower concentrations of 0A~P for regulation (higher affinity of 0A boxes to 0A~P) are placed under the low-threshold category. Whereas, genes that require higher concentrations of 0A~P for regulation (lower affinity of 0A boxes to 0A~P) are placed under the high-threshold category (Fujita, Gonzalez-Pastor, & Losick, 2005). Consistent with this idea, the genes involved in sporulation, an energy consuming process, require higher concentrations of 0A~P, and are placed in the high-threshold category (Fujita et al., 2005). Similarly, genes involved in biofilm formation (such as *tapA*, *epsA*), delaying sporulation (*sdp*) and cannibalism (*skf*) require lower concentrations of 0A~P and are placed in the low threshold category (Fujita et al., 2005). Studies have also shown that a gradual

increase in 0A~P levels is crucial for proper downstream gene expression to initiate and complete the sporulation process efficiently (Fujita et al., 2005; Vishnoi et al., 2013).

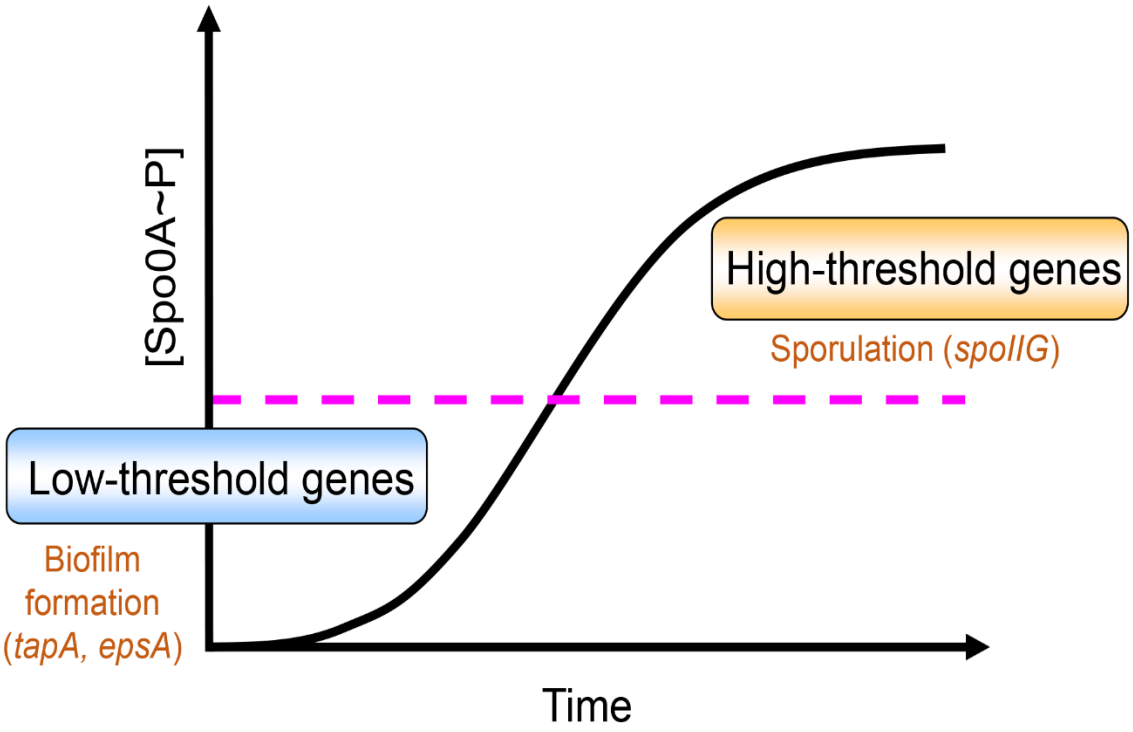


**Figure I-6. Categories of Spo0A regulon genes dependent on the 0A~P concentration.**
The 0A~P concentration gradually increases over time and genes in the Spo0A regulon are regulated in the 0A~P concentration dependent manner. The 0A~P threshold is shown (dotted pink line). Genes involved in biofilm formation (such as *tapA* and *epsA*) require low 0A~P concentration, and hence, fall in the low threshold category. Genes involved in sporulation (such as *spoIIG*) require higher 0A~P concentration, and therefore, are placed in the high threshold category.

I.iv.2 Regulation of the phosphorelay

Regulation of such an intricate signal transduction system is of extreme importance, for precise initiation and completion of cellular differentiation events. In accordance to that, several post transcriptional regulations are controlling the specific levels of all the components of this phosphorelay signaling cascade. At the heart of these complex signal transduction events is the transcriptional regulator, Spo0A. Studies have shown that, disruption or mutation of the *spo0A* gene rendering the protein unable to phosphorylate, results in cell death, which occurs due to the cells' inability to activate the survival pathways adopted under stress (Hoch, 1993). These signal transduction pathways are ultrasensitive and require precise levels of all components, including the response regulator Spo0A. Previous studies have shown that overexpression of a constitutively-active Spo0A mutant in vegetative cells, drastically reduces the sporulation efficiency to 5% (Fujita & Losick, 2005). This stresses the importance of gradual increase in Spo0A~P levels, which is maintained by feedback loops (Figure 1-7).

The *spo0A* gene is transcribed from two promoters, $P_V$ (vegetative growth) and $P_S$ (starvation/sporulation), acting under the control of two different sigma factors, $\sigma^A$ (Housekeeping sigma factor) and $\sigma^H$ (stationary phase sigma factor), respectively (Chibazakura, Kawamura, & Takahashi, 1991; Strauch, Trach, Day, & Hoch, 1992). Furthermore, 0A~P production through the phosphorelay, enhances the *spo0A* gene expression (Fujita & Sadaie, 1998). Under vegetative growth conditions, *spo0A* gene is transcribed by $\sigma^A$ through the relatively weak $P_V$ promoter. Under nutrient deprivation conditions, when the cells are starved,

transcription of *spo0A* gene switches to a stronger $P_S$ promoter under $\sigma^H$ control (Chibazakura et al., 1991).

*sigH* gene, which encodes $\sigma^H$ is repressed during vegetative growth, by the transition state regulator protein, AbrB (Chumsakul et al., 2011; Fujita & Sadaie, 1998; Strauch, Webb, Spiegelman, & Hoch, 1990). Upon entering stationary phase, production of 0A~P through the phosphorelay, represses AbrB, resulting in derepression of $\sigma^H$, along with several other AbrB-controlled genes (Strauch et al., 1990). Expression of several genes in the phosphorelay such as *kinA*, *spo0F* and *spo0A* is enhanced upon activation or derepression of $\sigma^H$ (Fujita & Sadaie, 1998).

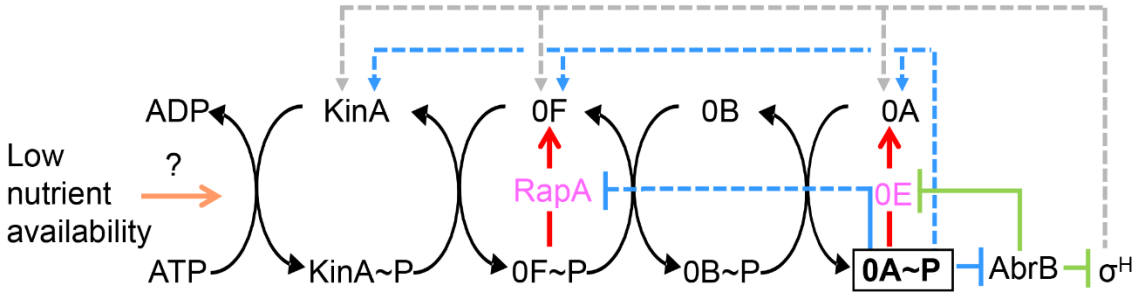


**Figure I-7. Schematic diagram of the feedback loops regulating the phosphorelay.** The intricate feedback loops involved in post-transcriptional regulation are illustrated. Activation is shown by pointed arrowheads and repression is shown by flat arrowheads. Post-transcriptional regulation by 0A~P (blue), AbrB (green) and $\sigma^H$ (gray) is shown here.

Along with $\sigma^H$, 0A~P is also involved in positively enhancing the expression of *kinA*, *spo0F* and *spo0A* (Chastanet & Losick, 2011; Chastanet et al., 2010; Fujita & Sadaie, 1998). These feedback loops regulating the levels of phosphorelay components, play a huge role in maintaining the precise levels of the components. Steady levels of phosphorelay components is critical, since excess of one

component can have inhibitory effects on the phosphorelay. Studies have shown that, increased levels of Spo0F inhibits KinA autophosphorylation both *in vitro* (Grimshaw et al., 1998) and *in vivo* (Chastanet et al., 2010; Narula et al., 2015).

To maintain the exact levels of these phosphorelay proteins, two phosphatases play antagonistic roles. RapA and Spo0E phosphatases remove phosphoryl groups from Spo0F~P and Spo0A~P, respectively (Perego, 2001; Perego, Glaser, & Hoch, 1996; Shafikhani & Leighton, 2004). To maintain the proper levels, *rapA* is repressed by 0A~P, and *spo0E* is repressed by AbrB (Chumsakul et al., 2011; Fujita et al., 2005; Shafikhani & Leighton, 2004).

### I.v Mother cell-specific Spo0A activity

The above mentioned tight feedback regulatory loops help in regulation of the 0A~P levels required to initiate this energy consuming cell survival process of sporulation. Gradual increase in 0A~P levels, which is achieved through the feedback regulation and phosphorelay, is very important for the proper initiation of sporulation (Fujita et al., 2005; Vishnoi et al., 2013). Once the 0A~P levels are reached, an alternative sigma factor, $\sigma^H$ is activated, which plays a crucial role in the remodeling of cell, and formation of asymmetric septation, a hallmark feature of sporulation (Britton et al., 2002; Stragier & Losick, 1996).

After asymmetric septation, sporulation specific sigma factors are activated in the different compartments of the cell: forespore (smaller compartment controlled by $\sigma^F$ initially and $\sigma^G$ later on) and mother cell (larger compartment controlled by $\sigma^E$ in the initial stages and $\sigma^K$ in the later stages). These sigma factors are in their

inactive state under 0A control, and require additional proteins to activate, for instance, the sigma factor $\sigma^F$ is activated by SpoIIE under 0A-control. Therefore, after asymmetric septation, Spo0A plays an important role of activation of cell-specific regulatory proteins like SpoIIE and many others, which activate the forespore and mother cell lines of gene expression (Fujita & Losick, 2003; Losick & Stragier, 1992; Stragier & Losick, 1996).

For several years, the compartmentalization of the sporulation sigma factors was a mystery in the field of sporulation. There were gaps in understanding, even after finding the individual contributing factors. For instance, the processing mechanism for pro-$\sigma^E$ (encoded by *spoIIGB*) to active $\sigma^E$ was known to be mediated by SpoIIGA (encoded by *spoIIGA*) with the help of SpoIIR under $\sigma^F$ control (Londono-Vallejo & Stragier, 1995). However, the mechanism by which $\sigma^E$ was confined to the mother cell was unknown.

One group studying localization of $\sigma^E$ to the mother cell compartment proposed a model. According to this model, pro-$\sigma^E$ localized to the mother cell face of the septum, and was processed into active $\sigma^E$ through the combined action of SpoIIGA & SpoIIR, and selectively released into the mother cell cytoplasm (Ju & Haldenwang, 1999). This model was disproved by Fujita and Losick in 2002, when they showed that pro-$\sigma^E$ was indeed a membrane protein, but distributed all along the cytoplasm and both membrane faces of the septum (Fujita & Losick, 2002). Their results suggested that, the preferential and persistent transcription of the *spoIIG* operon (encoding *spoIIGA* and *spoIIGB*) in the mother cell and the degradation of $\sigma^E$ in the forespore, contribute towards the selective accumulation

of $\sigma^E$ in the mother cell (Fujita & Losick, 2002). The results from this study also indicated that pro-$\sigma^E$ activation, which requires SpoIIR is critical for efficient sporulation and is properly timed, such that mature or active $\sigma^E$ does not appear until the asymmetric division is complete (Fujita & Losick, 2002).

Previously, the role of Spo0A was confirmed to be the initiation of sporulation, but later on it became clear, that Spo0A continues to function after the initiation phase of sporulation. Another study by Fujita and Losick (in 2003), revealed that Spo0A becomes a mother cell-specific transcription factor when the sporulating cell is divided into mother cell and forespore. Evidence presented in this study was a major finding towards understanding the role of Spo0A after asymmetric septation. In this study, the cells engineered to produce an activated form of Spo0A in the forespore, showed impaired sporulation. When the activated form of Spo0A was expressed in the mother cell, sporulation was normal. This study also used a newly devised inhibitor of Spo0A phosphorylation (Spo0A-N). The cells engineered to produce this inhibitor in the mother cell were defective in sporulation. Whereas, when the inhibitor was expressed in the forespore, sporulation was normal (Fujita & Losick, 2003).

According to the investigation, Spo0A itself along with the 0A-controlled promoters, accumulated to high levels after asymmetric division and preferentially in the mother cell (Figure I-8). Although it is established that Spo0A becomes a mother cell specific transcription factor, the function of Spo0A in the mother cell remains unclear. One speculation is that, Spo0A might be involved in regulating the genes under the $\sigma^E$ control(Fujita & Losick, 2003). It is important to elucidate

the regulatory mechanisms displayed by Spo0A in the mother cell, which may involve regulation of the mother cell line of gene expression.

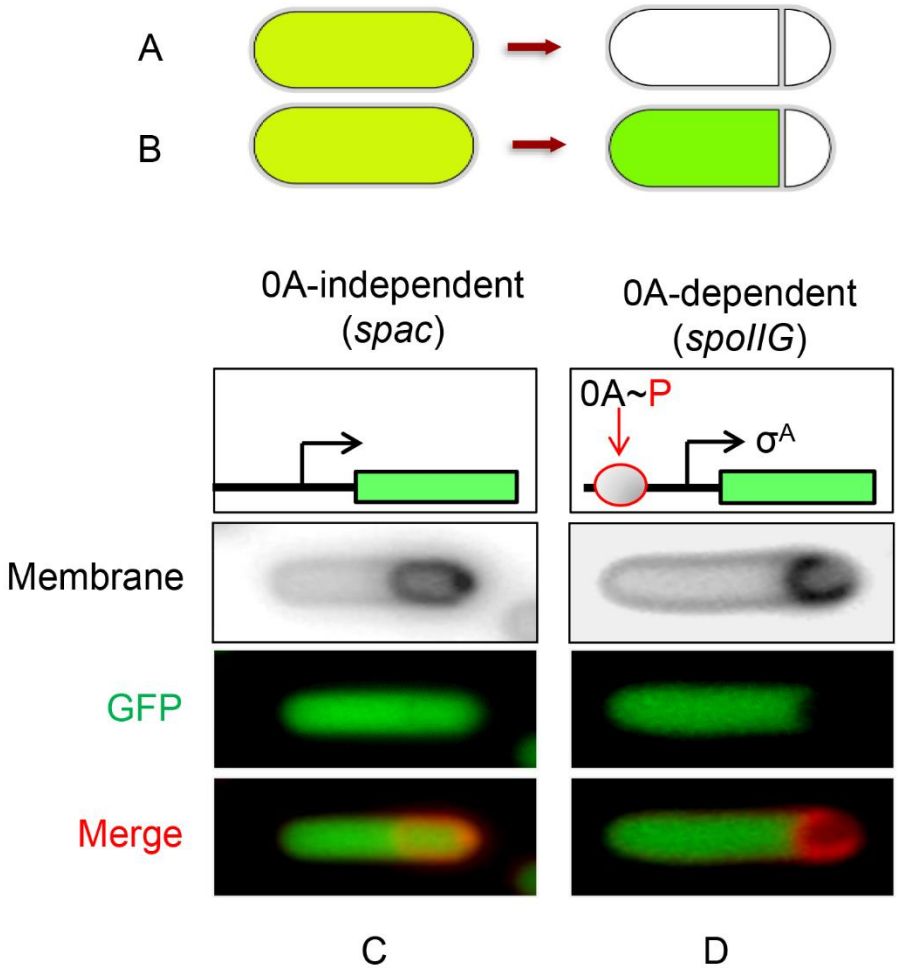


**Figure I-8. Role of Spo0A, as a mother cell-specific transcription factor.**
Mother cell-specific activity of Spo0A was first observed in 2002.
A) Schematic representation of what was believed to be the role of Spo0A earlier, Spo0A was believed to only initiate sporulation (Ferrari et al., 1985).
B) Schematic representation of the newly discovered role of Spo0A as a mother cell-specific transcription factor, after asymmetric septation (Fujita & Losick, 2002).
C) 0A-independent *spac* promoter fused to *gfp*. GFP signal (green) is observed throughout the cell.
D) 0A-dependent *spoIIG* promoter fused to *gfp*. GFP signal (green) is observed exclusively in the mother cell compartment.

## I.vi Scope of this Dissertation

Even with decades of research in the field of *Bacillus subtilis* sporulation; certain questions remain unanswered. How the cell arrives to the decision to sporulate or form biofilms is still debatable. The 0A~P levels regulated through the phosphorelay and the feedback loops play a role in the cell fate decision. One more interesting aspect is the relatively new found role of Spo0A as the mother cell-specific transcription factor. Research needs to be conducted to determine the function of Spo0A as the cell-specific transcription factor.

Within the confines of this thesis, I focused on two main questions: how is the transcriptional control of *spo0A* achieved, and what is the mechanism of 0A regulation in a mother cell specific gene. My primary goal for chapter II was to study the transcriptional control of *spo0A*. For this purpose, I mainly focused on the role of the three 0A boxes (0A1, 0A2, and 0A3) located upstream of the *spo0A* gene, by studying their binding patterns and role in promoter activity. In order to study the role of the 0A boxes in *spo0A* transcription, 0A box mutations with all possible combinations were constructed. Electrophoretic mobility shift assays were performed for assessing the relative binding affinity of 0A~P to the 0A boxes. In Chapter II, I provided the fundamental evidence of 0A~P binding with varied affinities to the three 0A boxes located upstream of *spo0A*. For studying the promoter activities in the absence of the 0A boxes, 0A box mutated and non-mutated promoters were transcriptionally fused to *lacZ* gene. Our unpublished data suggests the importance of two kinases, KinA (Sporulation kinase) and KinC (Biofilm kinase) in the cell fate decision by Spo0A. Hence, I was interested in

studying the transcriptional activity of *spo0A* in the absence of each of these kinases. For this purpose, promoter *lacZ* constructs were inserted in *kinA* knockout (ΔA) and *kinC* knockout (ΔC) strains. β-galactosidase assays were performed to study the mutated promoter activities in wild type, ΔA and ΔC knockout strains. In order to investigate the conservation of this regulatory mechanism through evolution, I conducted homology search using bioinformatics tools.

My main goal for chapter III and IV was to study the mother cell-specific activity of Spo0A. For this purpose, in Chapter III, I investigated a potential Spo0A target mother cell-specific gene, *spoIID*. The work started with the close study of the *spoIID* promoter region, resulting in identification of three putative 0A boxes. 0A box mutants (single, double and all mutated) were constructed. Along with studying the 0A~P binding, I also verified the binding site for a well-known *spoIID* binding protein, SpoIIID. I provided the key evidence of 0A~P binding to the three 0A boxes upstream of *spoIID* through Electrophoretic mobility shift assays. To assess the role of individual 0A boxes during the *spoIID* transcription, I assayed the box mutant promoters transcriptionally fused to *lacZ*. The results indicate that *spoIID* expression is positively regulated by 0A~P through binding to 0A1 and 0A2, whereas 0A~P binding to 0A3 box negatively regulates *spoIID* expression.

In Chapter IV, I studied the effect of mother cell-specific Spo0A activity on the sporulation process. For this purpose, I constructed a functional SpoIID-FLAG strain with SpoIID-FLAG inserted at a non-essential *amyE* locus along with native *spoIID* deletion. Assorted mutants were constructed by placing the SpoIID-FLAG strain under different 0A box and IIID box mutated promoters. For studying the

effects on sporulation, compartment-specific sporulation reporter strains were constructed. We used forespore-specific promoters such as $P_{spoIIQ}$ and $P_{sspA}$. These promoters are controlled by different sigma factors and are active at different times during sporulation. For visualizing the single cell effects, these promoters were fused with *gfp* and inserted in the assorted SpoIID-FLAG mutants with wild type and mutated promoters. Single cell analysis, using fluorescence microscopy, provided important morphological evidence regarding the bulging of forespore in the 0A3 box mutants. Expression levels of SpoIID were also assessed and revealed an altered SpoIID-FLAG expression in the 0A3 box mutants. This further led to designing induction experiments for observing whether sporulation is restored upon over-expressing SpoIID from an IPTG inducible promoter. Using bioinformatics tools, I also studied the promoter organization of *spoIID* across *Bacillus spp.*, and later compared it with other pathogenic *Bacillus spp.* and *Clostridium spp*. Overall, the results provided in this Chapter, elucidate that Spo0A controls forespore engulfment by regulating the expression of *spoIID*, a gene encoding lytic transglycosylase, essential for the first step of engulfment.

Taken together, the work described in this dissertation has allowed me to build two models: one for the transcriptional control of *spo0A* during early and prolonged starvation, and another for the mother cell-specific activity of Spo0A to control the engulfment process via *spoIID* regulation. My studies provide a better understanding of the complex transcriptional pathways of *spo0A* and, importantly, reveal the post- asymmetric septation function of Spo0A, as a mother cell-specific transcription factor controlling forespore engulfment.

# Chapter II: Investigating the Transcriptional Control of spo0A

## II.i Introduction

Under starvation conditions, the soil bacterium *Bacillus subtilis* initiates entry into either a unicellular (sporulation) or a multicellular (biofilm) differentiation pathway for survival (Gonzalez-Pastor, 2011; Piggot & Hilbert, 2004). These differentiation programs require the activation of a master regulator Spo0A (Ferrari et al., 1985; Hoch, 1993). The activation is achieved via phosphorelay, a His-Asp-His-Asp type phospho-transfer cascade (Burbulys et al., 1991). The phosphorelay starts with autophosphorylation of any of the three histidine kinases (KinA, KinB, and KinC), upon starvation (Jiang et al., 2000; LeDeaux, Yu, & Grossman, 1995). Then, the phosphoryl group from the phosphorylated kinase is transferred to two intermediate phosphotransferases Spo0F and Spo0B in this order, and thereafter to the response regulator, Spo0A (Burbulys et al., 1991). Phosphorylated Spo0A (0A~P) acts as a transcriptional regulator that directly or indirectly controls hundreds of genes involved in competence, cannibalism, biofilm formation, and sporulation (Fujita et al., 2005; Molle et al., 2003).

Among these 0A-controlled genes, a set of 121 genes is known to be under the direct control of 0A~P (Molle et al., 2003). It is suggested that KinC plays an essential role in triggering biofilm formation (Devi et al., 2015) (Yepes et al., 2012), whereas KinA appears to be primarily responsible for sporulation (Eswaramoorthy et al., 2010; Jiang et al., 2000). In addition to the kinases, the phosphorelay activity is controlled post-translationally by phosphatases. RapA phosphatase dephosphorylates Spo0F~P and Spo0E phosphatase dephosphorylates Spo0A~P (Ohlsen, Grimsley, & Hoch, 1994; Perego et al., 1996).

The expression of *spo0A* and other phosphorelay components is known to be regulated by the transcriptional feedback loops. During growth under nutrient-rich conditions, the gene for the transition state regulatory protein AbrB is actively transcribed by the house-keeping $\sigma^A$-RNA polymerase (RNAP) (Strauch et al., 1990). Thus, to maintain growth phase, AbrB represses a set of genes controlling stationary phase, biofilm formation, and sporulation (Banse, Chastanet, Rahn-Lee, Hobbs, & Losick, 2008; Chumsakul et al., 2011; Hamon, Stanley, Britton, Grossman, & Lazazzera, 2004; Strauch et al., 1989). Under such conditions, the *spo0A* gene is weakly transcribed from an upstream $P_V$ (promoter for vegetative phase) promoter under the control of the house-keeping $\sigma^A$-RNAP for maintaining the basal level of Spo0A (Chibazakura et al., 1991).

Upon starvation, Spo0A~P levels gradually increase through phosphorelay, leading to repression of the *abrB* gene (Fujita et al., 2005; Perego, Spiegelman, & Hoch, 1988). In turn, the transcription of the *sigH* (*spo0H*) gene encoding an alternative $\sigma^H$ subunit of RNAP is derepressed by the downregulation of the repressor AbrB (Fujita & Sadaie, 1998). Then, the increased levels of $\sigma^H$-RNAP trigger transcription from a downstream $P_S$ (promoter for sporulation/stationary phase) promoter of *spo0A* (Chibazakura et al., 1991). As a result, the transcription levels of the Spo0A- and $\sigma^H$-controlled *spo0F* and *spo0A* increase in a positive feedback mechanism (Fujita et al., 2005; Fujita & Sadaie, 1998; Predich, Nair, & Smith, 1992). Therefore, the transcriptional feedback loops contribute to the gradual increase in the Spo0A activity during nutrient starvation (Fujita & Losick, 2005; Vishnoi et al., 2013).

In addition to the above described indirect transcriptional feedback loops, the *spo0A* gene is known to be controlled directly by 0A~P (Chastanet & Losick, 2011) (Fujita & Sadaie, 1998) (Strauch et al., 1992). A previous study (Chastanet & Losick, 2011) indicates that binding of 0A~P, to three 0A boxes located in the Spo0A promoter region, governs a transcriptional switch between the two promoters $P_V$ and $P_S$. Although the study does not show direct evidence of 0A~P binding to these 0A boxes located in the promoter region, the model suggests that 0A~P binding to 0A2 causes repression of $P_S$ ($\sigma^H$-controlled, stationary/sporulation phase) promoter and transcription through $P_V$ ($\sigma^A$-controlled growth phase) promoter. Further, low levels of 0A (transcribed through the $P_V$ promoter) activate $\sigma^H$-RNAP resulting in the production of high levels of Spo0A. When starvation persists, the transcription from the $P_S$ promoter is further stimulated by relatively high levels of 0A~P bound to the 0A3 box. Under such conditions, 0A~P bound to the 0A1 box causes repression of the upstream $P_V$ promoter, and the repression of the $P_S$ promoter by 0A~P bound to the 0A2 box is prevented by the binding of 0A~P to the 0A3 box(Chastanet & Losick, 2011).

Although the previous studies attempted to characterize the mechanisms of promoter switching between $P_V$ and $P_S$ in response to starvation (Chastanet & Losick, 2011; Chibazakura et al., 1991), it is not clear how cells achieve *spo0A* expression using the promoter switching mechanism and how they decide their fate between biofilm formation or sporulation. In the following chapter, I provide direct experimental evidence of the 0A~P binding to the three 0A boxes in the *spo0A* promoter region. Secondly, I Investigate the transcriptional activity of *spo0A*

with the help of 0A box mutations and provide a model for the *spo0A* transcription during the early and prolonged starvation phases. With the help of Δ*kinA* and Δ*kinC* knockout strains, I perform transcriptional studies to find out the role of two different kinases in *spo0A* transcriptional control. Finally, I elucidate the evolution of the Spo0A protein in *Bacilli spp.* and *Clostridia spp.* through homology search.

## II.ii Materials and Methods

### II.ii.1 Strains, Plasmids and Primers

All strains used in this study are listed in Table II-2. The parent strain for all the transcriptional studies was the undomesticated and naturally competent DK1042 (NCIB 3610 background, BGSC3A38 as the *Bacillus* Genetic Stock Center strain number) (Konkol et al., 2013) as listed in Table II-1. *B. subtilis* strains were constructed by transformation with either chromosomal DNA or plasmid DNA as described by Harwood & Cutting (Harwood & Cutting, 1990). Standard recombinant DNA techniques including plasmid DNA construction and isolation using *Escherichia coli* DH5α were performed as described by Sambrook & Russell (Sambrook & Russell, 2001). For the deletion of some of the genes, the genomic DNA of the BKE (*Bacillus* knockout erythromycin) strains carrying the deletion of the target gene was used (Koo et al., 2017). Removal of the antibiotic resistance cassette from the BKE strain was performed according to the published procedures (Koo et al., 2017). The plasmids used in this study are listed in Table II-3. The oligonucleotide primers used are listed in Table II-4.

**Table II-1. List of Parental *Bacillus* strains used in this study**

| Strain | Genotype | Reference |
|---|---|---|
| ***B.subtilis* PY79** | Prototroph wild type | (Youngman, Perkins, & Losick, 1984) |
| **DK1042** | *comI*$^{Q12L}$ undomesticated competent wild type derived from NCIB3610 | (Koo et al., 2017) |

**Table II-2. . List of strains used in this study**

| Strain | ***B. subtilis* strains used for β-galactosidase assay** | Reference |
|---|---|---|
| **MF9768** | *amyE::Pspo0A*$^{wt}$*-lacZ spc comI*$^{Q12L}$ | This study |
| **MF9687** | *amyE::Pspo0A*$^{0A1*}$*-lacZ spc comI*$^{Q12L}$ | This study |
| **MF9688** | *amyE::Pspo0A*$^{0A2*}$*-lacZ spc comI*$^{Q12L}$ | This study |
| **MF9689** | *amyE::Pspo0A*$^{0A3*}$*-lacZ spc comI*$^{Q12L}$ | This study |
| **MF9690** | *amyE::Pspo0A*$^{0A1*2*}$*-lacZ spc comI*$^{Q12L}$ | This study |
| **MF9691** | *amyE::Pspo0A*$^{0A2*3*}$*-lacZ spc comI*$^{Q12L}$ | This study |
| **MF9692** | *amyE::Pspo0A*$^{0A1*3*}$*-lacZ spc comI*$^{Q12L}$ | This study |
| **MF9693** | *amyE::Pspo0A*$^{0A1*2*3*}$*-lacZ spc comI*$^{Q12L}$ | This study |
| **MF 9807** | *amyE::P*$_{\Delta v}$$^{wt}$*-lacZ* spc comI$^{Q12L}$ | This study |
| **MF 9983** | *ΔkinA amyE::Pspo0A*$^{wt}$*-lacZ spc comI*$^{Q12L}$ | This study |
| **MF 9987** | *ΔkinA amyE::Pspo0A*$^{0A1*}$*-lacZ spc comI*$^{Q12L}$ | This study |
| **MF 9988** | *ΔkinA amyE::Pspo0A*$^{0A2*}$*-lacZ spc comI*$^{Q12L}$ | This study |
| **MF 9989** | *ΔkinA amyE::Pspo0A*$^{0A3*}$*-lacZ spc comI*$^{Q12L}$ | This study |
| **MF 9990** | *ΔkinA amyE::Pspo0A*$^{0A1*2*}$*-lacZ spc comI*$^{Q12L}$ | This study |
| **MF 9991** | *ΔkinA amyE::Pspo0A*$^{0A2*3*}$*-lacZ spc comI*$^{Q12L}$ | This study |
| **MF 9992** | *ΔkinA amyE::Pspo0A*$^{0A1*3*}$*-lacZ spc comI*$^{Q12L}$ | This study |
| **MF 9993** | *ΔkinA amyE::Pspo0A*$^{0A1*2*3*}$*-lacZ spc comI*$^{Q12L}$ | This study |
| **MF 9984** | *ΔkinA amyE::P*$_{\Delta v}$$^{wt}$*-lacZ spc comI*$^{Q12L}$ | This study |
| **MF 9985** | *ΔkinC amyE::Pspo0A*$^{wt}$*-lacZ spc comI*$^{Q12L}$ | This study |
| **MF 9997** | *ΔkinC amyE::Pspo0A*$^{0A1*}$*-lacZ spc comI*$^{Q12L}$ | This study |
| **MF 9998** | *ΔkinC amyE::Pspo0A*$^{0A2*}$*-lacZ spc comI*$^{Q12L}$ | This study |
| **MF 9999** | *ΔkinC amyE::Pspo0A*$^{0A3*}$*-lacZ spc comI*$^{Q12L}$ | This study |
| **MF 10000** | *ΔkinC amyE::Pspo0A*$^{0A1*2*}$*-lacZ spc comI*$^{Q12L}$ | This study |
| **MF 10001** | *ΔkinC amyE::Pspo0A*$^{0A2*3*}$*-lacZ spc comI*$^{Q12L}$ | This study |
| **MF 10002** | *ΔkinC amyE::Pspo0A*$^{0A1*3*}$*-lacZ spc comI*$^{Q12L}$ | This study |
| **MF 10003** | *ΔkinC amyE::Pspo0A*$^{0A1*2*3*}$*-lacZ spc comI*$^{Q12L}$ | This study |
| **MF 9986** | *ΔkinC amyE::P*$_{\Delta v}$$^{wt}$*-lacZ spc comI*$^{Q12L}$ | This study |

**Table II-3. List of Plasmids used in this study**

| Plasmid | Description | Reference |
|---|---|---|
| **pMF998** | *amyE::Pspo0A$^{0A1*}$-spo0A spc* | This study |
| **pMF999** | *amyE::Pspo0A$^{0A2*}$-spo0A spc* | This study |
| **pMF1000** | *amyE::Pspo0A$^{0A3*}$-spo0A spc* | This study |
| **pMF1001** | *amyE::Pspo0A$^{0A1*2*}$-spo0A spc* | This study |
| **pMF1002** | *amyE::Pspo0A$^{0A2*3*}$-spo0A spc* | This study |
| **pMF1003** | *amyE::Pspo0A$^{0A1*3*}$-spo0A spc* | This study |
| **pMF1004** | *amyE::Pspo0A$^{0A1*2*3*}$-spo0A spc* | This study |
| **pMF1005** | *amyE::Pspo0A$^{0A1*}$-lacZ spc* | This study |
| **pMF1006** | *amyE::Pspo0A$^{0A2*}$-lacZ spc* | This study |
| **pMF1007** | *amyE::Pspo0A$^{0A3*}$-lacZ spc* | This study |
| **pMF1008** | *amyE::Pspo0A$^{0A1*2*}$-lacZ spc* | This study |
| **pMF1009** | *amyE::Pspo0A$^{0A2*3*}$-lacZ spc* | This study |
| **pMF1010** | *amyE::Pspo0A$^{0A1*3*}$-lacZ spc* | This study |
| **pMF1011** | *amyE::Pspo0A$^{0A1*2*3*}$-lacZ spc* | This study |
| **pMF1019** | *amyE::Pspo0A$^{wt}$-spo0A spc* | This study |

**Table II-4. List of Primers used in this study**

| Primers | Sequence |
|---|---|
| **omf18** | 5’-gccgaattcatcgatatttatggaaaaga-3’ |
| **omf28** | 5’-gccggatccttaagaagccttatgctctaa-3’ |
| **omf44** | 5’-gccaagcttatcgatatttatggaaaaga-3’ |
| **omf111** | 5’-gcgaagcttggtaaaatatacaaaagaagatttttcgaca-3’ |
| **omf117** | 5’-gatatgccactaatattggtgattaagcttggc-3’ |
| **om448** | 5’-acgtgaattcacttggaaatcttcttttgtatattttacc-3’ |
| **om449** | 5’-ggtaaaatatacaaaagaagatttccaagtgaattcacgt-3’ |
| **om450** | 5’-aaatgaaaccaagtgaacaaggaaacgtgaatttgtcgaa-3’ |
| **om451** | 5’-ttcgacaaattcacgtttccttgttcacttggtttcattt-3’ |
| **om452** | 5’-ctctgtttccaagtgaaaaatgaaatttgacaaacaagga-3’ |
| **om453** | 5’-tccttgtttgtcaaatttcatttttcacttggaaacagag-3’ |
| **om454** | 5’-gccaagcttatcgatatttatggaaaaga-3’ |
| **om455** | 5’-gccggatccgtagttaacaggattcaccc-3’ |

II.ii.2 Media and Culture Conditions

Luria-Bertani medium (LB) was used for the normal growth of *B. subtilis* (Sambrook & Russell, 2001). Cells harboring *lacZ* reporter fusions were cultured in liquid MSgg (Biofilm conditions) and DSM (sporulation conditions) with shaking at 37 °C. Samples were collected at the indicated time points and assayed for β-galactosidase activities. Threonine (1 mg $ml^{-1}$, final concentration) was added to the MSgg medium whenever threonine auxotroph strains were used. When appropriate, antibiotics were included at the following concentrations: 10 µg $ml^{-1}$ of tetracycline, 100 µg $ml^{-1}$ of spectinomycin, 20 µg $ml^{-1}$ of kanamycin, 5 µg $ml^{-1}$ chloramphenicol and 1 µg $ml^{-1}$ of erythromycin.

II.ii.3 Electrophoretic mobility shift assay

The his-tagged Spo0A protein was expressed in *E. coli* BL21(DE3) and purified as described previously (Devi et al., 2015; Eswaramoorthy et al., 2011; Fujita & Losick, 2003; Kiehler et al., 2017). A soluble form of the his-tagged KinC ($KinC^{\Delta TM1+2}$, the transmembrane deleted form of KinC) was expressed in *E. coli* BL21(DE3) and purified as described previously (Devi et al., 2015).

All autophosphorylation and phosphotransfer reactions were carried out as reported (Devi et al., 2015; Fujita & Losick, 2003; Kiehler et al., 2017). In brief, the reactions were performed in a 20 µl final reaction volume containing 50 mM Tris-HCl, pH 8.0, 5 mM $MgCl_2$, and 10% (v/v) glycerol. Proteins used for the phosphorylation assays were 1 µM of $KinC^{\Delta TM1+2}$ and 10 µM of Spo0A. The reaction was initiated by the addition of ATP to a final concentration of 400 µM.

Reaction mixtures were incubated for 30 min at 30 °C and then used for Electrophoretic mobility shift assays (EMSA).

DNA fragments used in this assay correspond to the region 211 bp upstream of the *spo0A* coding region and were amplified with primers omf18 (radiolabeled) and omf117 by PCR. PCR products containing wild-type and the mutated 0A-boxes were amplified by using DNA templates that contained each of these mutations. The 5' end of omf18 was labeled using [γ-$^{32}$P] ATP (Perkin-Elmer, 3000 Ci mmol-1, 10 mCi ml-1) and T4 polynucleotide kinase. A typical assay mixture contained 10 mM Tris-HCl, pH 7.5, 50 mM NaCl, 1 mM EDTA, 1 mM dithiothreitol (DTT), 5% (v/v) glycerol, 0.5 µg of BSA, 1 µg of Poly(dI-dC), a radioactive DNA probe (2000 c.p.m.), and various amounts of the purified proteins in a 20 µl total volume. After 30 min of incubation at room temperature, 4 µl of 6x loading dye (Thermo Scientific) was added to each of the reaction mixture (20 µl) and then the samples were loaded onto a native 6% (w/v) polyacrylamide gel and electrophoresed in 0.5 x TBE buffer. Radioactive species were detected by autoradiography after exposure to X-ray film. Spo0A was phosphorylated as described above and used at the indicated final concentrations as described in figure legends. Figure II-1 gives a brief illustration of the EMSA protocol.

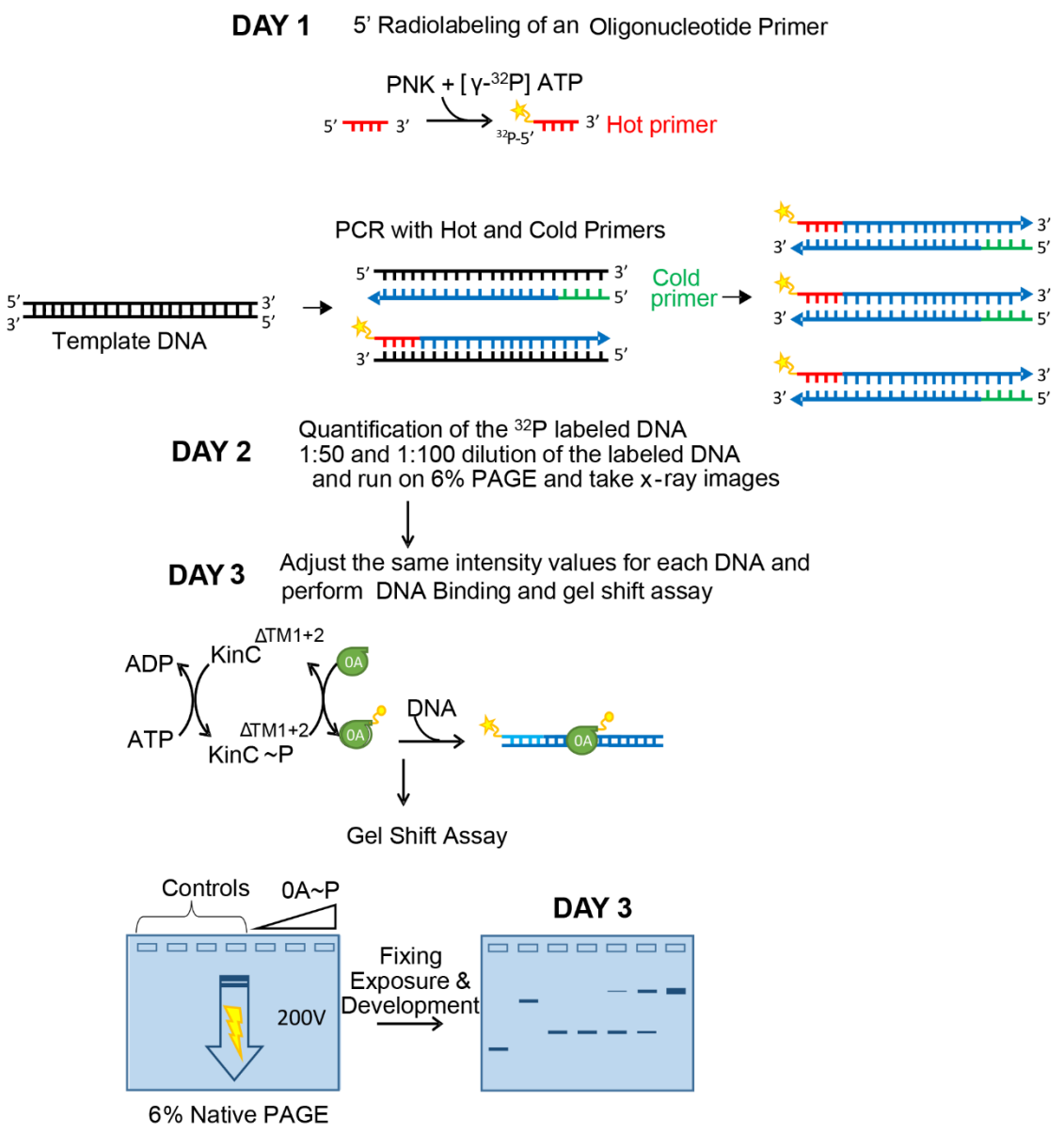


**Figure II-1. A general protocol for Electrophoretic mobility shift assay.**

## II.ii.4 β-galactosidase assays

β-galactosidase assays were performed as described by Harwood & Cutting (Harwood and Cutting 1990) from the samples collected for *B. subtilis* undomesticated strains grown under MSgg and DSM media as required at 37 °C.

II.ii.5 Homology search

Homology search was performed using the blast program (Johnson et al., 2008) with the *spo0A* (*B. subtilis* PY79) promoter region containing three 0A boxes, the promoter recognition elements of the $\sigma^A$ controlled $P_V$ promoter and the promoter recognition elements of the $\sigma^H$ controlled $P_S$ promoter against the bacterial genome database. CLUSTAL Omega program from EMBL-EBI was used for multiple sequence alignment of the promoter recognition sequences from different species. Pairwise sequence alignment was carried out to determine the percentage similarity between the selected candidate *spo0A* and Bacillus subtilis *spo0A* using the EMBOSS water program from EMBL-EBI (Madeira, Madhusoodanan, Lee, Tivey, & Lopez, 2019; Madeira, Park, et al., 2019).

## II.iii Results

II.iii.1 Direct experimental evidence of Spo0A~P binding to three upstream 0A boxes in the *spo0A* promoter region

Previously published studies (Chastanet & Losick, 2011; Chibazakura et al., 1991) on the two promoters ($P_V$ and $P_S$) upstream of the *spo0A* coding region have proposed a promoter switching model for the regulation of *spo0A*. Although, none of them provide direct evidence of Spo0A~P binding to the three upstream 0A boxes in the *spo0A* promoter region. This is the first study, providing direct experimental evidence of Spo0A~P binding to three upstream 0A boxes in the *spo0A* promoter region through Electrophoretic mobility shift assays. In order to achieve this goal, we started by construction of 0A box mutants. For this study, we

only used the first three 0A boxes (0A1, 0A2, and 0A3, hereafter) located between the $P_V$ and $P_S$ promoters upstream of the *spo0A*. The fourth 0A box (0A4) is located in the $P_S$ promoter and its role in promoter switching has not yet been established (Chastanet & Losick, 2011). The 0A box mutant combinations are illustrated in Figure II-2. These 0A box mutants were used as templates to amplify a 221 bp DNA fragment containing different 0A box mutations to be used for EMSA.

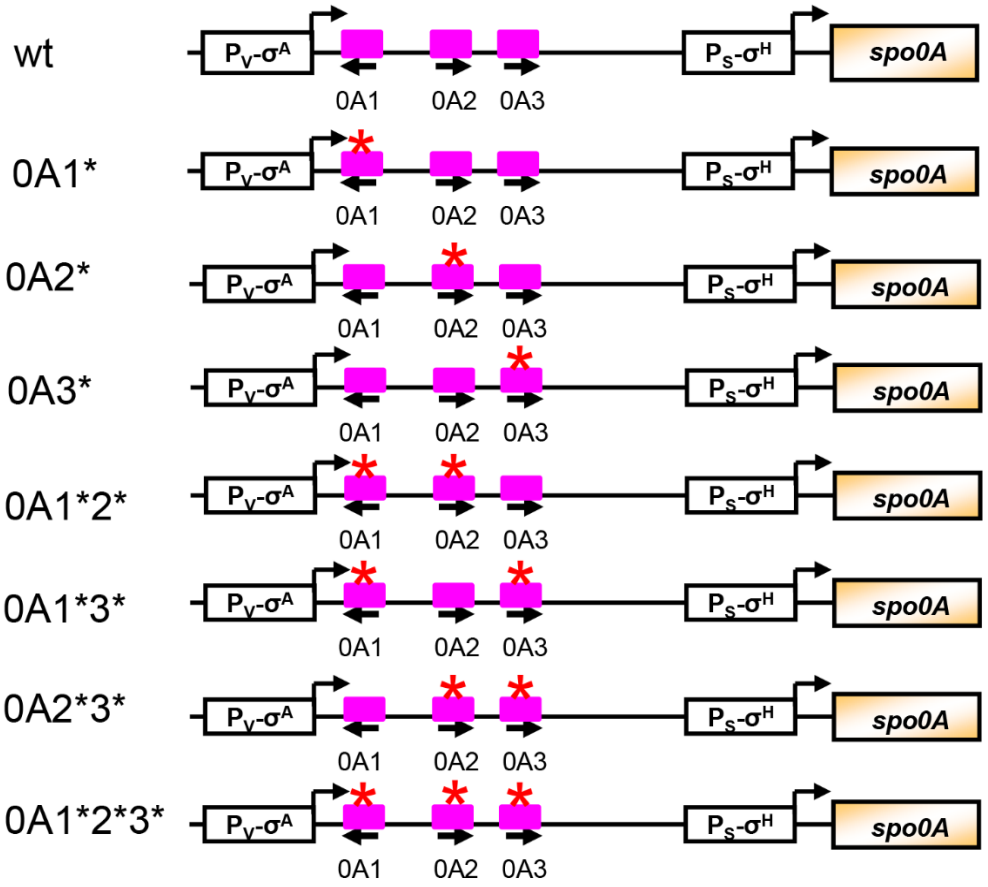


**Figure II-2. Schematic description of constructs with non-mutated and mutated 0A boxes in the *spo0A* promoter region.**
The upstream region of *spo0A* comprising of two promoters $P_V$ ($\sigma^A$-controlled, growth phase promoter) and $P_S$ ($\sigma^H$-controlled, stationary/sporulation phase promoter) is shown. The three 0A boxes on which the study focuses are shown (pink). The asterisk (red) on top of each 0A box denotes the mutation of that 0A box in the *spo0A* promoter region.

**Figure II-3. Electrophoretic mobility shift assays (EMSA) of the 0A~P bindings to the 0A boxes in the *spo0A* promoter region.**

(A) Results of Spo0A~P binding to wild-type and mutated *spo0A* promoter fragments as detected by EMSA. *Spo0A* promoter fragments (221 bp) containing all 0A-boxes (lane 1-6), 0A3* (lane 7-12), 0A1* (lane 13-18), 0A2* (lane 19-24), 0A2*3* (lane 25-30), 0A1*3* (lane 31-36), 0A1*2* (lane 37-42), 0A1*2*3* (lane 43-48) were amplified by PCR using primers (5' end labeled omf18 and omf117). Purified Spo0A was phosphorylated by $KinC^{\Delta TM1+2}$ in the presence of ATP. Varying concentrations of Spo0A~P (0 μM, lanes 1, 7, 13, 19, 25, 31, 37, and 43; 0.1 μM, lanes 2, 8, 14, 20, 26, 32, 38, and 44; 0.2 μM, lanes 3, 9, 15, 21, 27, 33, 39, and 45; 0.4 μM, lanes 4, 10, 16, 22, 28, 34, 40, and 46; 0.6 μM, lanes 5, 11, 17, 23, 29, 35, 41, and 47; 0.8 μM, lanes 6, 12, 18, 24, 30, 36, 42, and 48) were incubated with radiolabeled DNA and analyzed by 6% non-denaturing PAGE (see Materials and Methods). Free DNA (unbound and non-shifted) is indicated by white line. Bound (shifted) DNA is indicated by dashed lines.

(B) Relative levels of unbound DNA are plotted against different 0A~P concentrations.

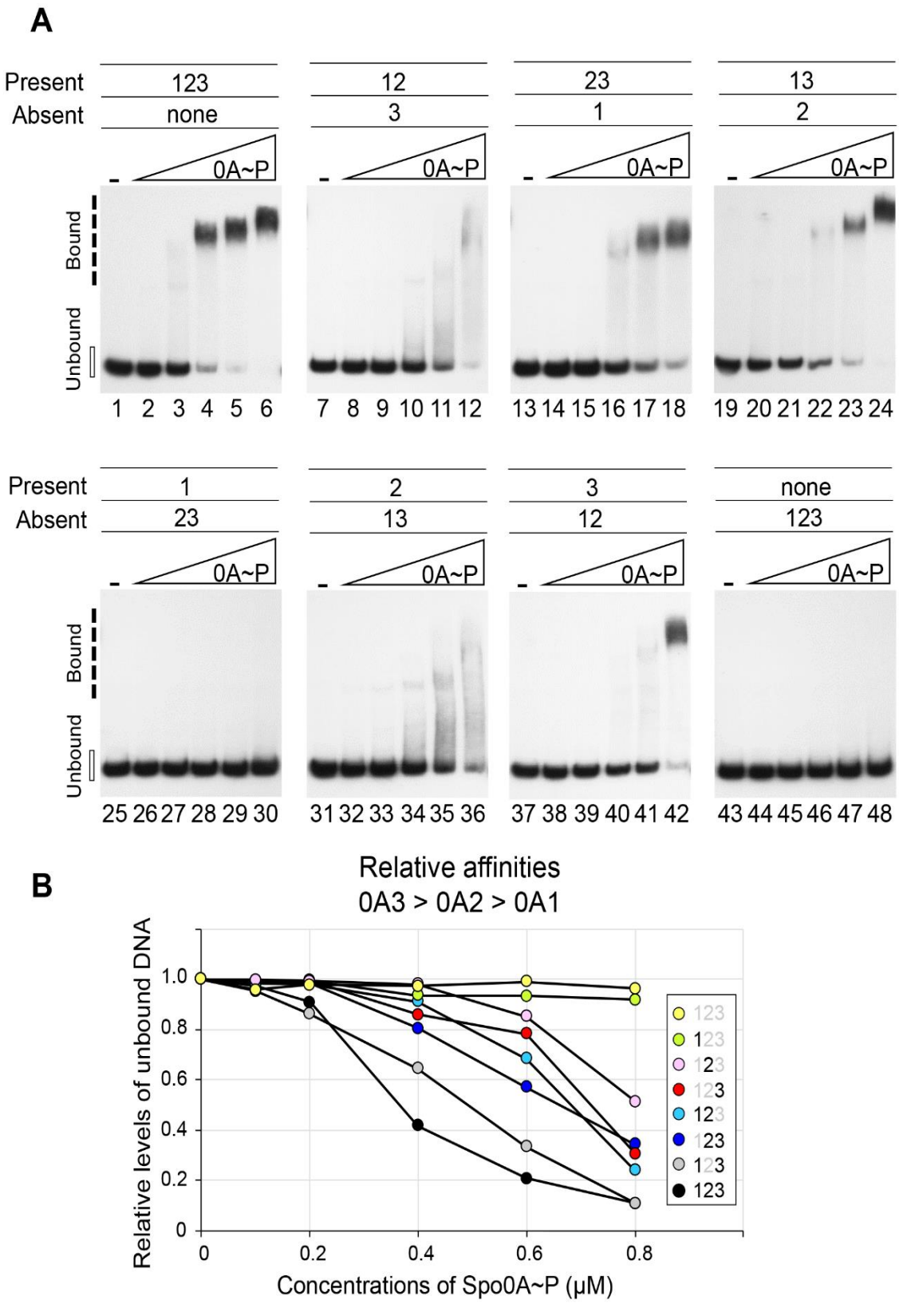
A
Present
Absent
123
none
12
3
23
1
13
2
1
23
2
13
3
12
none
123
0A~P
Bound
Unbound
1 2 3 4 5 6
7 8 9 10 11 12
13 14 15 16 17 18
19 20 21 22 23 24
25 26 27 28 29 30
31 32 33 34 35 36
37 38 39 40 41 42
43 44 45 46 47 48
B
Relative affinities
0A3 > 0A2 > 0A1
Relative levels of unbound DNA
1.0
0.8
0.6
0.4
0.2
0
0
0.2
0.4
0.6
0.8
Concentrations of Spo0A~P (μM)
123
123
123
123
123
123
123

Figure II-3 shows results from the Electrophoretic mobility shift assays for 0A~P binding to the three 0A boxes in the spo0A promoter region. When 0A~P concentration was increased, a discrete shifted band was observed in the wild type sequence (Figure II-3A lanes 4-6). This discrete shifted band disappeared when the 0A3 box was mutated (Figure II-3A lanes 10-12). When the 0A1 box was mutated, the discrete shifted band was still observed similar to wild type, but there was a slight difference in the unbound DNA pattern (Figure II-3A lanes 16-18). Upon mutating the 0A2 box, most of the discrete shifted bands disappeared and were only visible at the highest 0A~P concentration (Figure II-3A lanes 22-24).

In order to get a clear idea of the relative affinities of the 0A~P to three 0A boxes, double mutants data needs to be observed. When 0A1 and 0A3 boxes were mutated (i.e. only 0A2 present), the shifted bands showed a smear pattern at higher 0A~P concentrations (Figure II-3A lanes 34-36). When 0A1 and 0A2 boxes were mutated (i.e. only 0A3 present), a discrete shifted band was observed at the highest 0A~P concentration (Figure II-3A lanes 40-42). Upon mutating 0A2 and 0A3 boxes (i.e. only 0A1 present), there were no visible shifted bands (Figure II-3A lanes 25-30). Finally, when all three 0A boxes were mutated (0A1*2*3*), there was no shift in the DNA bands (Figure II-3A lanes 43-48). Thus the binding of 0A~P was abolished in this mutant DNA fragment. On close inspection of the EMSA images (Figure II-3), we can speculate the relative affinities to be 0A3>0A2>0A1.

Since the shifted pattern observed in 0A2*3* and 0A1*2*3* mutants was almost similar, we wanted to verify the binding of 0A~P to the 0A1 box. For this purpose, I performed another set of EMSA with increased 0A~P concentrations.

II.iii.2 Weaker binding of 0A~P to 0A1 box in the *spo0A* promoter region

As described above, in order to verify the binding of 0A~P to the 0A1 box, I conducted another set of EMSA using higher concentrations of 0A~P than previously used. Figure II-4 shows the results from the EMSA with higher 0A~P concentrations. Discrete shifted bands were observed as before, in the wild type *spo0A* promoter fragment with all the 0A boxes present (Figure II-4A lanes 5-10). Upon increasing 0A~P concentrations than before, we saw a smear pattern in the shifted bands of 0A2*3* mutant (i.e. only 0A1 present) (Figure II-4A lanes 17-20). This smear pattern was also observed in the last two lanes (Figure II-4A lanes 29 & 30) of the 0A1*2*3* mutant (all 0A boxes mutated). Since all the 0A boxes were mutated in this strain, the shift can be considered as non-specific binding. This non-specific binding was also observed in the last two lanes of the 0A2*3* mutant (Figure II-4A lanes 19 & 20). Nevertheless, the shifted smear pattern increased in the presence of the 0A1 box, indicating a binding to the 0A1 box.

Since this binding was only observed at higher concentrations, it suggests that 0A~P binding to 0A1 box is the weakest compared to the other two 0A boxes. The graphs in Figure II-4B also corroborate this data. The relative levels of unbound DNA were lower in the presence of 0A1 box (0A2*3* mutant) in comparison with the 0A1*2*3* mutant. Additionally, the relative levels of bound DNA were higher in the 0A2*3* mutant (in presence of 0A1 box) than the 0A1*2*3* mutant, which suggests a weaker but still existing binding of 0A~P to the 0A1 box.

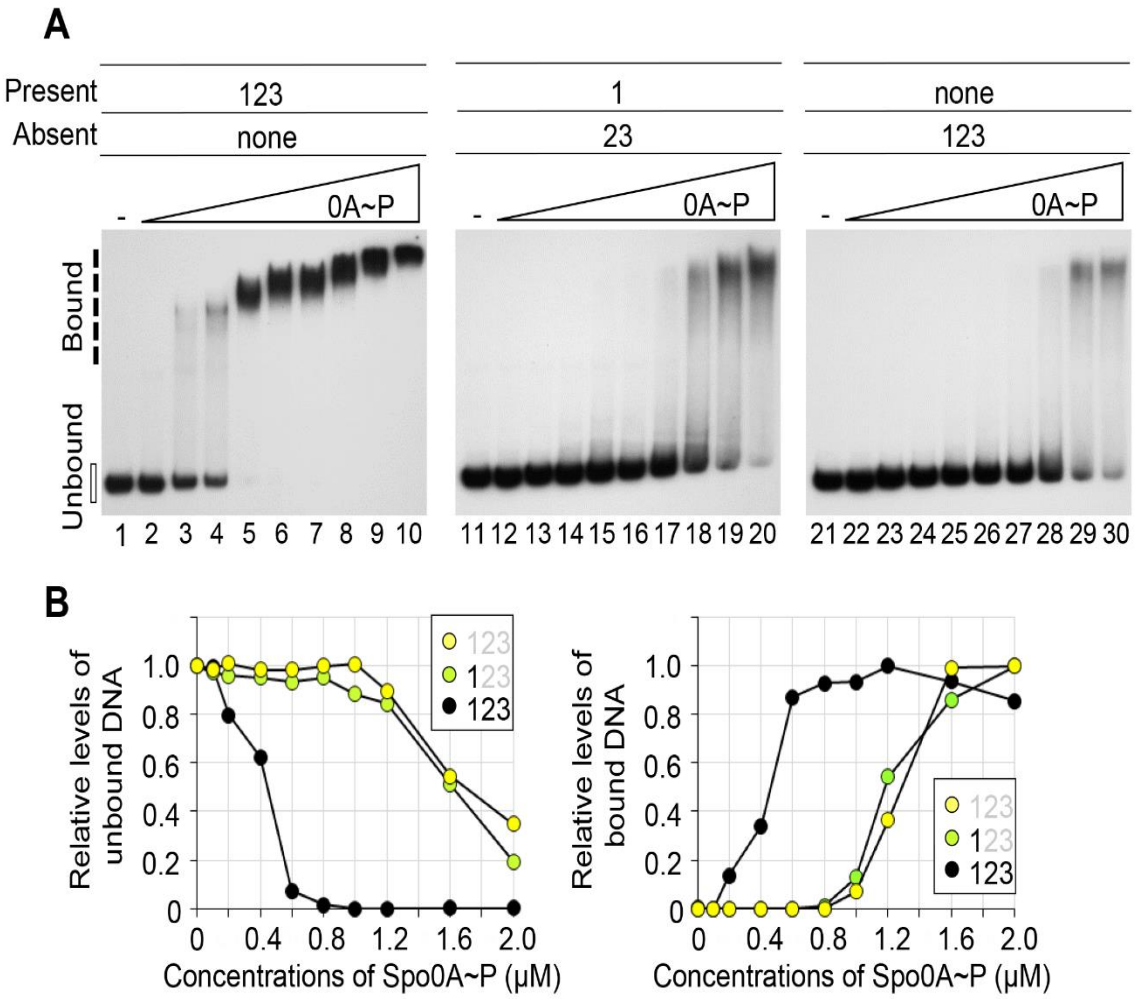


**Figure II-4. Electrophoretic mobility shift assays (EMSA) of the 0A~P bindings to the 0A boxes in the wild type, 0A2*3*, and 0A1*2*3* mutants.**

(A) Results of 0A~P binding to wild-type, 0A2*3*, and 0A1*2*3* as detected by EMSA. *spo0A* promoter fragments (221 bp) containing all 0A-boxes (lane 1-10), 0A2*3* (lane 11-20), 0A1*2*3* (lane 21-30) were amplified by PCR using primers (5' end-labeled omf18 and omf117). Purified Spo0A was phosphorylated by KinC$^{\Delta TM1+2}$ in the presence of ATP. Varying concentrations of Spo0A~P (0 μM, lanes 1, 11, and 21; 0.1 μM, lanes 2, 12, and 22; 0.2 μM, lanes 3, 13, and 23; 0.4 μM, lanes 4, 14, and 24; 0.6 μM, lanes 5, 15, and 25; 0.8 μM, lanes 6, 16, and 26; 1.0 μM, lanes 7, 17 and 27; 1.2 μM, lanes 8, 18 and 28; 1.6 μM, lanes 9, 19 and 29; 2.0 μM, lanes 10, 20 and 30) were incubated with radiolabeled DNA and analyzed by 6% non-denaturing PAGE (see Materials and Methods). Free DNA (unbound and non-shifted) is indicated by a white line. Bound (shifted) DNA is indicated by dashed lines.

(B) Relative levels of unbound DNA are plotted against varying Spo0A~P concentrations, on the left graph. Whereas, relative levels of bound DNA are plotted against varying Spo0A~P concentrations, on the right-hand side.

II.iii.3 0A box mutated *spo0A* promoters show different activities under sporulation and biofilm conditions

In order to determine the transcriptional activities of the 0A box mutated promoters, β-galactosidase assays were performed. For this purpose, *lacZ* gene was transcriptionally fused to wild type and 0A box mutated *spo0A* promoters. Apart from 0A box mutant strains, we also constructed $P_S$-*spo0A* strain, which had $P_V$ deletion (PΔV). These wild type and mutated *Pspo0A-lacZ* strains were cultured in liquid DSM (sporulation conditions) and MSgg (biofilm conditions). Then, cells were collected periodically and assayed for β-galactosidase activities (Figure II-5B, II-5C). As expected, β-galactosidase activities varied in DSM (sporulation) and MSgg (biofilm conditions). Under sporulation promoting conditions (DSM), β-galactosidase activity from *spo0A* promoters peaked at T4 (4 hrs. after the start of cultures) and declined at later time points (Figure II-5B). The highest transcriptional activity was observed in strain harboring mutation in the 0A2 box of *spo0A* promoter, under sporulation conditions. Since binding of 0A~P to 0A2 box causes repression of $P_S$ promoter, a de-repression is observed after mutating 0A2 box. Mutations in the 0A3 box of the *spo0A* promoter, resulted in lower transcriptional activities, confirming the role of 0A~P to 0A3 box in the activation of $P_S$ promoter of *spo0A*. Role of 0A3 box in the activation of $P_S$ promoter of spo0A was also evident upon the comparison of the transcriptional activities by 0A1*2*, 0A2*3*, and 0A1*3* double mutants. Among the above mentioned mutant strains, 0A1*2* mutant showed the highest activity, which dropped upon mutation of the 0A3 box in 0A2*3* and further lowered on mutating 0A1 along with 0A3.

**Figure II-5. β-Galactosidase assays measuring the transcriptional activity from wild type and mutated *spo0A* promoters under DSM and MSgg.**
(A) Schematic diagram of wild type and mutated *spo0A* promoters fused transcriptionally to the *lacZ* gene for measuring the β-galactosidase activity. Note that the superscripted x denotes the 0A box mutations in the promoter region. The β-galactosidase activity was measured in strains with wild type or mutated *spo0A* promoters fused transcriptionally to the *lacZ* gene. β-galactosidase samples were collected from cells grown in (B) DSM (sporulation media) or (C) Msgg (Biofilm media) at indicated time points. T2-T10 indicates 2-10 hours after the start of culture in both DSM and MSgg.

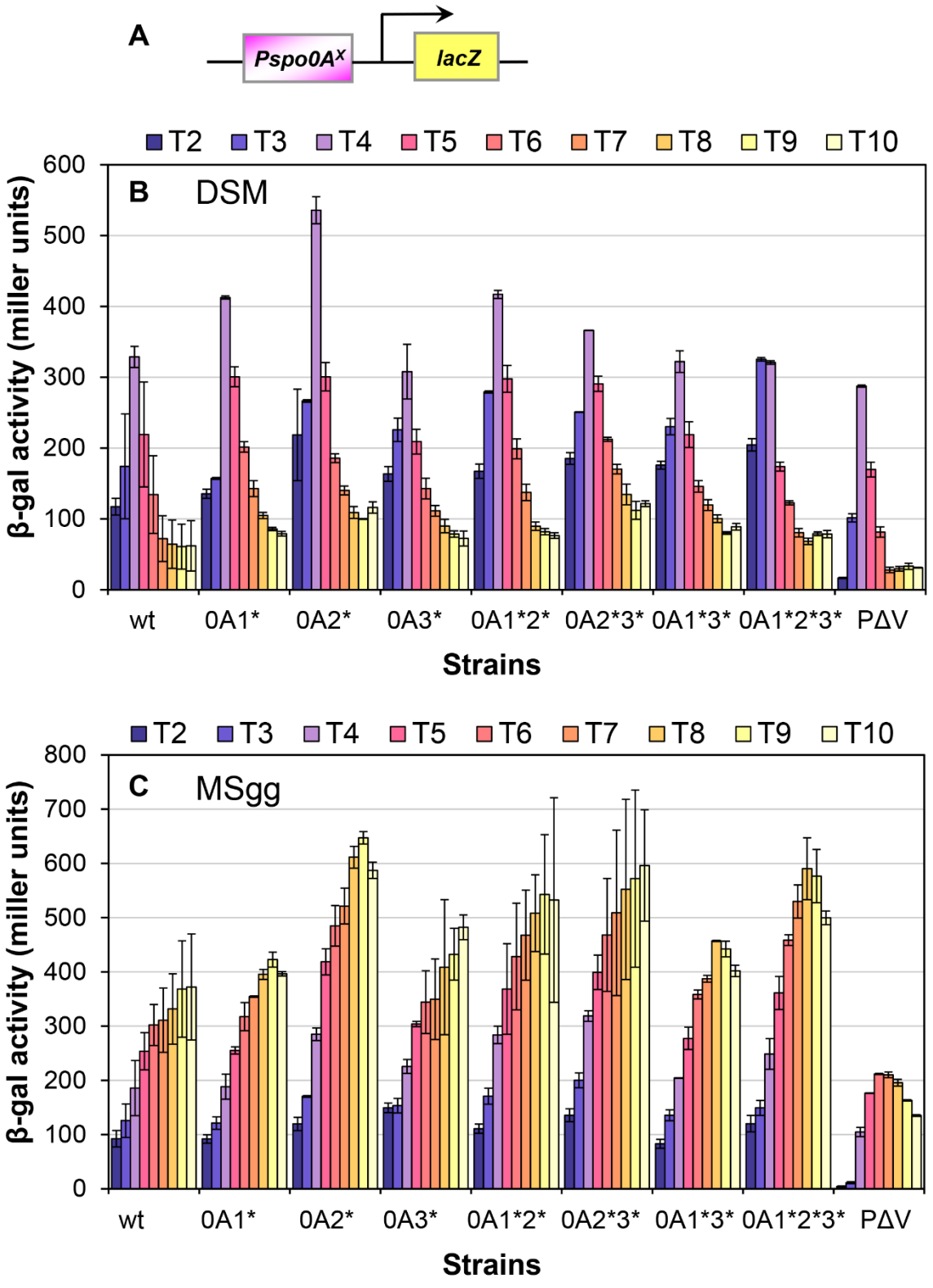
A
Pspo0A^X
lacZ
T2 T3 T4 T5 T6 T7 T8 T9 T10
B DSM
β-gal activity (miller units)
0
100
200
300
400
500
600
wt
0A1*
0A2*
0A3*
0A1*2*
0A2*3*
0A1*3*
0A1*2*3*
PΔV
Strains
T2 T3 T4 T5 T6 T7 T8 T9 T10
C MSgg
β-gal activity (miller units)
0
100
200
300
400
500
600
700
800
wt
0A1*
0A2*
0A3*
0A1*2*
0A2*3*
0A1*3*
0A1*2*3*
PΔV
Strains

Under DSM conditions, a strain harboring a deletion of $P_V$ promoter (PΔV), showed lower transcriptional activity than wild type promoter, and the activity further reduced at later time points. Under biofilm promoting conditions (MSgg), the strains showed a gradual increase in the *spo0A* transcriptional activities (Figure II-5C). The strain with the 0A2 box mutated showed the highest transcriptional activities at every sampling time point. Whereas, the strain with a deletion of $P_V$ promoter (PΔV), showed the lowest transcriptional activities amongst all the strains. Interestingly, the peak activity of PΔV shifted earlier than other strains and a gradual decline was visible at the later time points in this strain. The strain harboring all three 0A box mutations showed increased activity than wild type promoter, under both sporulation (DSM) and biofilm (MSgg) conditions, suggesting that the negative regulation by the 0A boxes plays a crucial role in *spo0A* transcription.

II.iii.4 0A box mutated *spo0A* promoter activities vary distinctly in Δ*kinA* and Δ*kinC* knockout strains

For elucidating the role of the two kinases, KinA and KinC in the *spo0A* transcription through phosphorelay, I studied the *spo0A* transcriptional activities in the 0A box mutated promoter strains in the kinase knockout backgrounds. Figure II-6BC and Figure II-7BC show the transcriptional activities of the 0A box mutated *spo0A* promoters under sporulation (DSM) and biofilm (MSgg) conditions, in the absence of *kinA* and *KinC*, respectively. In the absence of *kinA*, the transcriptional activity varied drastically under both DSM and MSgg conditions (Figure II-6).

Transcriptional activities remained elevated at later time points in the *kinA* deletion strains (ΔA) under DSM conditions (Figure II-6B). Interestingly, the strain with all three 0A boxes mutated showed highest transcriptional activity in DSM under ΔA background (Figure II-6B). Transcriptional activity of PΔV ($P_V$ promoter deletion) was the lowest under DSM condition. On the other hand, under MSgg conditions, transcriptional activity of PΔV was higher than the wild type and some other mutants (Figure II-6C). The strain with the 0A2 box mutated showed the highest transcriptional activity under the MSgg conditions. Under the *ΔkinA* background, the peak transcriptional activities of the mutants varied in both DSM and MSgg conditions (Figure II-6BC).

Strains with *kinC* deletion (ΔC) background under DSM conditions, showed earlier shift in the peak activity and lower activity at later time points when compared to the wild type background strains (Figure II-5B and II-7B). 0A2 box mutated promoter showed the highest transcriptional activity in ΔC background under the DSM conditions. The transcriptional activity of PΔV ($P_V$ promoter deletion) was the lowest under DSM and MSgg condition (Figure II-7BC). Similar to DSM, peak activities shifted earlier in the strains with *kinC* deletion (ΔC) under MSgg conditions (Figure II-7C). Interestingly, under MSgg conditions, strain with 0A1, 0A2, and 0A3 mutated (0A1*2*3*) showed the highest transcriptional activity with *kinC* deletion (ΔC) (Figure II-7C). Moreover, under MSgg conditions, in ΔC background, the transcriptional activities of 0A1*3* and 0A1*2*3* showed constant climb, while other mutant activities peaked and gradually declined after five to six hours (Figure II-7C).

**Figure II-6. β-Galactosidase assays measuring the transcriptional activity from wild type and mutated *spo0A* promoters under DSM and MSgg in Kinase A (*kinA*) deletion background strains**

(A) Schematic diagram of wild type and mutated *spo0A* promoters fused transcriptionally to the *lacZ* gene in a strain which has *kinA* deletion for measuring the β-galactosidase activity. Note that the superscripted x denotes the 0A box mutations in the promoter region. β-galactosidase activity was measured in *kinA* deletion strains with wild type or mutated *spo0A* promoters fused transcriptionally to the *lacZ* gene. The β-galactosidase samples were collected from cells grown in (B) DSM (sporulation media) or (C) MSgg (Biofilm media) at indicated time points. T2-T10 indicates 2-10 hours after the start of culture in both DSM and MSgg.

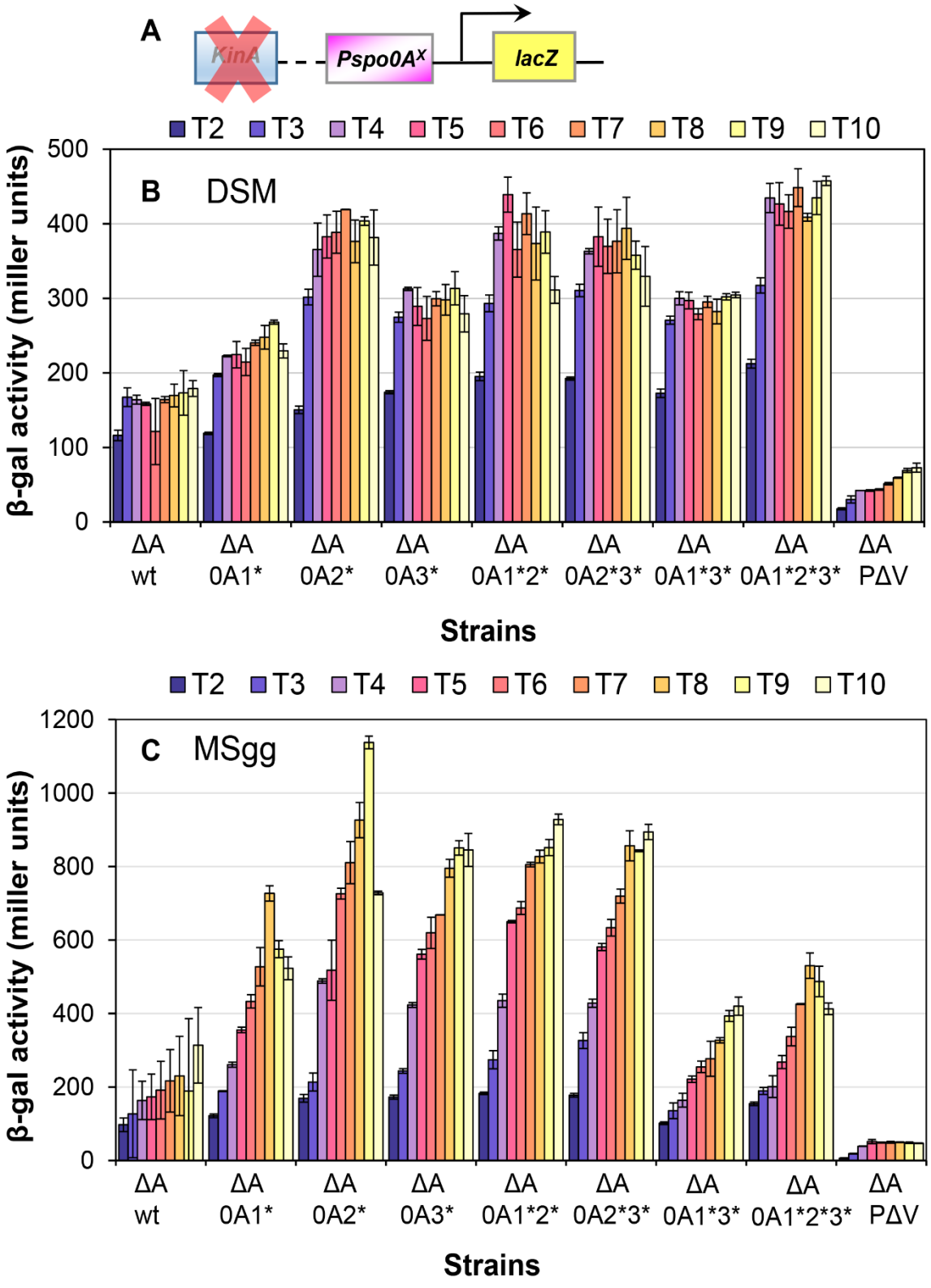
A
KinA
Pspo0A^X
lacZ
T2 T3 T4 T5 T6 T7 T8 T9 T10
B DSM
β-gal activity (miller units)
0
100
200
300
400
500
ΔA wt
ΔA 0A1*
ΔA 0A2*
ΔA 0A3*
ΔA 0A1*2*
ΔA 0A2*3*
ΔA 0A1*3*
ΔA 0A1*2*3*
ΔA PΔV
Strains
T2 T3 T4 T5 T6 T7 T8 T9 T10
C MSgg
β-gal activity (miller units)
0
200
400
600
800
1000
1200
ΔA wt
ΔA 0A1*
ΔA 0A2*
ΔA 0A3*
ΔA 0A1*2*
ΔA 0A2*3*
ΔA 0A1*3*
ΔA 0A1*2*3*
ΔA PΔV
Strains

**Figure II-7. β-Galactosidase assays measuring the transcriptional activity from wild type and mutated *spo0A* promoters under DSM and MSgg in Kinase C (kinC) deletion background strains**

(A) Schematic diagram of wild type and mutated *spo0A* promoters fused transcriptionally to the *lacZ* gene in a strain which has *kinC* deletion for measuring the β-galactosidase activity. Note that the superscripted x denotes the 0A box mutations in the promoter region. The β-galactosidase activity was measured in *kinC* deletion strains with wild type or mutated *spo0A* promoters fused transcriptionally to the *lacZ* gene. β-galactosidase samples were collected from cells grown in (B) DSM (sporulation media) or (C) Msgg (Biofilm media) at indicated time points. T2-T10 indicates 2-10 hours after the start of culture in both DSM and MSgg.

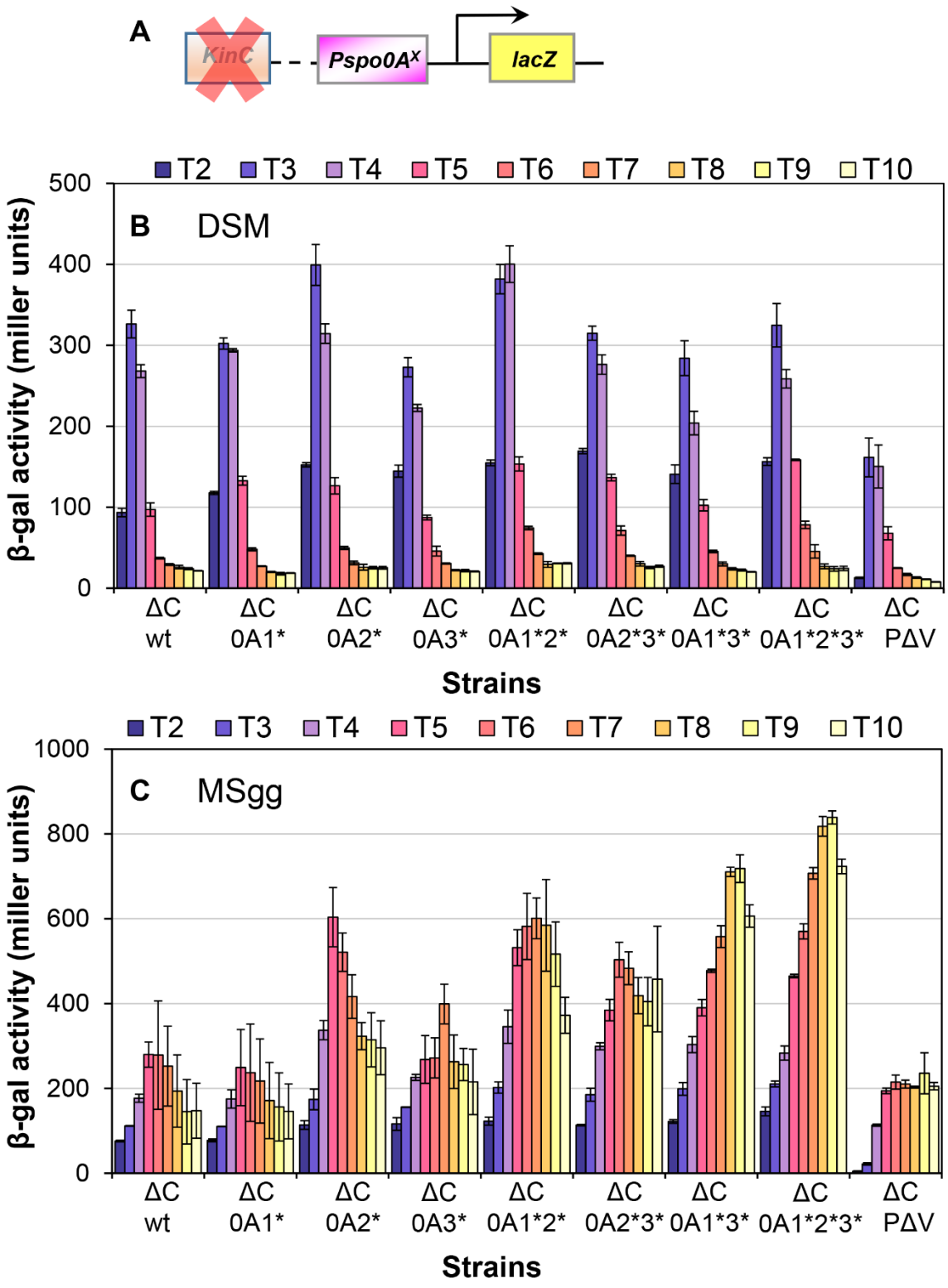
A
KinC
Pspo0A^X
lacZ
B DSM
T2 T3 T4 T5 T6 T7 T8 T9 T10
β-gal activity (miller units)
0
100
200
300
400
500
ΔC wt
ΔC 0A1*
ΔC 0A2*
ΔC 0A3*
ΔC 0A1*2*
ΔC 0A2*3*
ΔC 0A1*3*
ΔC 0A1*2*3*
ΔC PΔV
Strains
C MSgg
T2 T3 T4 T5 T6 T7 T8 T9 T10
β-gal activity (miller units)
0
200
400
600
800
1000
ΔC wt
ΔC 0A1*
ΔC 0A2*
ΔC 0A3*
ΔC 0A1*2*
ΔC 0A2*3*
ΔC 0A1*3*
ΔC 0A1*2*3*
ΔC PΔV
Strains

II.iii.5 Homology search shows that the *spo0A* promoter organization is conserved among *Bacillus* species, but not among pathogenic spore formers.

Spo0A is the transcriptional regulator that is activated through a multi-component phosphorelay in *Bacillus subtilis* (Burbulys et al., 1991; Trach et al., 1991). Orthologues of Spo0A have been found in a variety of firmicutes, including *Bacillus spp*. and *Clostridium spp* (Sauer, Santangelo, Treuner, Buchholz, & Durre, 1995). In order to study the promoter organization of *spo0A* in other firmicutes, especially among the pathogenic variety, I carried out the homology search using bioinformatics tools. I started by performing a BLAST search using the NCBI website (Johnson et al., 2008). Several *Bacillus spp.* and *Bacillus subtilis subsp.* showed similarity with the *spo0A* upstream (238bp upstream from the start codon) promoter region. Few of those selected candidates are listed in the upper panel of Table II-5. Following that, I compared the upstream and coding region of *spo0A* in *Bacillus subtilis* with certain pathogenic spore formers listed in the bottom panel of Table II-5. The individual comparison was done using pairwise sequence alignment from EMBOSS water by EMBL-EBI (Madeira, Madhusoodanan, et al., 2019). Figure II-8 shows the sequence alignment in *Bacillus subtilis* and the various pathogenic spore formers from *Bacillus* and *Clostridium sp*. The *spo0A* gene in *Bacillus subtilis* has two promoters, $P_V$ promoter (-35 and -10 regions for the $\sigma^A$-RNAP) and $P_S$ promoter (-35 and -10 regions for the $\sigma^H$-RNAP). Other *Bacillus* pathogenic species and several *Clostridium* spp. showed similar organization of the two promoters, although the sequences were not conserved (Table II-5 and Figure II-8).

**Table II-5. Sequence homology for the upstream and coding region of *spo0A***

| | | Identity to *spo0A* in *B. subtilis* 168 | | | | | |
|---|---|---|---|---|---|---|---|
| | | Nucleotides | | | | | Amino acids |
| ***Bacillus* species** | **Accession number** | **0A boxes[1]** | **$\sigma^{A2}$** | **$\sigma^{H3}$** | **Upstream region[6]** | **Coding region[7]** | **Coding region[8]** |
| *Bacillus sp. KBS0812* | CP041757.1 | 100% | 100% | 100% | 100% | 100% | 100% |
| *Bacillus vallismortis strain DSM 11031* | CP026362.1 | 100% | 100% | 100% | 99% | 94% | 100% |
| *Bacillus cereus MBGJa3* | CP026523.1 | 100% | 100% | 100% | 99% | 96% | 100% |
| *Bacillus gibsonii FJAT-10019* | CP017070.1 | 100% | 100% | 100% | 100% | 99% | 100% |
| *Bacillus subtilis subsp. natto strain BEST 195* | CP014471.1 | 100% | 100% | 100% | 100% | 100% | 100% |
| *Bacillus sp. BSn5* | CP002468.1 | 100% | 100% | 100% | 100% | 99% | 100% |
| *Bacillus subtilis subsp. spizizenii SW83* | CP030925.1 | 100% | 100% | 100% | 100% | 99% | 100% |
| *Bacillus intestinalis strain T30* | CP011051.1 | 100% | 100% | 100% | 99% | 97% | 100% |
| *Bacillus tequilensis EA-CB0015* | CP048852.1 | 100% | 100% | 100% | 99% | 96% | 100% |
| **Pathogenic spore formers** | **Accession number** | **0A boxes** | **$\sigma^{A4}$** | **$\sigma^{H5}$** | **Upstream region** | **Coding region** | **Coding region** |
| *Bacillus licheniformis ATCC 14580* | CP000002.3 | Not found | Found | Found | 71% | 80% | 97% |
| *Bacillus cytotoxicus NVH 391-98* | CP000764.1 | Not found | Found | Found | 51% | 71% | 88% |
| *Bacillus anthracis str. Ames* | AE016879.1 | Not found | Found | Found | 50% | 71% | 89% |
| *Bacillus thuringiensis serovar. Konkukian str. 97-27* | AE017355.1 | Not found | Found | Found | 48% | 71% | 89% |
| *Clostridioides difficile 630* | CP010905.2 | Not found | Found | Found | 51% | 59% | 71% |
| *Clostridium botulinum BKT015925* | CP002410.1 | Not found | Found | Found | 50% | 57% | 75% |
| *Clostridium perfringens ATCC 13124* | CP000246.1 | Not found | Found | Found | 52% | 58% | 75% |

0A boxes[1], 0A1: TCGACAA, 0A2: TTGTCAA, 0A3: AGTCGAA

$\sigma^{A2}$, TTCACT (-35) - 17 bp space - TAAAAT (-10)

$\sigma^{H3}$, in Bs, GAGGGTAT (-35) - 11 bp space - GTCGAAT (-10)

$\sigma^{A4}$, in Clostridium, TGGTAT (-35) - 17 bp space -TAAAAT (-10)

$\sigma H^{5}$, in Clostridium, GGAATA (-35) - 11 bp space - GTCGAAT (-10)

Upstream region[6], 238 bp from the start codon ATG

spo0A coding region[7], 804 bp in Bs

Spo0A coding region[8], 267 aa in Bs


**Figure II-8. Sequence alignment for the *spo0A* upstream region in the pathogenic spore-formers.**

0A boxes and start codons are highlighted in green and magenta, respectively. The consensus promoter for $\sigma^A$-RNAP (Blue) in *B. subtilis* is TTCACT in the -35 element and TAAAAT in the -10 element with 17 bp spacing between these two elements. The consensus promoter for $\sigma^H$-RNAP (Red) in *B. subtilis* is GAGGGTAT in the -35 element and GTCGAAT in the -10 element with 11 bp spacing between these two elements. The consensus promoter for $\sigma^A$-RNAP (Blue) in *Clostridium* species is TGGTAT in the -35 element and TAAAAT in the -10 element with 17 bp spacing between these two elements. The consensus promoter for $\sigma^H$-RNAP (Red) in *Clostridium* species is GGAGGAATA in the -35 element and GTCGAAT in the -10 element with 11 bp spacing between these two elements. Bs, *Bacillus subtilis*; Ba, *Bacillus anthracis* str. Ames; Bt, *Bacillus thuringiensis* serovar. Konkukian str. 97-27; Bl, *Bacillus licheniformis* ATCC 14580; Bcy, *Bacillus cytotoxicus* NVH 391-98; Cd, *Clostridioides difficile* 630; Cb, *Clostridium botulinum* BKT015925; Cp, *Clostridium perfringens* ATCC 13124.

In *Bacillus subtilis*, the *spo0A* promoter region contains two promoters, $P_V$ and $P_S$, respectively. The $P_V$ promoter is controlled by $\sigma^A$-RNAP and the $P_S$ promoter is controlled by $\sigma^H$-RNAP. These two promoters, along with the three 0A boxes are conserved among several *Bacillus spp*. listed in the upper panel of Table II-5. Although the 0A boxes were not found in other pathogenic *Bacillus* and *Clostridium spp.*, different promoter sequences for $\sigma^A$-RNAP and $\sigma^H$-RNAP were found in those pathogenic *spp.* (Figure II-8). This indicates that the promoter organization in these pathogenic *spp.* is not conserved.

The 2.4 and 4.2 regions on the RNAP encoding gene are indicated to interact with the -10 and -35 promoter recognition elements, respectively, in the promoter region of a gene (Lonetto, Gribskov, & Gross, 1992). Interestingly, when I compared the *sigA* (encoding $\sigma^A$-RNAP) and *sigH* (encoding $\sigma^H$-RNAP) genes in all the strains listed in Table II-5, I found that the 2.4 and 4.2 regions in these genes were conserved in the *Bacillus* strains examined (Figure II-9 and Figure II-10). Few residues were conserved in the *Clostridium spp*. studied and few conserved and semi-conserved substitutions were found (Figure II-9 and Figure II-10).

```
Bs     WWIRQAITRAIADQARTIRIPVHMVETINKLIRVQRQLLQDLGREPTPEEIAEDMDLTPEKVREILKIAQEPVSLETPIGEE 273
BcM    WWIRQAITRAIADQARTIRIPVHMVETINKLIRVQRQLLQDLGREPTPEEIAEDMDLTPEKVREILKIAQEPVSLETPIGEE 273
Bg     WWIRQAITRAIADQARTIRIPVHMVETINKLIRVQRQLLQDLGREPTPEEIAEDMDLTPEKVREILKIAQEPVSLETPIGEE 273
Bsk    WWIRQAITRAIADQARTIRIPVHMVETINKLIRVQRQLLQDLGREPTPEEIAEDMDLTPEKVREILKIAQEPVSLETPIGEE 273
Bv     WWIRQAITRAIADQARTIRIPVHMVETINKLIRVQRQLLQDLGREPTPEEIAEDMDLTPEKVREILKIAQEPVSLETPIGEE 273
Bsn5   WWIRQAITRAIADQARTIRIPVHMVETINKLIRVQRQLLQDLGREPTPEEIAEDMDLTPEKVREILKIAQEPVSLETPIGEE 273
BsnB   WWIRQAITRAIADQARTIRIPVHMVETINKLIRVQRQLLQDLGREPTPEEIAEDMDLTPEKVREILKIAQEPVSLETPIGEE 273
Bi     WWIRQAITRAIADQARTIRIPVHMVETINKLIRVQRQLLQDLGREPTPEEIAEDMDLTPEKVREILKIAQEPVSLETPIGEE 273
BtE    WWIRQAITRAIADQARTIRIPVHMVETINKLIRVQRQLLQDLGREPTPEEIAEDMDLTPEKVREILKIAQEPVSLETPIGEE 273
Bss    WWIRQAITRAIADQARTIRIPVHMVETINKLIRVQRQLLQDLGREPTPEEIAEDMDLTPEKVREILKIAQEPVSLETPIGEE 273
Bcy    WWIRQAITRAIADQARTIRIPVHMVETINKLIRVQRQLLQDLGREPTPEEIGEEMDLAPEKVREILKIAQEPVSLETPIGEE 275
Ba     WWIRQAITRAIADQARTIRIPVHMVETINKLIRVQRQLLQDLGREPSPEEIGEEMDLAPEKVREILKIAQEPVSLETPIGEE 275
Bt     WWIRQAITRAIADQARTIRIPVHMVETINKLIRVQRQLLQDLGREPSPEEIGEEMDLAPEKVREILKIAQEPVSLETPIGEE 275
Bl     WWIRQAITRAIADQARTIRIPVHMVETINKLIRVQRQLLQDLGREPTPEEIAEDMDLTPEKVREILKIAQEPVSLETPIGEE 273
Cd     WWIRQAITRAIADQARTIRIPVHMVETINKLIRVSRQLLQELGRDPKPEEIAKEMEMTEDKVREIMKIAQDPVSLETPIGEE 292
Cb     WWIRQAITRAIADQARTIRIPVHMVETINKLIRVSRQLLQELGREPQPEEIAKIMEMPVDKVREIMKIAQEPVSLETPIGEE 270
Cp     WWIRQAITRAIADQARTIRIPVHMVETINKLIRIQRQLVQELGRDPLPEELSKQMDMPVDKVREILKIAQEPVSLETPIGEE 268
       **************************************:.***:*:***:* ***:.: *::  :*****:****:***********

Bs     DDSHLGDFIEDQEATSPSDHAAYELLKEQLEDVLDTLTDREENVLRLRFGLDDGRTRTLEEVGKVFGVTRERIRQIEAKALR 355
BcM    DDSHLGDFIEDQEATSPSDHAAYELLKEQLEDVLDTLTDREENVLRLRFGLDDGRTRTLEEVGKVFGVTRERIRQIEAKALR 355
Bg     DDSHLGDFIEDQEATSPSDHAAYELLKEQLEDVLDTLTDREENVLRLRFGLDDGRTRTLEEVGKVFGVTRERIRQIEAKALR 355
Bsk    DDSHLGDFIEDQEATSPSDHAAYELLKEQLEDVLDTLTDREENVLRLRFGLDDGRTRTLEEVGKVFGVTRERIRQIEAKALR 355
Bv     DDSHLGDFIEDQEATSPSDHAAYELLKEQLEDVLDTLTDREENVLRLRFGLDDGRTRTLEEVGKVFGVTRERIRQIEAKALR 355
Bsn5   DDSHLGDFIEDQEATSPSDHAAYELLKEQLEDVLDTLTDREENVLRLRFGLDDGRTRTLEEVGKVFGVTRERIRQIEAKALR 355
BsnB   DDSHLGDFIEDQEATSPSDHAAYELLKEQLEDVLDTLTDREENVLRLRFGLDDGRTRTLEEVGKVFGVTRERIRQIEAKALR 355
Bi     DDSHLGDFIEDQEATSPSDHAAYELLKEQLEDVLDTLTDREENVLRLRFGLDDGRTRTLEEVGKVFGVTRERIRQIEAKALR 355
BtE    DDSHLGDFIEDQEATSPSDHAAYELLKEQLEDVLDTLTDREENVLRLRFGLDDGRTRTLEEVGKVFGVTRERIRQIEAKALR 355
Bss    DDSHLGDFIEDQEATSPSDHAAYELLKEQLEDVLDTLTDREENVLRLRFGLDDGRTRTLEEVGKVFGVTRERIRQIEAKALR 355
Bcy    DDSHLGDFIEDQEATSPADHAAYELLKEQLEDVLDTLTDREENVLRLRFGLDDGRTRTLEEVGKVFGVTRERIRQIEAKALR 357
Ba     DDSHLGDFIEDQEATSPADHAAYELLKEQLEDVLDTLTDREENVLRLRFGLDDGRTRTLEEVGKVFGVTRERIRQIEAKALR 357
Bt     DDSHLGDFIEDQEATSPADHAAYELLKEQLEDVLDTLTDREENVLRLRFGLDDGRTRTLEEVGKVFGVTRERIRQIEAKALR 357
Bl     DDSHLGDFIEDQEATSPSDHAAYELLKEQLEDVLDTLTDREENVLRLRFGLDDGRTRTLEEVGKVFGVTRERIRQIEAKALR 357
Cd     EDSHLGDFIPDDDAPAPAEAAAYSLLKEQIEDVLGSLNDREQKVLKLRFGLEDGRARTLEEVGKEFDVTRERIRQIEAKALR 374
Cb     EDSHLGDFIPDDEAPAPAEAAAFTMLKEQLINVLDTLTPREEKVLRLRFGLDDGRARTLEEVGKEFNVTRERIRQIEAKALR 352
Cp     EDSHLGDFIPDDDAPAPAEAAAFTMLKEQLINVLDTLTPREEKVLRLRFGLDDGRARTLEEVGKEFNVTRERIRQIEAKALR 350
       :******** *::* :*:: **: :****: :**.:*. **::**:*****:***:******* *.***************

Bs     KLRHPSRSKRLKDFLE 371
BcM    KLRHPSRSKRLKDFLE 371
Bg     KLRHPSRSKRLKDFLE 371
Bsk    KLRHPSRSKRLKDFLE 371
Bv     KLRHPSRSKRLKDFLE 371
Bsn5   KLRHPSRSKRLKDFLE 371
BsnB   KLRHPSRSKRLKDFLE 371
Bi     KLRHPSRSKRLKDFLE 371
BtE    KLRHPSRSKRLKDFLE 371
Bss    KLRHPSRSKRLKDFLE 371
Bcy    KLRHPSRSKRLKDFLE 373
Ba     KLRHPSRSKRLKDFLE 373
Bt     KLRHPSRSKRLKDFLE 373
Bl     KLRHPSRSKRLKDFLE 373
Cd     KLRHPSRSKKLRDYLD 390
Cb     KLRHPSRSKKLKDYLD 368
Cp     KLRHPSRSKKLKDYLD 366
       *********:*:*:*:
```

**Figure II-9. Alignment of the promoter-recognition regions (2.4 and 4.2) of $\sigma^A$ in *Bacillus* and *Clostridium* species.**

Regions 2.4 and 4.2 of *B. subtilis* $\sigma^A$ are highlighted in blue**.** The strains shown here are the same as in Table II-5. An asterisk (*) indicates a conserved residue, a colon (:) indicates a conserved substitution, and a period (.) indicates a semi-conserved substitution.

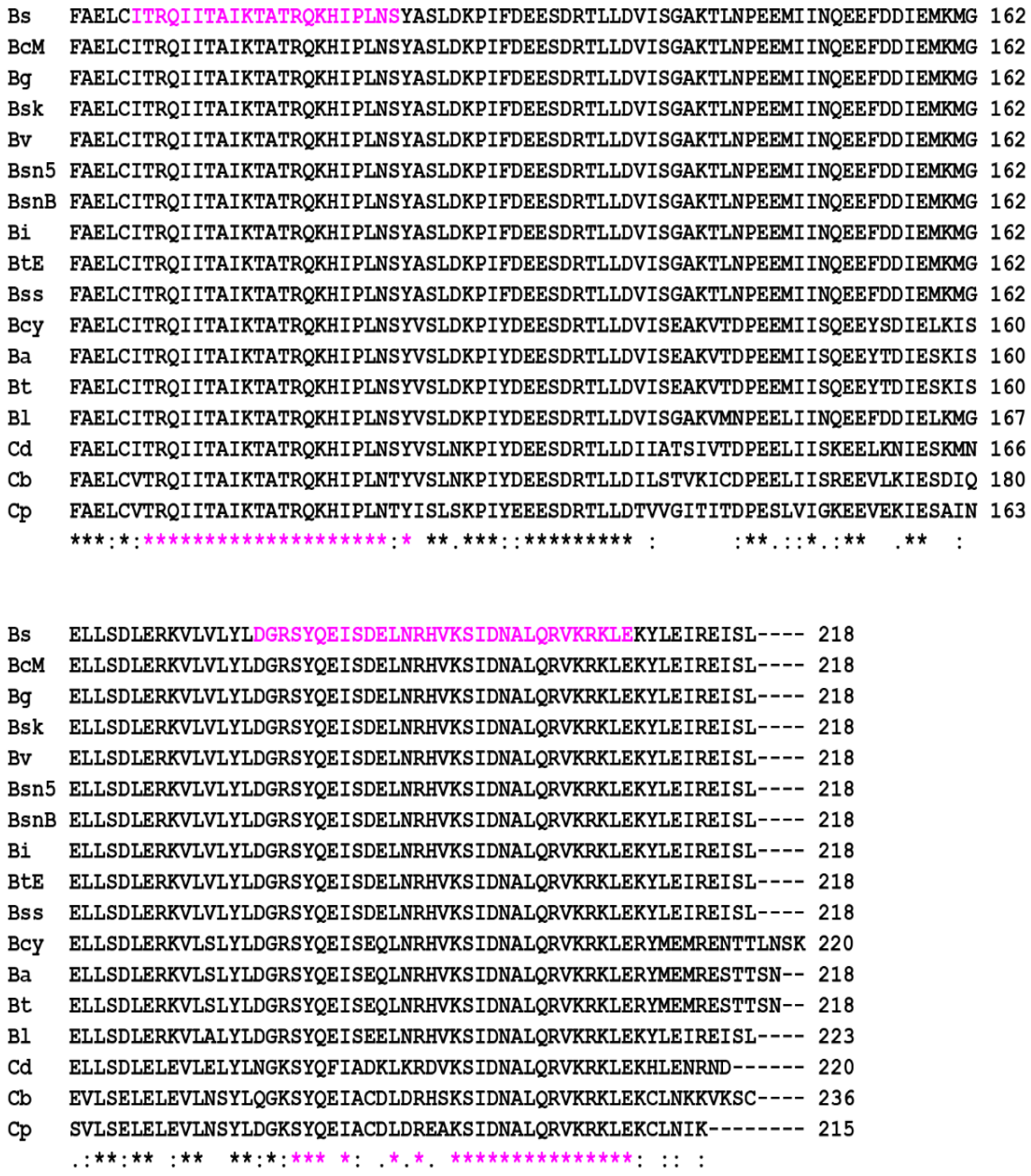


**Figure II-10. Alignment of the promoter-recognition regions (2.4 and 4.2) of $\sigma^H$ in *Bacillus* and *Clostridium* species.**

Regions 2.4 and 4.2 of *B. subtilis* $\sigma^H$ are highlighted in blue**.** The strains shown here are the same as in Table II-5. An asterisk (*) indicates a conserved residue, a colon (:) indicates a conserved substitution, and a period (.) indicates a semi-conserved substitution.

## II.iv Discussion

Spo0A, the transcriptional regulator of cell differentiation in *Bacillus subtilis* under environmental stress is activated via a multi-component phosphorelay cascade (Burbulys et al., 1991) (Trach et al., 1991). A gradual accumulation of Spo0A~P via the phosphorelay is essential for proper initiation of the cell differentiation pathways (Fujita & Losick, 2005) (Eswaramoorthy, Guo, & Fujita, 2009) (Vishnoi et al., 2013). Several positive and negative feedback loops help in maintaining the required levels of Spo0A. The concentration of phosphorelay components is very critical, and a higher concentration of one component acts as negative feedback to block the phosphorelay and ultimately, levels of 0A~P. Apart from these feedback loops, the level of 0A is also regulated by transcription from two different promoters, $P_V$ promoter ($\sigma^A$-controlled) transcribing relatively lower levels of 0A and $P_S$ promoter ($\sigma^H$-controlled) transcribing higher levels of 0A during the stationary phase of the cell cycle. Furthermore, 0A~P binding to 0A boxes in the promoter region of *spo0A* aids in *spo0A* transcription from either $P_V$ or $P_S$ promoter. It has been observed that the cell fate decision to choose a differentiation pathway; either biofilm or sporulation, depends majorly on the cellular levels of 0A~P and several other factors such as the kinases driving the phosphorelay.

In order to further study this phenomenon, I investigated the transcriptional control of *spo0A*, in this Chapter. For the extent of this dissertation, I focused on assessing the role of three 0A boxes on the expression patterns of *spo0A*. Through the electrophoretic mobility shift assay (EMSA), I provided fundamental

experimental evidence of 0A~P binding to the three 0A boxes in the upstream region of *spo0A* promoter with different binding affinities. This evidence helped us in further building the model for *spo0A* transcription (Figure II-11).

In order to study the biological role of these 0A boxes in *spo0A* transcription, I assayed the β-galactosidase activities of different 0A box mutated promoter fusion strains fused to *lacZ*. These assays were conducted in two different media specific for promoting sporulation (DSM) and promoting biofilms (MSgg). The wild type promoter showed a gradual rise in activity levels and peaked around four hours after the start of culture. After four hours, the activity levels gradually dropped under sporulation conditions (DSM), whereas under biofilm conditions (MSgg) wild type promoter strain activity levels continued to rise till the last time point of collection (ten hours after the start of culture). This trend has been observed several times in the *spo0A* experiments. Upon observation of the 0A box mutated promoter strains, the results corroborated with the 0A~P binding assays (EMSA) shown in this Chapter and are summarized in a *spo0A* transcription model shown in Figure II-11.

Over-induction of KinA and KinC have shown to promote sporulation under nutrient-rich and starvation conditions, however, KinC induction reduced the sporulation efficiency as compared to KinA induction (Eswaramoorthy et al., 2010) (Eswaramoorthy et al., 2009) (Vishnoi et al., 2013). Artificially inducing KinA or KinC using IPTG (isopropyl-β-D-thiogalactopyranoside) has also shown to increase the biofilm reporter activities in another experiment (unpublished data). In this chapter, I wanted to study the *spo0A* transcription activity in the absence of

*kinA* and *kinC* in the undomesticated (biofilm background) strain with or without mutated 0A boxes. Under sporulation conditions (DSM), the promoter activity stayed elevated or was derepressed at the later stages of culture, in the absence of *kinA*, suggesting a negative feedback regulation of 0A transcription through KinA. Under biofilm promoting conditions (MSgg), promoter activities in the absence of *kinA* were similar to the wild type background strains, except for the PΔV strain, which showed the least promoter activity in the absence of *kinA*. In the absence of KinA, the major kinase for sporulation, 0A~P does not reach its threshold level, and therefore there is no activation of $\sigma^H$. Since the $\sigma^H$ is inactive, there is no *spo0A* transcription from $P_S$ promoter, further keeping low levels of 0A. This explains the minimal activity from PΔV strain in the *kinA* knockout background.

In the absence of *kinC*, the promoter activity trends observed under the sporulation conditions (DSM), were similar to those observed in the wild type background strains. However, the activities were slightly lower at the later time points in the absence of *kinC*. Under biofilm promoting conditions (MSgg), promoter activities quickly peaked in the absence of *kinC*, the major biofilm kinase. These elevated promoter activities can lead to accelerated accumulation of 0A~P, which can cause abnormal activation or repression of either sporulation or biofilm formation.

To further study the conservation of the *spo0A* promoter organization, I utilized some bioinformatics tools for homology search. Firstly, the BLAST search of the *spo0A* upstream promoter region (238 bp from the start codon) showed similarity

with other *Bacillus spp*. and *Bacillus subtilis subsp*. Following that, certain pathogenic *Bacillus spp*. and *Clostridium spp*. were analyzed using multiple sequence alignment and pairwise sequence alignment tools from EMBL-EBI (Madeira, Madhusoodanan, et al., 2019) (Madeira, Park, et al., 2019). As shown in Figure II-8, all the pathogenic species consist of two promoters; one recognized by $\sigma^A$ and another by $\sigma^H$. Although, the promoter sequences in these pathogenic species are not conserved as in *Bacillus spp*. This might be due to the fact that the pathogenic bacteria share a different habitat (host organisms) as compared to the soil-dwelling *Bacillus spp*. Survival strategies are important for both the environmental and pathogenic spp., but the evolution might be separate since the habitats are varied.

Based on the transcriptional assays in two different conditions (Biofilm and sporulation) we have built a model for the transcriptional control of *spo0A*, which is illustrated in Figure II-11. According to this model, 0A~P binding to the three 0A boxes in the *spo0A* promoter region influences the *spo0A* transcription either from $P_V$ or $P_S$ promoter. During the early phases of starvation, KinC drives the phosphorelay, producing low levels of 0A~P. These 0A~P levels are not sufficient to repress AbrB, which represses several sporulation genes including sigma factor $\sigma^H$. Hence *spo0A* transcription continues from a relatively weak $P_V$ promoter driven by sigma factor $\sigma^A$. $P_V$ transcription might be affected by 0A~P binding to the 0A3 box. Slowly 0A~P levels increase, and after prolonged hours of starvation, KinA threshold is reached, driving the phosphorelay to produce more 0A~P. Readily available 0A~P binds to all the 0A boxes in the *spo0A* upstream region, as well as

depresses $\sigma^H$ (via AbrB repression). Transcription of *spo0A* now starts from the strong $P_S$ promoter driven by $\sigma^H$. At the same time, 0A~P binding to 0A1 box blocks *spo0A* transcription from the $P_V$ promoter.

**Figure II-11. Model illustrating the role of 0A boxes in the transcriptional control of *spo0A*.**

(A) Schematic representation of the *spo0A* promoter region. The $P_V$ and $P_S$ promoter recognition sites are shown in pink. Three 0A boxes are shown in green. Each of the 0A boxes was mutated (mutated sequence is shown in red) and binding affinity of 0A~P (with EMSA) was determined to be 0A3 > 0A2 > 0A1.

(B) During the early stages of starvation, phosphorelay is driven by KinC, producing low levels of 0A~P. $\sigma^H$ is repressed (blue downward arrow) by AbrB and hence transcription from $P_S$ is inactive (gray). $\sigma^A$ is active (red upward arrow) and weakly transcribes *spo0A* transcripts from $P_V$ promoter. Binding of 0A~P to 0A3 box might affect the $P_V$ transcripts.

(C) After a few hours of starvation, phosphorelay is still driven by KinC, 0A~P levels are intermediate and more 0A~P binds to different 0A boxes in the *spo0A* promoter region, according to the binding affinity. AbrB repression by 0A~P activates $\sigma^H$ (cyan upward arrow), and binding of 0A~P to the 0A3 box aids in *spo0A* transcription from the strong $P_S$ promoter.

(D) During prolonged starvation, the KinA threshold is reached, resulting in phosphorelay driven by KinA, producing high levels of 0A~P. $\sigma^H$ is now highly active (red upward arrow) and transcribing *spo0A* from $P_S$ promoter in high quantities. 0A~P, present in high levels, now binds to all the 0A boxes upstream of *spo0A*. Binding of 0A~P to 0A1 represses $P_V$ promoter (gray), along with a decreased $\sigma^A$ activity (blue downward arrow).

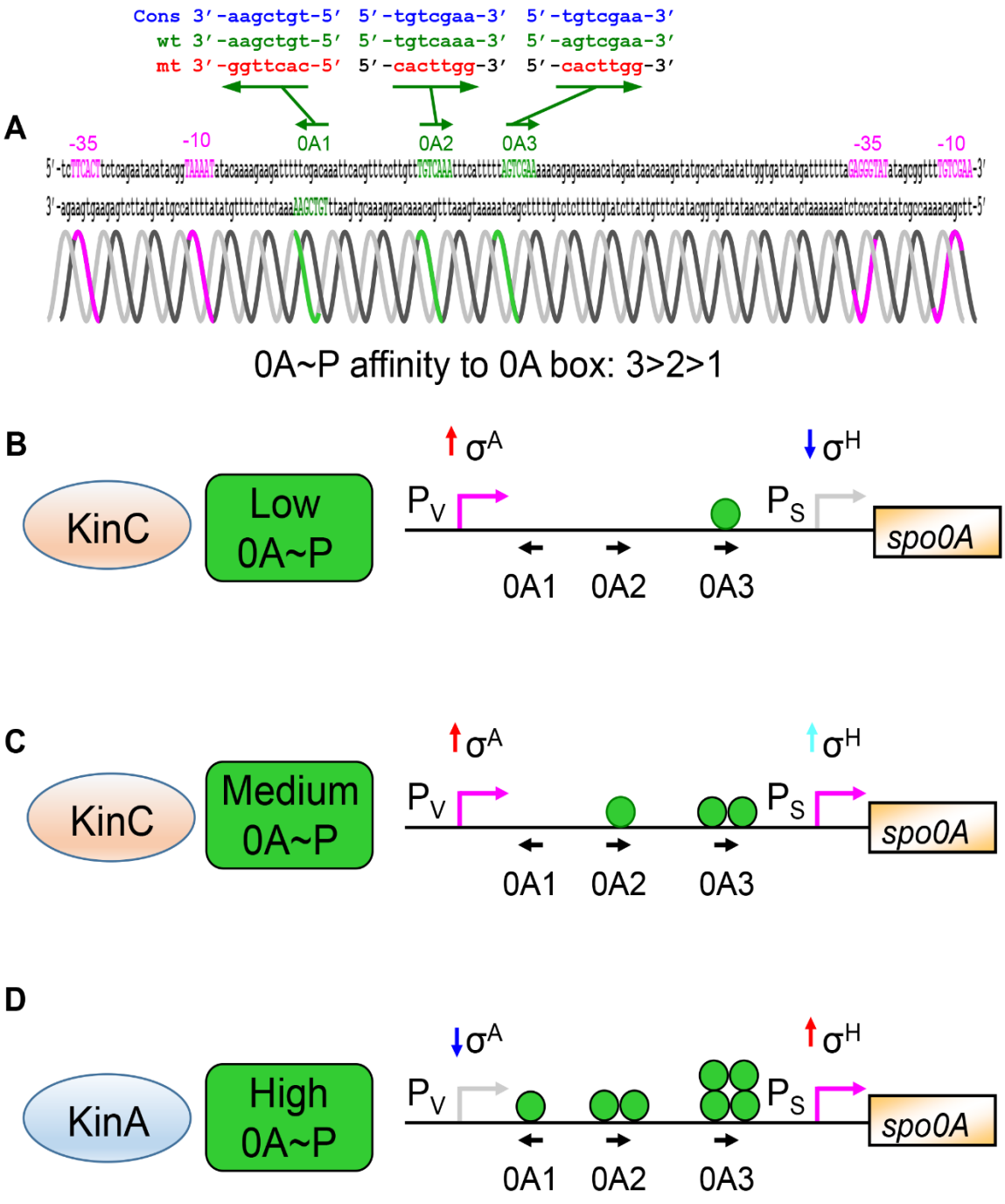
Cons 3′-aagctgt-5′ 5′-tgtcgaa-3′ 5′-tgtcgaa-3′
wt 3′-aagctgt-5′ 5′-tgtcaaa-3′ 5′-agtcgaa-3′
mt 3′-ggttcac-5′ 5′-cacttgg-3′ 5′-cacttgg-3′
A
-35
-10
0A1
0A2
0A3
-35
-10
0A~P affinity to 0A box: 3>2>1
B
KinC
Low 0A~P
σA
σH
PV
PS
spo0A
0A1
0A2
0A3
C
KinC
Medium 0A~P
σA
σH
PV
PS
spo0A
0A1
0A2
0A3
D
KinA
High 0A~P
σA
σH
PV
PS
spo0A
0A1
0A2
0A3

# Chapter III: Identification of a Spo0A Target Gene that Controls Forespore Engulfment, a Hallmark of Spore Morphogenesis

## III.i Introduction

*Bacillus subtilis*, a gram-positive soil-bacterium, is a highly studied model organism for cell differentiation. Upon experiencing prolonged starvation, this bacterium undergoes asymmetric division by forming a septum at one of the poles giving rise to two unequal sized compartments. The smaller compartment is called the forespore, and the larger compartment is called the mother cell. Sporulation is an energy-consuming process, and upon asymmetric (polar) septation, the cell commits to this process. Both the forespore and the mother cell have strictly controlled gene expression systems. Eventually, the forespore is engulfed by the mother cell compartment, in a phagocytic-like process which involves migration of the mother cell membranes around the forespore, generating a cell within a cell. Thus engulfment marks a point of no return for the starving *Bacillus* cells. Upon engulfment, the spore matures inside the mother cell and prepares for dormancy with the help of the mother cell. Eventually, the mother cell lyses, releasing the mature spore into the environment.

Spo0A is the master regulator for transcription of genes involved in sporulation. Spo0A is activated (phosphorylated) via a four-component phosphorelay involving a histidine-kinase (KinA, KinB, or KinC) and two phosphotransferases (Spo0F and Spo0B) participating in a his-asp-his-asp transfer cascade. When 0A~P reaches a certain threshold level, asymmetric cell division is triggered followed by activation of compartment-specific sigma factors in a Spatio-temporal manner. After asymmetric division, genes in the mother cell and the forespore compartment are specifically transcribed by $\sigma^E$ and $\sigma^F$ RNA polymerases, respectively (Haldenwang,

1995) (Kroos et al., 1999). Operons (*spoIIG* and *spoIIA*) including genes encoding $\sigma^E$ and $\sigma^F$ are also under the direct control of 0A~P (Molle et al., 2003). Transcription of *spoIIG* and *spoIIA* operons starts before the asymmetric division, gradually increases over the course of starvation, and spikes only in the mother cell compartment after the asymmetric division (Fujita et al., 2005; Fujita & Losick, 2003). These mother cell preferential transcriptions are controlled by the increasing abundance of 0A~P in the mother cell relative to the forespore compartment (Fujita & Losick, 2003).

It has also been demonstrated that, when the newly devised Spo0A inhibitor is expressed specifically in the mother cell compartment, sporulation becomes defective (Fujita & Losick, 2003). Thus, these results suggest that the mother cell-specific localization of 0A~P is essential for the completion of sporulation (Fujita & Losick, 2003).

The importance of this mother cell-specific 0A~P activity for the progression of sporulation has not been understood. Also, there have been no studies focusing on the 0A~P regulated mother cell-specific genes. In order to study these mechanisms, I perused the literature in search of a candidate gene regulated by 0A~P in the mother cell compartment. There is only one such mother cell specific gene, *spoIID*, detected via chromatin immunoprecipitation (chIP) assay to be under 0A~P control (Molle et al., 2003). The data from this study suggest that *spoIID* is a possible target of Spo0A and provide a potential clue to explore the importance of the mother cell-specific activation of Spo0A.

SpoIID is a membrane protein (Abanes-De Mello, Sun, Aung, & Pogliano, 2002; Gutierrez, Smith, & Pogliano, 2010) and forms a complex with SpoIIP (Frandsen & Stragier, 1995), and SpoIIM (Smith & Youngman, 1993) that are also transmembrane proteins. SpoIIM serves as a scaffold protein that facilitates complex formation with SpoIID (lytic transglycosylase) and SpoIIP (amidase/endopeptidase), leading to specific localization of DMP to the mother cell side of the septum (Abanes-De Mello et al., 2002; Morlot, Uehara, Marquis, Bernhardt, & Rudner, 2010). DMP complex is involved in peptidoglycan degradation during the engulfment process (Gutierrez et al., 2010). Enzymatic activities of each of DMP proteins become evident only upon the assembly of each protein into the DMP complex.

Figure III-1 provides an illustration of processes involved in the engulfment of forespore by the mother cell. The DMP proteins play a crucial role in the first step of engulfment, peptidoglycan degradation. This separates the septal peptidoglycan from the transverse peptidoglycan and helps in the movement of the mother cell membrane towards the forespore pole (Meyer, Gutierrez, Pogliano, & Dworkin, 2010) (Morlot et al., 2010). Once the septal peptidoglycan is degraded, new peptidoglycan is synthesized which gets sandwiched between the two membranes after the completion of the engulfment process. Peptidoglycan synthesis also facilitates the membrane migration of the mother cell. Another contributing factor is the zipper-like interaction between the forespore membrane proteins SpoIIQ and mother cell membrane protein SpoIIIAH, facilitated by GerM (Blaylock, Jiang, Rubio, Moran, & Pogliano, 2004; Rodrigues, Ramirez-Guadiana, Meeske, Wang,

& Rudner, 2016). SpoIIIAH is localized at the membrane and further recruits additional mother cell proteins (Doan & Rudner, 2007) (Fredlund, Broder, Fleming, Claussin, & Pogliano, 2013).

Out of the DMP protein-coding genes, *spoIID* alone has been detected to be a potential target of Spo0A (Molle et al., 2003), these findings allow us to hypothesize that Spo0A~P helps to regulate the $\sigma^E$-dependent expression of *spoIID* after asymmetric division, leading to the completion of forespore engulfment by the mother cell. However, there have been no detailed studies directly characterizing the effect of Spo0A on the expression of *spoIID*. The limitation of the study is mainly due to the lack of Spo0A mutations specifically blocking gene expression in the mother cell compartment, but not asymmetric division. Therefore, the physiological significance of 0A~P binding to the *spoIID* promoter region is unclear.

In the following chapter, I provide direct experimental evidence of the binding of 0A~P to the three 0A binding sites (0A boxes), in the *spoIID* promoter region. I further, characterize each of the 0A boxes through transcriptional studies on the reporter mutants and present a model for the regulation of 0A~P along with mother cell transcription factor $\sigma^E$ RNA polymerase and another DNA binding protein, SpoIIID.

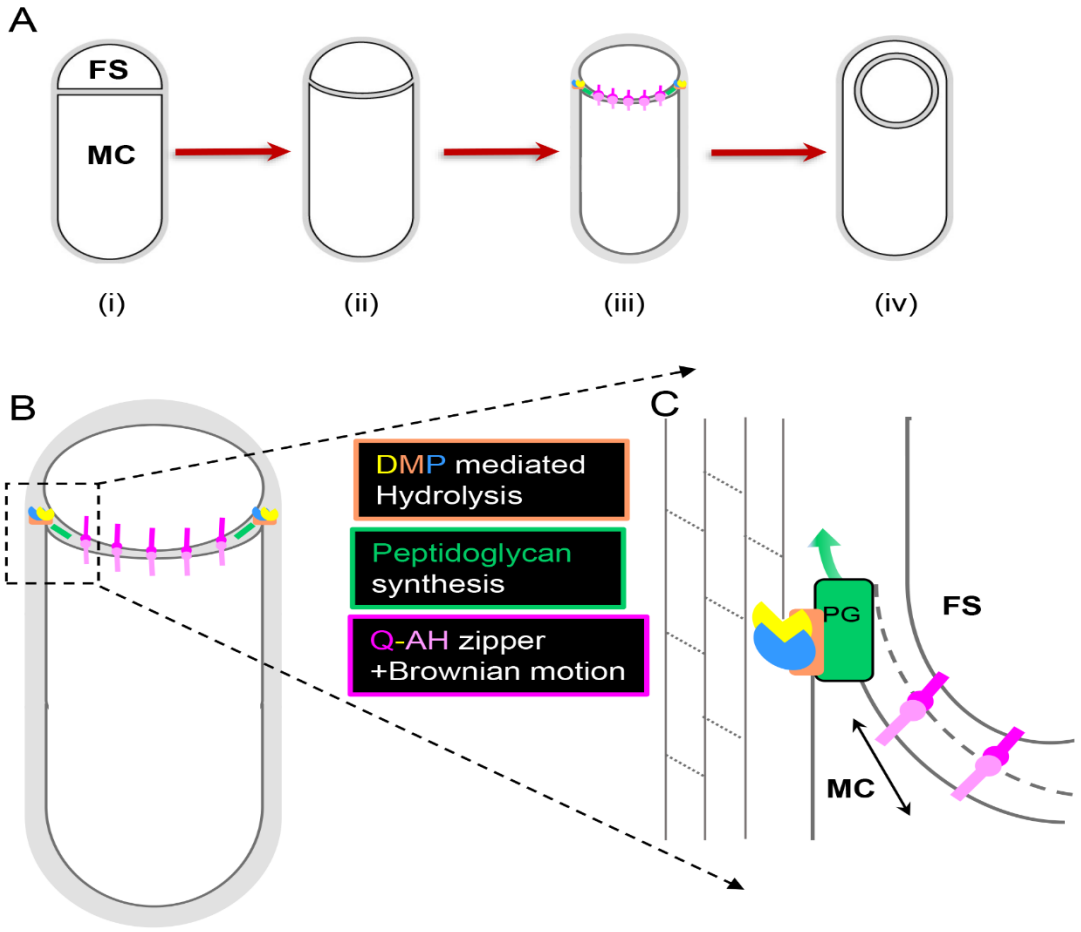


**Figure III-1. Schematic illustration of steps involved in Engulfment.**

A) Morphological changes during spore formation are shown. (i) After asymmetric septation, the cell divides into a smaller forespore (FS) and a larger mother cell (MC). (ii) The septum curves and protrudes toward the mother cell. (iii) The mother cell membrane migrates towards the forespore pole. The different factors contributing to the engulfment process are shown in the inset (panel C). (iv) Fully engulfed forespore surrounded by two membranes sandwiching a thin layer of peptidoglycan.

B) Enlarged image of the cell with proteins contributing to the membrane migration and engulfment process.

C) A detailed description of different factors playing a role during forespore engulfment. Proteins SpoIID (yellow), and SpoIIP (blue) degrade peptidoglycan and are held together by SpoIIM (orange), a scaffolding protein. These three proteins play a necessary role of detaching septal peptidoglycan which facilitates the membrane movement. Membrane movement is also facilitated by the new peptidoglycan synthesis marked by the PG box and arrow (green). Another factor that aids the membrane migration is the zipper-like interaction between the forespore membrane protein SpoIIQ (labeled Q, bright pink) and the mother cell membrane protein SpoIIIAH (labeled AH, light pink).

## III.ii Materials and Methods

### III.ii.1 Strains, Plasmids and Primers

The *B. subtilis* strains used in this study are derived from the prototrophic laboratory wild type strain PY79 (Youngman et al., 1984), a derivative of strain 168 (Zeigler et al., 2008). All the *B. subtilis* strains for this study, listed in Table III-1 were constructed by transformation with either chromosomal DNA or plasmid DNA as described by Harwood and Cutting (Harwood & Cutting, 1990). The standard recombinant DNA techniques including plasmid DNA construction and isolation using *Escherichia coli* DH5α were performed as described by Sambrook and Russell (Sambrook & Russell, 2001). Plasmids pDG1728 (*amyE* integration vector for a β-galactosidase reporter) (Guerout-Fleury, Frandsen, & Stragier, 1996) and pDG1730 (*amyE* integration vector) (Guerout-Fleury et al., 1996) were used for cloning of the DNA fragments. The resulting plasmids were inserted by double crossover recombination into either the *thrC* or *amyE* locus of the *B. subtilis* chromosome. The plasmids used in this study are listed in Table III-2. The oligonucleotide primers used are listed in Table III-3.

**Table III-1. List of *B. Subtilis* Strains used for β-galactosidase assay**

| Strain | Genotype | Reference |
|---|---|---|
| **MF8353** | *amyE::PspoIID$^{WT}$-lacZ spc* | This study |
| **MF8355** | *amyE::PspoIID$^{0A1*}$-lacZ spc* | This study |
| **MF8357** | *amyE::PspoIID$^{0A2*}$-lacZ spc* | This study |
| **MF8359** | *amyE::PspoIID$^{0A3*}$-lacZ spc* | This study |
| **MF8361** | *amyE::PspoIID$^{IIID*}$-lacZ spc* | This study |
| **MF8363** | *amyE::PspoIID$^{0A1*2*}$-lacZ spc* | This study |
| **MF8365** | *amyE::PspoIID$^{0A1*2*3*}$-lacZ spc* | This study |

| | | |
|---|---|---|
| **MF8367** | *amyE::PspoIID$^{0A1*2*3*IIID*}$-lacZ spc* | This study |
| **MF8423** | *amyE::PspoIID$^{0A1*3*}$-lacZ spc* | This study |
| **MF8425** | *amyE::PspoIID$^{0A2*3*}$-lacZ spc* | This study |
| **MF8874** | *amyE::PspoIID$^{0A3*IIID*}$-lacZ spc* | This study |

**Table III-2. List of Plasmids used in this study**

| Plasmid | Description | Reference |
|---|---|---|
| **pDR244** | *cre* plasmid with temperature-sensitive replication origin in *B. subtilis* | (Koo et al., 2017) |
| **pMF925** | *amyE::PspoIID$^{WT}$-lacZ spc* | This study |
| **pMF920** | *precursor of pMF926* | This study |
| **pMF926** | *amyE::PspoIID$^{0A1*}$-lacZ spc* | This study |
| **pMF858** | *precursor of pMF927* | This study |
| **pMF927** | *amyE::PspoIID$^{0A2*}$-lacZ spc* | This study |
| **pMF858** | *precursor of pMF921* | This study |
| **pMF928** | *amyE::PspoIID$^{0A3*}$-lacZ spc* | This study |
| **pMF859** | *precursor of pMF929* | This study |
| **pMF929** | *amyE::PspoIID$^{IIID*}$-lacZ spc* | This study |
| **pMF922** | *precursor of pMF930* | This study |
| **pMF930** | *amyE::PspoIID0A$^{1*2*}$-lacZ spc* | This study |
| **pMF923** | *precursor of pMF931* | This study |
| **pMF931** | *amyE::PspoIID0A$^{1*2*3*}$-lacZ spc* | This study |
| **pMF924** | *precursor of pMF932* | This study |
| **pMF932** | *amyE::PspoIID0A$^{1*2*3*IIID*}$-lacZ spc* | This study |
| **pMF946** | *prepcursor of pMF949* | This study |
| **pMF949** | *amyE::PspoIID0A$^{1*3*}$-lacZ spc* | This study |
| **pMF947** | *precursor of pMF950* | This study |
| **pMF950** | *amyE::PspoIID0A$^{2*3*}$-lacZ spc* | This study |

**Table III-3. List of Primers used in this study**

| Primers | Sequence |
|---|---|
| **om244** | 5’-ccggaattcgctttgttgatttcgagccgtatattc-3’ |
| **om245** | 5’-cggaagcttctcacctccttgtgagtatagaatgtg-3’ |
| **om294** | 5’-cattatgcgcaaaatagcaaaaaag-3’ |
| **om295** | 5’-tgattgcgaattgtttcatattcag-3’ |
| **om374** | 5’-tttcccggttcaacgagagtcatattagcttgtccc-3’ |
| **om375** | 5’-cgttgaaccgggaaactttatttgtcatttacgtat-3’ |
| **om376** | 5’-tagcggaaccctgcccatagactagactagagtcg-3’ |
| **om377** | 5’-ggcagggttccgctaatatgactctcgttttggaca-3’ |
| **om378** | 5’-ggctctagaggctttcagcgcttcaggtttaaag-3’ |
| **om412** | 5’-ggcgaattcgcagacatcgaacgtgtaaat-3’ |

| | |
|---|---|
| **om418** | 5’-taaaccggttctaaagtttcccggttcaacgagagt-3’ |
| **om419** | 5’-tttagaaccggtttacgtattctttttttgct-3’ |
| **om420** | 5’-ctagccggttctcccgagcaggaggcagctgaat-3’ |
| **om421** | 5’-gggagaaccggctagtctagtctatgggcaggg-3’ |
| **om422** | 5’-tcccgagcaggaggcagctgaagcttggc-3’ |
| **om423** | 5’-taaaccggttctaaagtttcccggttcaacgagagt-3’ |
| **om424** | 5’-cgttgaaccgggaaactttaaacccggtttacgtat-3’ |

III.ii.2 Culture Conditions

Luria-Bertani (LB) medium (Sambrook & Russell, 2001) was used for routine growth of *E. coli* and *B. subtilis*. Difco sporulation medium (DSM) was used for the sporulation of *B. subtilis* (Harwood & Cutting, 1990). Cell growth in liquid media was checked using a spectrophotometer by reading the optical density at 600 nm ($OD_{600}$). 1.5% agar was included in the media for making solid agar plates.

For typical culture conditions, the overnight culture in 5 ml LB was transferred to 10 ml of fresh LB at $OD_{600}$ = 0.05 and shaken at 37 °C at 150 rpm until $OD_{600}$ = 0.5. Cells were then transferred to 20 ml DSM supplemented at OD600 = 0.05.

When appropriate, antibiotics were included at the following concentrations: 10 µg $ml^{-1}$ of tetracycline, 100 µg $ml^{-1}$ of spectinomycin, 20 µg $ml^{-1}$ of kanamycin, 5 µg $ml^{-1}$ of chloramphenicol and 1 µg $ml^{-1}$ of erythromycin.

III.ii.3 Electrophoretic mobility shift assay

The his-tagged Spo0A protein was expressed in *E. coli* BL21(DE3) and purified as described previously (Devi et al., 2015; Eswaramoorthy et al., 2011; Fujita & Losick, 2003; Kiehler et al., 2017). A soluble form of the his-tagged KinC

(KinC$^{\Delta TM1+2}$, the transmembrane deleted form of KinC) was expressed in *E. coli* BL21(DE3) and purified as described previously (Devi et al., 2015).

All autophosphorylation and phosphotransfer reactions were carried out as reported (Devi et al., 2015; Fujita & Losick, 2003; Kiehler et al., 2017). In brief, the reactions were performed in a 20 µl final reaction volume containing 50 mM Tris-HCl, pH 8.0, 5 mM $MgCl_2$, and 10% (v/v) glycerol. Proteins used for the phosphorylation assays were 1 µM of KinC$^{\Delta TM1+2}$ and 10 µM of Spo0A. The reaction was initiated by the addition of ATP to a final concentration of 400 µM. Reaction mixtures were incubated for 30 min at 30 °C and then used for Electrophoretic mobility shift assays (EMSA).

DNA fragments used in this assay correspond to the region 151 bp upstream of the *spoIID* coding region and were amplified with primers omf294 (radiolabeled) and omf295 by PCR. PCR products containing wild-type and the mutated 0A- and IIID- boxes were amplified by using DNA templates that contained each of these mutations. The 5' end of omf294 was labeled using [γ-$^{32}$P] ATP (Perkin-Elmer, 3000 Ci mmol-1, 10 mCi ml-1) and T4 polynucleotide kinase. A typical assay mixture contained 10 mM Tris-HCl, pH 7.5, 50 mM NaCl, 1 mM EDTA, 1 mM dithiothreitol (DTT), 5% (v/v) glycerol, 0.5 µg of BSA, 1 µg of Poly(dI-dC), a radioactive DNA probe (2000 c.p.m.), and various amounts of the purified proteins in a 20 µl total volume. After 30 min of incubation at room temperature, 4 µl of 6x loading dye (Thermo Scientific) was added to each of the reaction mixture (20 µl) and then the samples were loaded onto a native 6% (w/v) polyacrylamide gel and electrophoresed in 0.5 x TBE buffer. Radioactive species were detected by

autoradiography after exposure to X-ray film. Spo0A was phosphorylated as described above and used at the indicated final concentrations as described in figure legends. The general protocol for EMSA is provided in Figure II-1, in the previous chapter.

III.ii.4 β-galactosidase assay

The β-galactosidase activity was determined by performing the β-galactosidase assay as described by Harwood & Cutting (Harwood & Cutting, 1990). The samples for this assay were collected periodically by growing *B. subtilis* strains under DSM media at 37 °C.

**III.iii Results**

III.iii.1 Direct evidence of 0A~P binding to three 0A boxes in the *spoIID* promoter region

0A~P is active in the mother-cell compartment after asymmetric septation and this mother-cell specific activity of Spo0A is very important for the sporulation process (Fujita & Losick, 2002, 2003). Nevertheless, the mechanism of 0A~P regulation in the mother-cell has not been studied till date. Our candidate gene for studying the mother-cell specific regulation of 0A~P is *spoIID*, a cell wall hydrolase (lytic transglycosylase) involved in the engulfment stage of sporulation(Morlot et al., 2010).

The first step in studying the 0A~P regulation of *spoIID* was to investigate the promoter region of *spoIID*. Upon careful observation, we identified three possible sites for 0A~P binding (0A boxes). To experimentally determine the 0A~P binding

to the possible 0A boxes, strains with mutated 0A boxes and the combinations were constructed. All these different 0A box mutant combinations are shown in Figure III-2. The mutant combinations were fused to different reporters for further characterization of these 0A boxes.

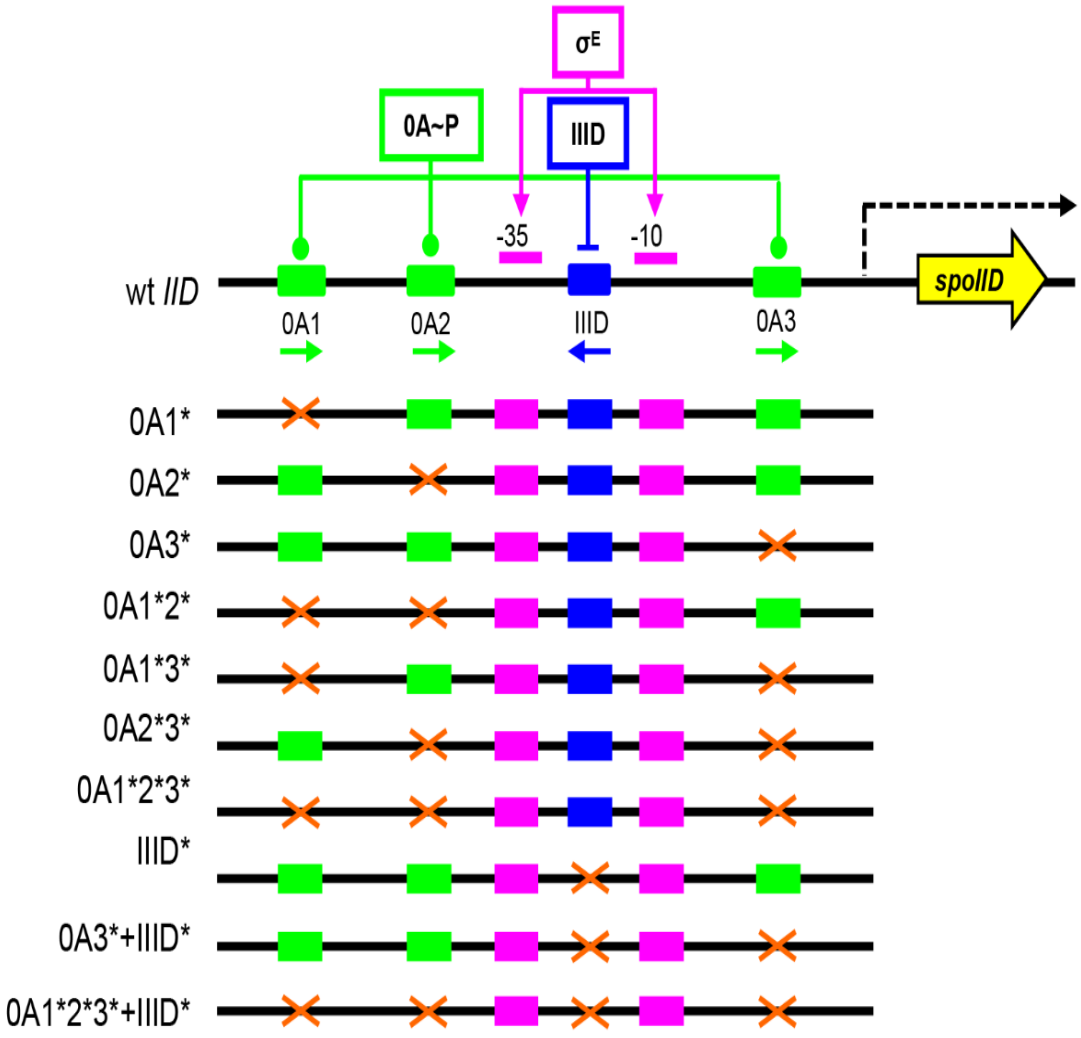


**Figure III-2. Schematic diagram of binding sites for Spo0A~P, SpoIIID, and $\sigma^E$-RNAP to the *spoIID* promoter.**
Different 0A box and IIID box mutant combinations are shown below the wild type *spoIID* promoter. Three possible 0A boxes (green) are located in the wild-type *spoIID* promoter along with the binding sites for $\sigma^E$-RNAP (pink) and one SpoIIID box (blue). The X (orange) indicates mutation in that binding site.

Electrophoretic mobility shift assays were performed using the wild type and mutated DNA fragments (151 bp) obtained by PCR with radiolabeled primers (5' end-labeled omf294 and omf295). Phosphorylated 0A~P was generated with our artificial two-component system (using soluble KinC) (Devi et al., 2015). Upon incubation of the radiolabeled DNA fragments with varying concentrations of 0A~P (0, 2.5, and 5 μM) analysis was done by running the samples on 6% non-denaturing PAGE. Radioactive species were detected after exposure of dried gels to X-ray films. Our results indicate that wild type *spoIID* promoter DNA fragment migrates slowly producing a smear pattern on the gel under increasing 0A~P concentrations (Figure III-3B lanes 1-3). This smear or shift of DNA provides evidence for the presence of 0A box/boxes for 0A~P binding. Upon mutating the first possible 0A box (Figure III-3A) (0A1 box, hereafter), the smear pattern suggesting binding of DNA fragment to 0A~P was still visible, but the highly shifted band on the top portion disappeared (Figure III-3B lanes 4-6). These results suggest that the 0A~P binding to 0A1 is abolished. When the DNA fragment containing the mutated 0A2* was examined, the shifted bands were detected with a modest resemblance to the wild type DNA bands (Figure III-3B lanes 7-9). When the DNA fragment containing the mutated 0A3* was examined, the smeared shifted bands migrated slightly above the free DNA, but the highly retarded bands on the top portion observed in the wild type, 0A1*, and 0A2* disappeared (Figure III-3B lanes 10-12). These results suggest that 0A~P is able to bind to each of the 0A boxes, but with different affinities. To verify this, two of three 0A boxes were mutated in all combinations and examined with EMSA. When the DNA fragment

containing the mutated 0A1*2* (i.e. only 0A3 present) was examined, the shifted bands showed similarities to those observed in the 0A1* (Figure III-3B, lanes 4-6), but the free DNA bands varied (Figure III-3B, lanes 13-15). When the DNA fragment containing the mutated 0A1*3* (i.e. only 0A2 present) was examined, the shifted bands had a similar pattern to 0A3* (Figure III-3B, lanes 10-12), but with a minute difference (Figure III-3B, lanes 16-18). When the DNA fragment containing the mutated 0A2*3* (i.e. only 0A1 present) was examined, the bands were only modestly shifted above the free DNA (Figure III-3B, lanes 19-21). Finally, when the DNA fragment with mutations in all the possible 0A-boxes was inspected it showed no binding to the 0A~P (Figure III-3B lanes 22-24). Thus the EMSA provides evidence of 0A~P binding to three 0A boxes in the promoter region of *spoIID*. We also compared the relative intensities of the shifted (bound) and non-shifted (unbound or free) DNA containing at least one intact 0A box. Our comparison suggests that the relative binding affinities are 0A3 ≥ 0A2 > 0A1.

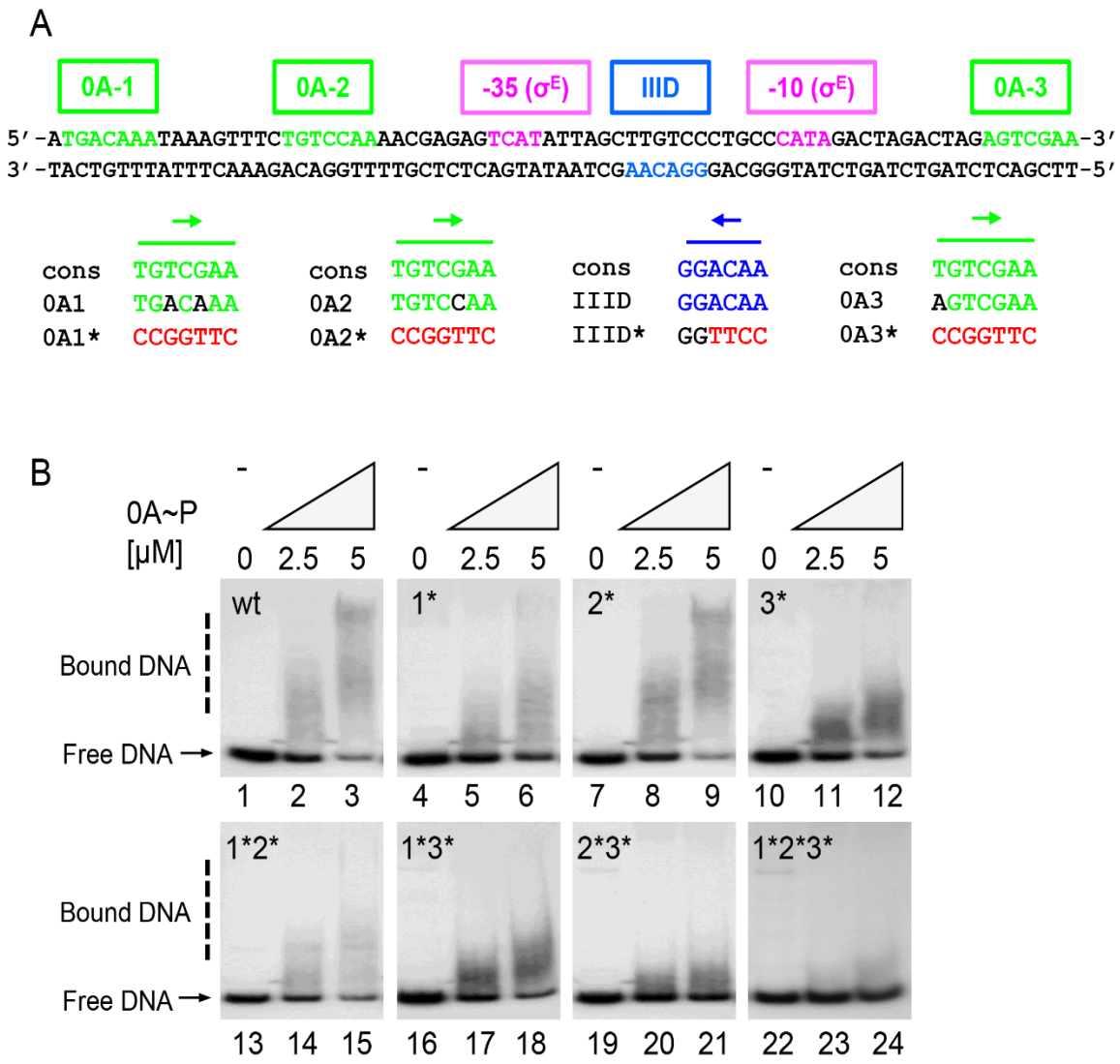


**Figure III-3. Electrophoretic mobility shift assays (EMSA) of the 0A~P binding to the 0A boxes in the *spoIID* promoter region.**

(A) Nucleotide sequence of the *spoIID* promoter region. The -35 and -10 promoter elements for the $\sigma^E$-RNA polymerase (pink), IIID box (blue), the wild type 0A boxes (green), and mutated (red) sequences of the 0A boxes and IIID box are indicated.

(B) Results of 0A~P binding to wild-type and mutated *spoIID* promoter fragments as detected by EMSA. *spoIID* promoter fragments (151 bp) containing all 0A-boxes (lane 1-3), 0A1* (lane 4,5,6), 0A2* (lane 7,8,9), 0A3* (lane 10,11,12), 0A1*2* (lane 13,14,15), 0A1*3* (lane 16,17,18), 0A2*3* (lane 19,20,21), 0A1*2*3* (lane 22,23,24) were amplified by PCR using primers (5' end-labeled omf294 and omf295). Purified Spo0A was phosphorylated by $KinC^{\Delta TM1+2}$ in the presence of ATP. Varying concentrations of 0A~P (0 μM, lanes 1, 4, 7, 10, 13, 16, 19, and 22; 2.5 μM, lanes 2, 5, 8, 11,14,17, 20, and 23; 5 μM, lanes 3, 6, 9, 12, 15, 18, 21, and 24) were incubated with radiolabeled DNA and analyzed by 6% non-denaturing PAGE (see Materials and Methods). Free DNA (unbound and non-shifted) is indicated by black arrow. Bound (shifted) DNA is indicated by dashed lines.

III.iii.2 Confirmation of SpoIIID binding site present in the *spoIID* promoter region

Another DNA-binding protein, SpoIIID also regulates *spoIID* expression by binding to a six-nucleotide region in the *spoIID* promoter (Eichenberger, Fujita, Jensen, Conlon, & Rudner, 2004). This SpoIIID binding site (also known as IIID box) is located between the $\sigma^E$-RNA polymerase recognition sites within the *spoIID* promoter region. In order to confirm the IIID box in the *spoIID* promoter region, we performed EMSA using purified SpoIIID and wild-type and IIID box mutated *spoIID* promoter DNA fragments. Wild type DNA fragment showed a shifted band upon increasing SpoIIID concentrations (Figure III-4 lanes 1-3). IIID box mutated DNA fragment showed no shifting even at higher SpoIIID concentrations (Figure III-4 lanes 4-6). Thus our results confirm the previously reported IIID box to be the single location for SpoIIID binding.

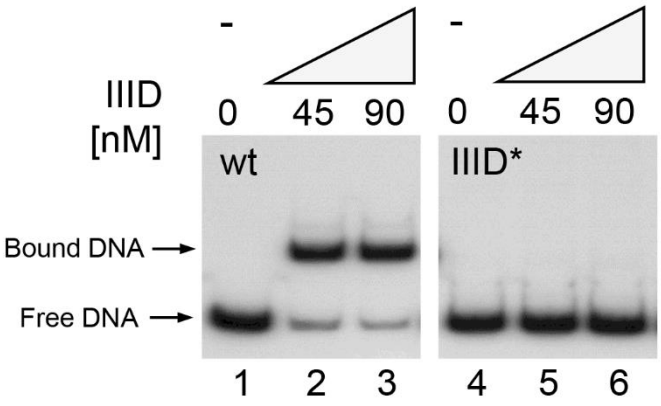


**Figure III-4. Electrophoretic mobility shift assay for SpoIIID binding to the IIID box in the *spoIID* promoter region.**
Results of SpoIIID binding to wild-type and mutated (IIID*) *spoIID* promoters as detected by EMSA. *spoIID* promoter fragments (151 bp) containing wild type IIID (lane 1-3), and mutated IIID (IIID*) (lane 4-6) were amplified by PCR using primers (5' end-labeled omf294 and omf295). Varying concentrations of purified SpoIIID (0 nM, lanes 1 and 4; 45 nM, lanes 2 and 5; 90 nM, lanes 3 and 6) were incubated with radiolabeled DNA and analyzed on 6% non-denaturing PAGE (see Materials and Methods).

III.iii.3 β-Galactosidase assay reveals the positive regulation by 0A1 and 0A2 box and repression by 0A3 and IIID box

The data shown above suggest that Spo0A plays an important role in controlling the mother-cell specific expression of *spoIID*. However, it has been technically difficult to demonstrate this possibility due to the lack of a Spo0A mutation that leads to proper asymmetric division but specifically blocks gene expression in the mother cell compartment. As a first step to overcome these technical difficulties and to examine whether Spo0A directly controls *spoIID* expression, we systematically introduced nucleotide substitutions into each of the three 0A boxes and one IIID box. Then, we constructed a series of *lacZ* fusions to the *spoIID* promoter DNA fragments containing single or combinations of the 0A box mutations (0A1*, 0A2*, 0A3*), and IIID box mutation (IIID*) (Note that the asterisk indicates the mutated 0A and IIID boxes in the *spoIID* promoter). Each of the resulting *lacZ* fusion constructs was integrated at the non-essential *amyE* locus of the wild type strain (Figure III-5A). I cultured these strains in liquid Difco Sporulation Medium (DSM) under shaking conditions starting from one hour, after entry into sporulation (~3 hours into culture) up to six hours. I further assayed these samples in order to measure the wild type and mutated *spoIID* promoter activities during sporulation (Figure III-5B).

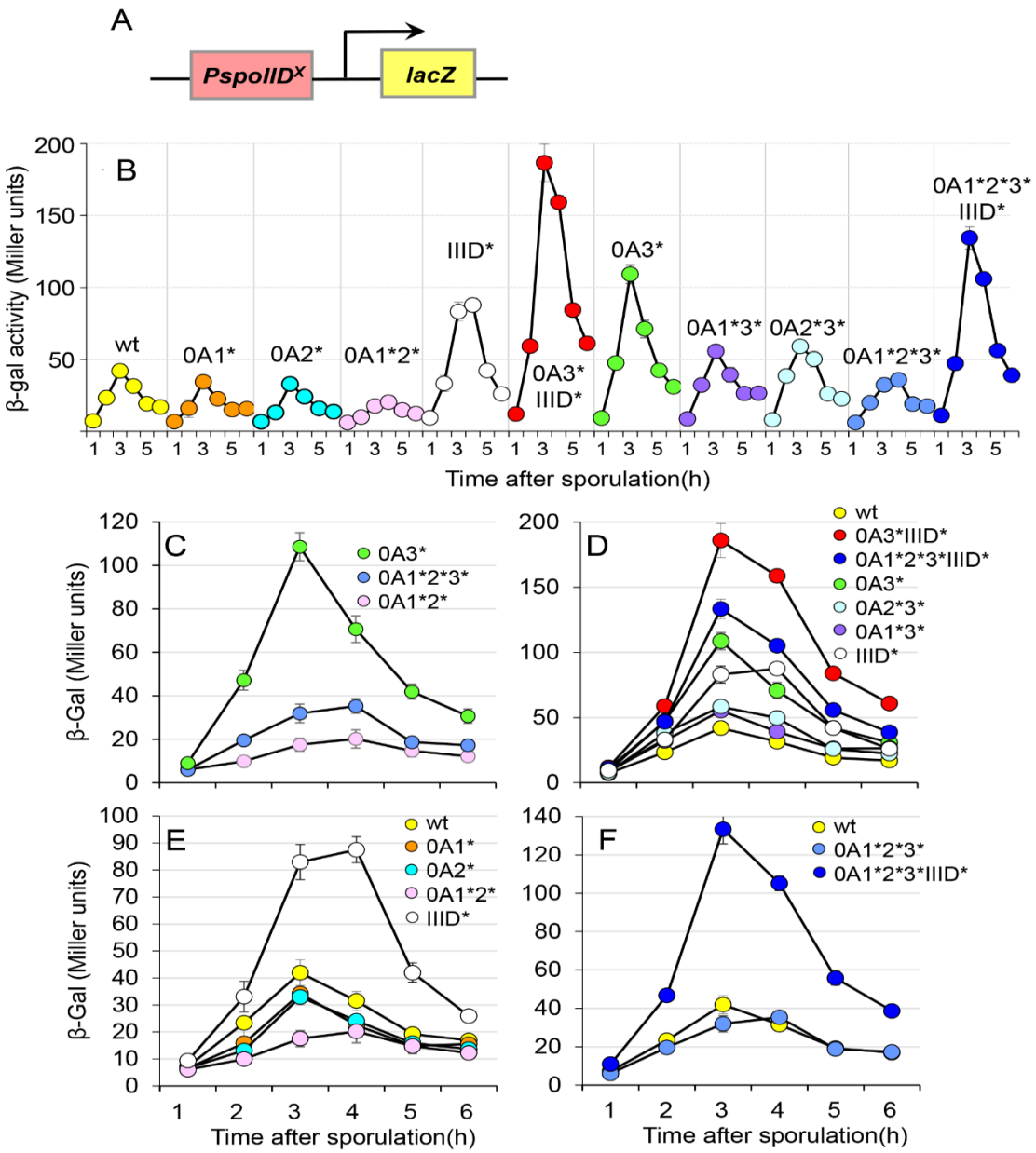


**Figure III-5. β-galactosidase assays to detect transcriptional activities of the wild type and the mutated *spoIID* promoters fused to *lacZ*.**

(A) Schematic diagram of *spoIID* promoter fusion to *lacZ*. (B) Individual β-galactosidase activities of the wild type and the mutated *spoIID* promoters fused to *lacZ*, arranged in one graph. Cells were grown in Difco sporulation medium (DSM) and samples were assayed from one hour to six hours after entry into sporulation. (C) to (F) Representative β-galactosidase data for comparison. The activity values represent the results of at least three independent experiments with standard deviations. The student t-test assuming equal variance was used for comparison between the peak activities of the wild type and mutant strains. The resulting p values were as follows: 0A1*, <0.05; 0A2*, <0.05; 0A3*, <0.001; 0A1*2*, <0.001; 0A2*3*, <0.001; 0A1*3*, <0.001; 0A1*2*3*, <0.05; IIID*, <0.001; IIID*0A3*, <0.001; and IIID*0A1*2*3*, <0.001. P <0.05 is significant.

As shown in Figure III-5BE, the reporter activities in the strain harboring each of the 0A1* and 0A2* mutations showed modestly lower values than in the wild type strain. These activities were further reduced by the combination of the two 0A1* and 0A2* mutations (0A1*2*), as compared to those in the single box mutation (0A1* or 0A2*) (Figure III-5BE). These results imply that 0A1 and 0A2 act as positive regulatory elements by the direct binding of 0A~P in a synergistic manner.

In contrast to the 0A1* and 0A2* mutants, the reporter activities displayed higher values in the strains harboring the 0A3* mutation than in the wild type strain (Figure III-5BCD). When the 0A3* mutation was introduced into each of the 0A1* and 0A2* mutants, the reporter activities increased in these mutant strains (0A1*3* and 0A2*3*) as compared with those in each of the single mutants (0A1* and 0A2*) (Figure III-5BDE). These results suggest that the *spoIID* expression is repressed by binding of 0A~P to the 0A3 box. However, in the 0A1*2*3* mutant, the reporter activities showed slightly lower levels, and the peak time point was shifted one hour later than in the wild type strain (Figure III-5BF). These results indicate that 0A~P strictly controls the *spoIID* expression by maintaining the balance between opposing effects of the positive (0A1 and 0A2) and negative (0A3) regulations.

We further found that the reporter activities are higher in the IIID* mutant than in the wild type strain (Figure III-5BD). These results directly verified that SpoIIID acts as a negative regulator for the *spoIID* expression as described previously (Eichenberger et al., 2004). As shown in Figure III-5BD, the reporter activities displayed highest values in the 0A3* and IIID* double mutant (0A3*IIID*) than all

other strains tested, supporting the observations that *spoIID* expression is repressed by the direct binding of 0A~P and SpoIIID to each of the 0A3 and IIID boxes, respectively.

According to Figure III-5D, the reporter activities increase over time more significantly in the 0A3*IIID* mutant than in the 0A1*2*3*IIID* mutant and both of these reporter activities gradually increased during 2 - 3 hrs. after the onset of sporulation. In the 0A3*IIID* mutant, 0A~P binds to the 0A1 and 0A2 boxes and stimulates transcription from the $\sigma^E$-RNAP dependent promoter. In contrast, transcription from the 0A1*2*3*IIID* promoter is solely dependent on $\sigma^E$-RNAP, but not 0A~P. Thus, we speculate that the gradual increase in the reporter activities in the 0A3*IIID* mutant may arise from an increase in 0A~P levels due to de novo activation of phosphorelay in a mother cell-specific manner.

Figure III-5F demonstrates that the reporter activities in the strain harboring 0A1*2*3*IIID* increased significantly as compared with the strain harboring 0A1*2*3*. These results suggest that the 0A1*2*3* promoter activity is repressed by SpoIIID while the 0A1*2*3*IIID* promoter activity is derepressed in the absence of SpoIIID. All of the reporter activity levels declined around after T3, likely due to the inactivation of $\sigma^E$-RNAP. These results suggest that the major role of SpoIIID is to help maintain the appropriate level of SpoIID as a fine-tuning device.

### III.iv Discussion

In earlier studies, Spo0A had been shown to play a pivotal role in asymmetric division and as a master regulator for entry into sporulation (Hoch, 1993) (Burbulys et al., 1991). In addition to these previous studies, it was later discovered that Spo0A activity increases after asymmetric division and is confined to the mother cell compartment (Fujita & Losick, 2002) (Fujita & Losick, 2003). Not only does the Spo0A activity increases in a compartment-specific manner inside the mother cell, but this Spo0A activity is also crucial for proper sporulation (Fujita & Losick, 2003). Years after this discovery, there have been no detailed studies directly characterizing the role of Spo0A in controlling mother cell-specific gene expression. We identified one such gene, *spoIID*, which is expressed in the mother cell under the control of $\sigma^E$-RNAP and DNA binding protein SpoIIID.

Another previous study has suggested that 0A~P appears to bind to the promoter region of *spoIID* (Molle et al., 2003). In that study, a constitutively active form of Spo0A, named Spo0A-Sad67, was artificially synthesized under the control of an isopropyl β-D-thiogalactopyranoside (IPTG)-inducible promoter under sporulation conditions and the Spo0A-bound DNA fragments were successfully obtained by chromatin immunoprecipitation experiments using anti-Spo0A antibodies. The genes obtained by the chromatin immunoprecipitation experiments were also verified by gene microarray analysis with and without Spo0A-Sad67 induction. The authors further demonstrated in vitro experiments that the C-terminal DNA binding domain of Spo0A directly binds to the *spoIID* promoter region with electrophoretic mobility shift assays (EMSA). Under these

assay conditions, little or no mRNA signal derived from *spoIID* was detected in transcriptional profiling experiments by gene microarray analysis. These results can be explained by the fact that *spoIID* is transcribed only in the mother cell compartment by $\sigma^E$-RNAP at later times of sporulation (Eichenberger et al., 2003) and the mRNA samples in that experiment were prepared from growing cells with and without Spo0A-Sad67 induction before asymmetric division (Molle et al., 2003). Nonetheless, these data suggest that *spoIID* is a possible target of Spo0A and provide a potential clue to explore the importance of the mother cell-specific activation of Spo0A. However, there have been no detailed studies directly characterizing the effect of Spo0A on the expression of a mother cell specific gene, like *spoIID*. The limitation of the study is mainly due to the lack of Spo0A mutations specifically blocking gene expression in the mother cell compartment, but not asymmetric division. Therefore, the physiological significance of 0A~P binding to the *spoIID* promoter region is unclear.

In this chapter, I provided a first-ever, direct experimental evidence of 0A~P binding to three Spo0A binding sites (0A boxes) in the *spoIID* promoter region, through Electrophoretic mobility shift assays (EMSA). The shifted bands seen with the wild type *spoIID* promoter fragment had a smear pattern. This smear pattern indicates the presence of different DNA-protein complexes with different binding affinity. We observed changes in the smear patterns of the shifted DNA bands with the use of mutated promoter fragments. Construction of combination of 0A box mutants (listed in Figure III-1) helped us in analyzing the relative binding affinity of

0A~P to each of the 0A boxes. According to the results, the relative 0A~P binding affinities are 0A3 ≥ 0A2 > 0A1.

Once the 0A~P binding to three 0A boxes in the *spoIID* promoter region was confirmed, it was clear that the binding of this master regulator has a role in modifying the gene expression. I proceeded with β-galactosidase assays in order to further characterize the role of these different 0A boxes in the *spoIID* expression. Since *spoIID* is under the $\sigma^E$-RNAP control, the transcriptional assay time points were chosen to encompass the $\sigma^E$-RNAP activity. The 0A1 and 0A2 boxes are located upstream to the $\sigma^E$-RNAP recognition sites, therefore, based on the published studies, I hypothesized that these boxes play a role in the positive regulation of *spoIID* expression (Satola, Baldus, & Moran, 1992). Similarly, as the 0A3 box is located downstream to the $\sigma^E$-RNAP recognition sites, it suggested a role in the negative regulation of the *spoIID* expression. The transcriptional assays presented in this chapter, corroborated the above-mentioned hypothesis.

Thus the results presented in this chapter prove that binding of 0A~P to the 0A1 and 0A2 boxes (upstream to the $\sigma^E$-RNAP recognition sites) positively regulates *spoIID* expression. Whereas, binding of 0A~P to the 0A3 box (downstream to the $\sigma^E$-RNAP recognition sites) represses the *spoIID* expression. Based on the transcriptional activities of the wild-type and mutated *spoIID* promoters, Figure III-5 shows the model for *spoIID* regulation by Spo0A~P along with $\sigma^E$-RNAP and SpoIIID.

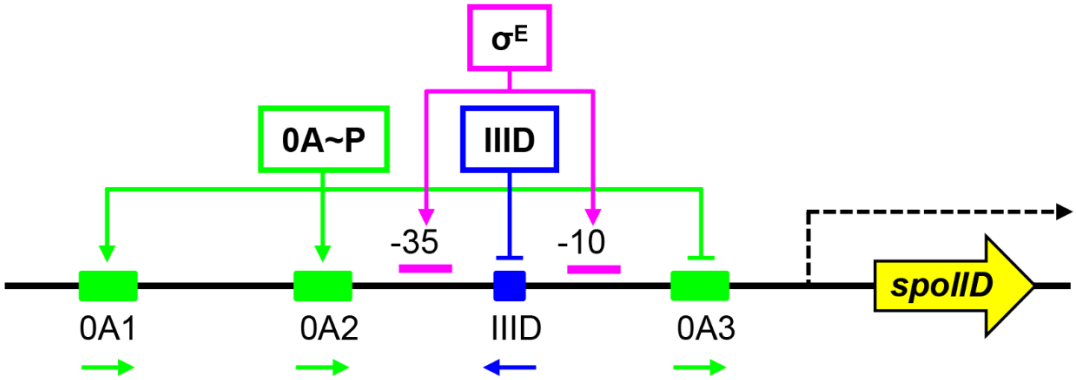


**Figure III-6. The model for *spoIID* regulation by Spo0A~P along with $\sigma^E$-RNAP and SpoIIID.**
The model for *spoIID* regulation by Spo0A~P based on our transcriptional studies is shown. 0A boxes (green) and IIID box (blue) are shown along with the arrows indicating their orientation. $\sigma^E$-RNAP recognition elements (pink) are shown. Positive regulation at the binding site is shown by a pointed arrow and negative regulation is shown by a flat arrow. Our results suggest that Spo0A~P positively regulates *spoIID* expression by binding to 0A1 and 0A2 and represses *spoIID* expression by binding at 0A3. SpoIIID is already known to repress the expression of this $\sigma^E$-RNAP controlled *spoIID* promoter.

Traditionally, Spo0A has been known to be activated via phosphorelay only prior to asymmetric division (Hoch, 1993) (Grossman, 1995) (Piggot & Hilbert, 2004). The present data indicate that the reporter activities for the modified *spoIID* promoter that is dependent on both 0A~P and $\sigma^E$-RNAP (0A3*) increase over time more significantly than those for the modified *spoIID* promoter that is dependent solely on $\sigma^E$-RNAP (0A1*2*3*). Therefore, the data presented in this chapter suggest that the phosphorelay activity continues in the mother cell compartment after asymmetric division and the resulting increased level of 0A~P contributes to the mother cell-specific transcriptional activation of the $\sigma^E$-RNAP controlled gene, *spoIID*.

# Chapter IV: Elucidating the Molecular Mechanisms of Forespore Engulfment Controlled by Spo0A

## IV.i Introduction

Spo0A had been shown to play a crucial role in asymmetric division and thus to act as a master regulator for entry into sporulation (Hoch, 1993) (Burbulys et al., 1991). In addition to these previous studies, it was later found that Spo0A activity increases after asymmetric division and is confined to the mother cell compartment (Fujita & Losick, 2002) (Fujita & Losick, 2003). One of the essential steps of sporulation, governed by the mother cell genes is engulfment. It is a phagocytic-like process in which mother cell membranes migrate around the forespore(Morlot et al., 2010).

The first step in engulfment is the cell wall hydrolysis, which is carried out by the SpoIID-SpoIIM-SpoIIP (DMP) complex (Gutierrez et al., 2010; Meyer et al., 2010; Ojkic, Lopez-Garrido, Pogliano, & Endres, 2016). A complex formation of a membrane-anchored transglycosylase encoded by *spoIID* and an amidase/endopeptidase encoded by *spoIIP* is mediated by a scaffold protein SpoIIM, leading to specific localization of DMP to the polar septal membrane (Morlot et al., 2010). Enzymatic activities of each subunit become evident only when each protein is assembled into the DMP complex. As a result, the complex pulls the mother cell membranes circumferentially and continuously around the forespore, leading to engulfment (Morlot et al., 2010). Each of the genes for DMP is known to be transcribed by $\sigma^E$-RNAP and thus specifically synthesized in the mother cell compartment (Eichenberger et al., 2003).

Among the three $\sigma^E$-RNAP-controlled genes, *spoIID* is the only one that is additionally regulated by 0A~P as suggested previously (Molle et al., 2003) and

described in this study. Based on available research, it appears that SpoIIP and SpoIIM are constitutively transcribed by $\sigma^E$-RNAP and available at all times for the DMP complex formation in the mother cell compartment.

It is also known that premature and simultaneous expression of all three components (DMP) interfere with sporulation (Eichenberger, Fawcett, & Losick, 2001). A recent study using cryo-electron tomography suggests possible novel mechanisms for engulfment mediated by DMP, in which limited numbers of the DMP complex degrade the peptidoglycan ahead of the engulfing membrane, generating an irregular and uneven membrane front in the form of finger-like projections (Khanna et al., 2019). DMP activity is known to be a rate-limiting step for membrane migration during engulfment (Abanes-De Mello et al., 2002; Meyer et al., 2010). These results suggest that the timing and levels of DMP complex formation are important for engulfment.

Upon surveying these facts, I hypothesize that the mother cell-specific Spo0A activity might be responsible to regulate the forespore engulfment via its role in *spoIID* regulation. In the previous Chapter, I established that *spoIID* expression is regulated by 0A~P upon binding to three 0A boxes in the *spoIID* promoter region. In the following Chapter, I further elucidate the mechanism of *spoIID* regulation by 0A~P, acting as a mother cell-specific transcription factor. The results presented here indicate that the timing and level of *spoIID* expression which is mediated by 0A~P, is important for proper engulfment. I also propose that 0A~P regulated *spoIID* expression is the rate-limiting step in the DMP complex formation, crucial for proper engulfment and sporulation.

## IV.ii Materials and Methods

### IV.ii.1 Strains, Plasmids and Primers

The *B. subtilis* strains used in this work are derived from the prototrophic laboratory wild type strain PY79 (Youngman et al., 1984), a derivative of strain 168 (Zeigler et al., 2008). The parental strains are listed in Table IV-1. All *B. subtilis* strains listed in Table IV-2 were constructed by transformation with either chromosomal DNA or plasmid DNA as described by Harwood and Cutting (Harwood & Cutting, 1990). The standard recombinant DNA techniques including plasmid DNA construction and isolation using *Escherichia coli* DH5α were performed as described by Sambrook and Russell (Sambrook & Russell, 2001). For studying SpoIID levels, a 3x FLAG tag was fused in-frame at the C-terminal of the *spoIID* coding region using joining PCR. Plasmid pDG1664 (*thrC* integration vector) (Guerout-Fleury et al., 1996) and pDG1730 (*amyE* integration vector) (Guerout-Fleury et al., 1996) were used for cloning of the DNA fragments. The resulting plasmids were inserted by double crossover recombination into either the *thrC* or *amyE* locus of the *B. subtilis* chromosome. The plasmids used in this study are listed in Table IV-3. The oligonucleotide primers used are listed in Table IV-4.

**Table IV-1. List of Parental strains used in this study**

| Strain | Genotype | Reference |
|---|---|---|
| ***B.subtilis* PY79** | Prototroph wild type | Youngman, Perkins, & Losick, 1984 |
| **MF7390** | *ΔspoIID::erm trpC2* KO of 168 BKE31350 Locus tag BSU36750 | BGSC |
| **MF7397** | *ΔspoIID::erm* (7390→PY79) | This study |
| **MF7436** | *ΔspoIID* (pDR244→7397) | This study |

**Table IV-2. List of *B. subtilis* strains used in this study**

| **Strains for immunoblots and spore counts and IPTG induction experiments** | | |
|---|---|---|
| **Strain** | **Genotype** | **Reference** |
| **MF8582** | *amyE::Phy-spank-spoIID-FLAG spc* | This study |
| **MF8583** | *ΔspoIID amyE::Phy-spank-spoIID-FLAG spc* | This study |
| **MF8586** | *ΔspoIID amyE::PspoIID$^{wt}$-spoIID-FLAG spc* | This study |
| **MF8589** | *ΔspoIID amyE::PspoIID$^{0A1*}$-spoIID-FLAG spc* | This study |
| **MF8592** | *ΔspoIID amyE::PspoIID$^{0A2*}$-spoIID-FLAG spc* | This study |
| **MF8595** | *ΔspoIID amyE::PspoIID$^{0A3*}$-spoIID-FLAG spc* | This study |
| **MF8598** | *ΔspoIID amyE::PspoIID$^{0A1*2*}$-spoIID-FLAG spc* | This study |
| **MF8601** | *ΔspoIID amyE::PspoIID$^{0A1*3*}$-spoIID-FLAG spc* | This study |
| **MF8604** | *ΔspoIID amyE::PspoIID$^{0A2*3*}$-spoIID-FLAG spc* | This study |
| **MF8607** | *ΔspoIID amyE::PspoIID$^{0A1*2*3*}$-spoIID-FLAG spc* | This study |
| **MF8610** | *ΔspoIID amyE::PspoIID$^{0A1*2*3*IIID*}$-spoIID-FLAG spc* | This study |
| **MF8613** | *ΔspoIID amyE::PspoIID$^{IIID*}$-spoIID-FLAG spc* | This study |
| **MF8879** | *ΔspoIID amyE::PspoIID$^{0A3*IIID*}$-spoIID-FLAG spc* | This study |
| **MF9174** | *ΔclpP::erm amyE::Phy-spank-spoIID-FLAG spc* | This study |
| **MF9176** | *ΔftsH::erm amyE::Phy-spank-spoIID-FLAG spc* | This study |
| **Strains for microscopic examination of sporulation** | | |
| **Strain** | **Genotype** | **Reference** |
| **MF200** | *thrC::PspoIIQ-gfp erm* | (Eswaramoorthy et al., 2009) |
| **MF6476** | *thrC::PsspA-gfp erm* | This study |
| **MF8853** | *ΔspoIID thrC::PspoIIQ-gfp erm amyE::PspoIID$^{WT}$-FLAG spc* | This study |
| **MF8854** | *ΔspoIID thrC::PspoIIQ-gfp erm amyE::PspoIID$^{0A1*}$-spoIID-FLAG spc* | This study |
| **MF8855** | *ΔspoIID thrC::PspoIIQ-gfp erm amyE::PspoIID$^{0A2*}$-spoIID-FLAG spc* | This study |
| **MF8856** | *ΔspoIID thrC::PspoIIQ-gfp erm amyE::PspoIID$^{0A3*}$-spoIID-FLAG spc* | This study |
| **MF8857** | *ΔspoIID thrC::PspoIIQ-gfp erm amyE::PspoIID$^{0A1*2*}$-spoIID-FLAG spc* | This study |
| **MF8858** | *ΔspoIID thrC::PspoIIQ-gfp erm amyE::PspoIID$^{0A1*3*}$-spoIID-FLAG spc* | This study |

| | | |
|---|---|---|
| **MF8859** | *ΔspoIID thrC::PspoIIQ-gfp erm amyE::PspoIID$^{0A2*3*}$-spoIID-FLAG spc* | This study |
| **MF8860** | *ΔspoIID thrC::PspoIIQ-gfp erm amyE::PspoIID$^{0A1*2*3*}$-spoIID-FLAG spc* | This study |
| **MF8861** | *ΔspoIID thrC::PspoIIQ-gfp erm amyE::PspoIID$^{0A1*2*3*IIID*}$-spoIID-FLAG spc* | This study |
| **MF8862** | *ΔspoIID thrC::PspoIIQ-gfp erm amyE::PspoIID$^{IIID*}$-spoIID-FLAG spc* | This study |
| **MF8863** | *ΔspoIID thrC::PsspA-gfp erm amyE::PspoIID$^{WT}$-FLAG spc* | This study |
| **MF8864** | *ΔspoIID thrC::PsspA-gfp erm amyE::PspoIID$^{0A1*}$-spoIID-FLAG spc* | This study |
| **MF8865** | *ΔspoIID thrC::PsspA-gfp erm amyE::PspoIID$^{0A2*}$-spoIID-FLAG spc* | This study |
| **MF8866** | *ΔspoIID thrC::PsspA-gfp erm amyE::PspoIID$^{0A3*}$-spoIID-FLAG spc* | This study |
| **MF8867** | *ΔspoIID thrC::PsspA-gfp erm amyE::PspoIID$^{0A1*2*}$-spoIID-FLAG spc* | This study |
| **MF8868** | *ΔspoIID thrC::PsspA-gfp erm amyE::PspoIID$^{0A1*3*}$-spoIID-FLAG spc* | This study |
| **MF8869** | *ΔspoIID thrC::PsspA-gfp erm amyE::PspoIID$^{0A2*3*}$-spoIID-FLAG spc* | This study |
| **MF8870** | *ΔspoIID thrC::PsspA-gfp erm amyE::PspoIID$^{0A1*2*3*}$-spoIID-FLAG spc* | This study |
| **MF8871** | *ΔspoIID thrC::PsspA-gfp erm amyE::PspoIID$^{0A1*2*3*IIID*}$-spoIID-FLAG spc* | This study |
| **MF8872** | *ΔspoIID thrC::PsspA-gfp erm amyE::PspoIID$^{IIID*}$-spoIID-FLAG spc* | This study |
| **MF8883** | *ΔspoIID thrC::PspoIIQ-gfp erm amyE::PspoIID$^{0A3*IIID*}$-spoIID-FLAG spc* | This study |
| **MF8884** | *ΔspoIID thrC::PsspA-gfp erm amyE::PspoIID$^{0A3*IIID*}$-spoIID-FLAG spc* | This study |

**Table IV-3. List of Plasmids used in this study**

| Plasmid | Description | Reference |
|---|---|---|
| **pDR244** | *cre* plasmid with temperature-sensitive replication origin in *B. subtilis* | (Koo et al., 2017) |
| **pMF752** | *thrC::PsspA-gfp erm* | This study |
| **pMF959** | *amyE::Phy-spank-spoIID-FLAG spc* | This study |
| **pMF960** | *amyE::PspoIID-spoIID-FLAG spc* | This study |
| **pMF961** | *amyE:: PspoIID$^{0A1*}$-spoIID-FLAG spc* | This study |
| **pMF962** | *amyE:: PspoIID$^{0A2*}$-spoIID-FLAG spc* | This study |
| **pMF963** | *amyE:: PspoIID$^{0A3*}$-spoIID-FLAG spc* | This study |
| **pMF964** | *amyE:: PspoIID$^{0A1*2*}$-spoIID-FLAG spc* | This study |
| **pMF965** | *amyE:: PspoIID$^{0A1*3*}$-spoIID-FLAG spc* | This study |
| **pMF966** | *amyE:: PspoIID$^{0A2*3*}$-spoIID-FLAG spc* | This study |
| **pMF967** | *amyE:: PspoIID$^{0A1*2*3*}$-spoIID-FLAG spc* | This study |
| **pMF968** | *amyE:: PspoIID$^{0A1*2*3*IIID*}$-spoIID-FLAG spc* | This study |

| | | |
|---|---|---|
| **pMF969** | *amyE:: PspoIID$^{IIID*}$-spoIID-FLAG spc* | This study |
| **pMF985** | *amyE::PspoIID$^{0A3*IIID*}$ -spoIID-FLAG spc* | This study |

**Table IV-4. List of Primers used in this study**

| Primers | Sequence |
|---|---|
| **om244** | 5'-ccggaattcgctttgttgatttcgagccgtatattc-3' |
| **om245** | 5'-cggaagcttctcacctccttgtgagtatagaatgtg-3' |
| **om344** | 5'-gccggatccgacaaatgtggatgactttacc-3' |
| **om412** | 5'-ggcgaattcgcagacatcgaacgtgtaaat-3' |
| **om420** | 5'-ctagccggttctcccgagcaggaggcagctgaat-3' |
| **om421** | 5'-gggagaaccggctagtctagtctatgggcaggg-3' |
| **om422** | 5'-tcccgagcaggaggcagctgaagcttggc-3' |
| **om425** | 5'-gccgtcgacagcaggaggcagctgaatatgaaac-3' |
| **om426** | 5'-gccgcatgcgacaaatgtggatgactttacc-3' |
| **om427** | 5'-ctttttcgccatatatttattcaaaaacgcatc-3' |
| **om428** | 5'-gaataaatatatggcgaaaaaggattataaggatcatgatggtg-3' |
| **om429** | 5'-gacgcccaatgagcgtctttttctacttgtcgtcatcgtctttgtagtc-3' |
| **om430** | 5'-gacaagtagaaaaagacgctcattgggcgtc-3' |
| **om433** | 5'-ctttaaacctgaagcgctgaaagcc-3' |
| **om434** | 5′-ggctttcagcgcttcaggtttaaag-3′ |

IV.ii.2 Culture Conditions

Luria-Bertani (LB) medium (Sambrook & Russell, 2001) was used for routine growth of *E. coli* and *B. subtilis*. Difco sporulation medium (DSM) was used for the sporulation of *B. subtilis* (Harwood & Cutting, 1990). Cell growth in liquid media was checked using a spectrophotometer by reading the optical density at 600 nm ($OD_{600}$). 1.5% agar was included in the media for making solid agar plates.

For typical culture conditions, the overnight culture in 5 ml LB was transferred to 10 ml of fresh LB at $OD_{600}$ = 0.05 and shaken at 37 °C at 150 rpm until $OD_{600}$ = 0.5. Cells were then transferred to 20 ml DSM supplemented at OD600 = 0.05. Cells of a strain harboring an IPTG-inducible *spoIID* were grown under similar

conditions to the non-inducible strains, with the addition of IPTG to culture media where appropriate. For Time-lapse microscopy, cells grown in fresh LB were spotted on DSM plates and incubated overnight at 37°C. The colonies growing on DSM agar plates for 12 hrs. were resuspended in 1X T-Base and spotted on special agarose pads made with MSgg + 0.005% Glutamate facilitating the starvation conditions.

When appropriate, antibiotics were included at the following concentrations: 10 µg $ml^{-1}$ of tetracycline, 100 µg $ml^{-1}$ of spectinomycin, 20 µg $ml^{-1}$ of kanamycin, 5 µg $ml^{-1}$ of chloramphenicol and 1 µg $ml^{-1}$ of erythromycin. Isopropyl Beta-D-thiogalactopyranoside (IPTG) was added to the medium at the indicated concentrations when appropriate.

### IV.ii.3 Viable and Spore Count Assays

For assessing the sporulation capability of different mutant strains, viable and spore count assays were performed. The total numbers of viable cells in the sporulation medium were determined by plating serial dilutions of cells on DSM agar plates and then counting the colonies. These serial dilutions were incubated in a water-bath at 80 °C for 10 min and then plated again on DSM plates in order to obtain the spore counts. The detailed description of viable and spore count assays is given in Figure IV-1.

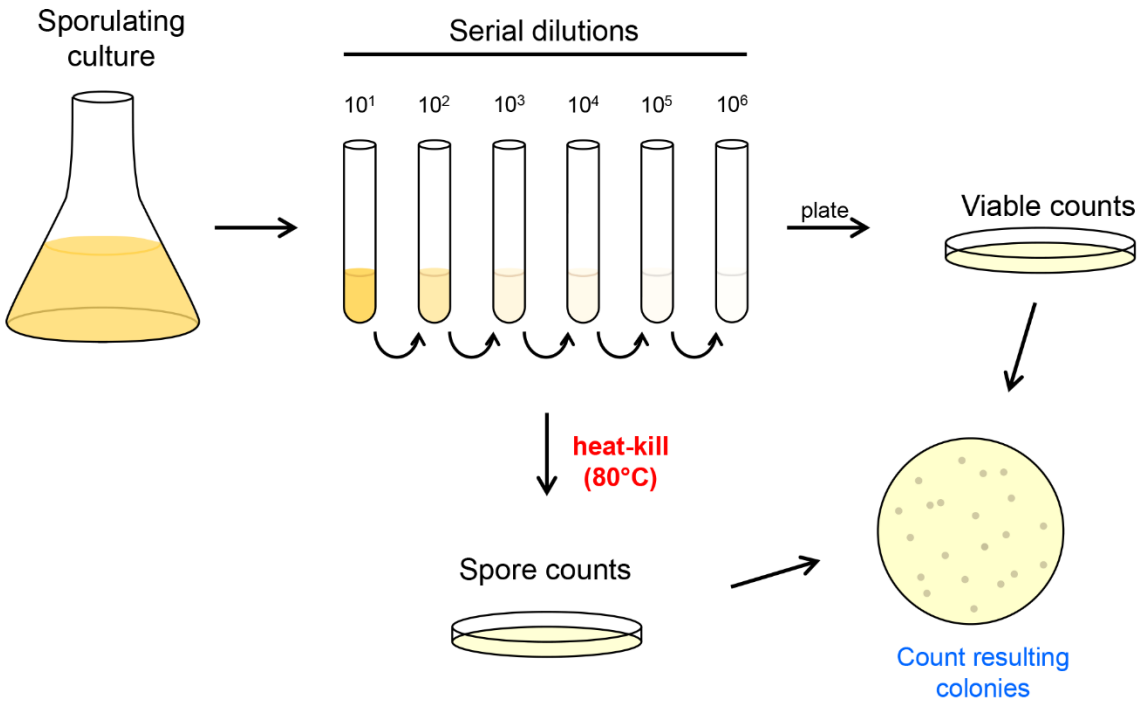


**Figure IV-1. A detailed description of Viable and Spore count assays.**
A drawing indicating the method for performing Viable and Spore count assays in DSM culture. Wild-type and mutant strains are grown in DSM and samples are taken at a certain time-point and processed as shown above in order to assess the sporulation ability of the cultures.

### IV.ii.4 Fluorescence Microscopy

Cells expressing fluorescent proteins were imaged using an Olympus BX61 microscope with an Olympus UPlanFL N 100x Microscope Objective and a Hamamatsu Photonics Camera C4742-95. For Time-lapse Microscopy, slides were mounted and imaging was done over a period of 9 hours, taking images of the fixed field every half an hour. Data collection and image processing were performed using SlideBook image analysis software (Intelligent Imaging Innovations, Inc.).

IV.ii.5 Immunoblots

Immunoblot analysis was performed with monoclonal anti-FLAG M2 (Sigma-Aldrich), polyclonal anti-SpoIID antibodies (a gift from David Rudner) (Doan & Rudner, 2007), and polyclonal anti-$\sigma^A$ antibodies (Fujita, 2000). Anti-Mouse IgG (whole molecule)-Alkaline Phosphatase (Sigma-Aldrich) was used as the secondary antibody for Monoclonal anti-FLAG M2. Anti-Rabbit IgG (Fc), Alkaline Phosphatase Conjugate (Promega) was used as the secondary antibody for polyclonal anti-SpoIID and anti-$\sigma^A$ antibodies. BCIP/NBT (5-bromo-4-chloro-3-indolyl-phosphate/nitro blue tetrazolium) color development substrate (Promega) was for the colorimetric detection of alkaline phosphatase on the secondary antibody. The intensities of each band were quantified with an image analyzer (FluorChem; Alpha Innotech). $\sigma^A$, a constitutively expressed protein, was used as a loading control. The protein levels were normalized to both the levels of $\sigma^A$ and then the levels of each of the corresponding proteins in the wild-type strain. For quantification of cellular concentration of SpoIID, the purified FLAG-BAP™ fusion protein was serially diluted and processed for immunoblot analysis with monoclonal anti-FLAG M2. Crude cell extracts containing SpoIID-FLAG were also serially diluted, run on the same gel with the purified FLAG-BAP™ fusion protein, and processed for immunoblot using monoclonal anti-FLAG M2. Then, the SpoIID-FLAG protein levels were determined with a serially diluted FLAG-BAP™ fusion protein as a standard.

III.ii.5 Bioinformatics Approach

A homology search was performed using the blast program (Johnson et al., 2008) with the *spoIID* (*B. subtilis* PY79) promoter region containing three 0A boxes, one IIID box, and the -35 and -10 elements of the $\sigma^E$ promoter against the bacterial genome database. CLUSTAL Omega program from EMBL-EBI was used for multiple sequence alignment of promoter recognition sequences in different species. Pairwise sequence alignment was carried out to determine the percentage similarity between the selected candidate *spoIID* and *Bacillus subtilis spoIID* using EMBOSS water program from EMBL-EBI (Madeira, Park, et al., 2019) (Sauer et al., 1995).

## IV.iii Results

IV.iii.1 Strains with a mutated 0A3 box produce less number of spores

To assess the biological significance of the mother cell-specific Spo0A activity, I tested whether 0A~P and SpoIIID binding to the *spoIID* promoter region plays a role in controlling sporulation. In order to accomplish this task, I systematically constructed a series of strains that express SpoIID under the control of the *spoIID* promoter containing either single or combinations of the mutated 0A1*, 0A2*, 0A3*, and IIID* boxes. For this purpose, first, a 3x FLAG tag sequence was fused in-frame at the C-terminal of the *spoIID* coding region. Second, the FLAG-tagged *spoIID* construct was placed under the control of either the wild type or the mutated *spoIID* promoter. Then, each of the resulting constructs was introduced as a single

copy at the *amyE* locus of the chromosome of a strain harboring the *spoIID* gene knockout.

The cells of these newly constructed SpoIID-FLAG strains under the control of wild- type and mutated *spoIID* promoters were cultured under sporulation conditions in DSM. Spore count assays were performed at 6 (T6) and 20 (T20) hours after the onset of sporulation as described in Materials and Methods.

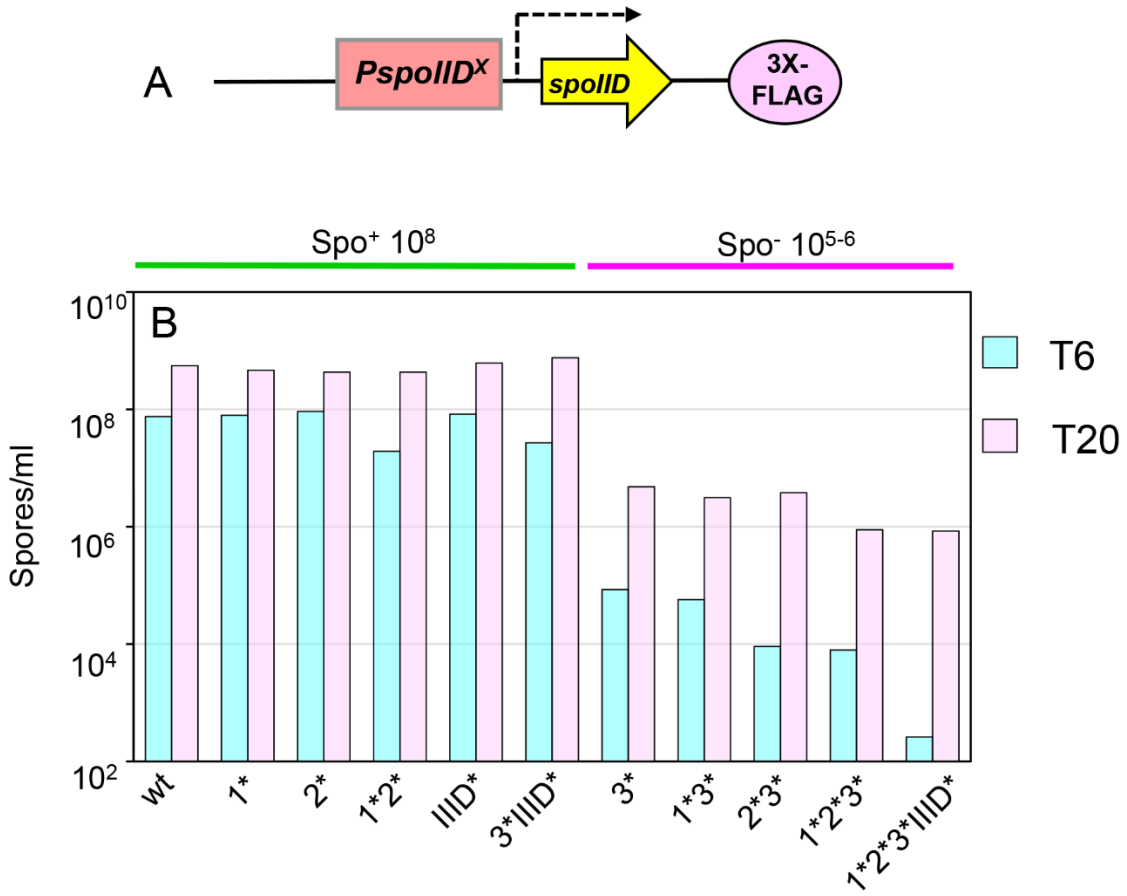


**Figure IV-2. Spore count assays of SpoIID-FLAG strains under the control of wild-type and mutated *spoIID* promoters.**
(A) Schematic diagram of SpoIID-FLAG strains under the control of different *spoIID* promoters. (B) Graph showing spores/ml counted at an early time point (T6) and a late time point (T20). Cells were cultured under sporulation conditions in DSM at T6 (cyan) or six hours and T20 (pink) or twenty hours after the onset of sporulation. Spore count assays were performed as described in Materials and Methods. Note that the asterisk indicates the mutated 0A box and IIID box in the *spoIID* promoter.

Wild type strain formed $10^7$ spores $ml^{-1}$ at an early time point (T6) and $10^8$ spores $ml^{-1}$ at a late time point (T20). Strains with either 0A1*, 0A2*, or IIID* mutation formed similar levels of spores to those in the wild type strain (Figure IV-2). Whereas, 0A3*, 0A1*3*, 0A2*3*, 0A1*2*3*, or 0A1*2*3*IIID* mutants produced fewer numbers of spores ($10^{2-4}$ spores $ml^{-1}$ culture at T6 and $10^{5-6}$ spores $ml^{-1}$ culture at T20) than the wild type strain ($10^7$ spores $ml^{-1}$ culture at T6 and $10^8$ spores $ml^{-1}$ culture at T20) (Figure IV-2). Strains with either the 0A1*2*3* or 0A1*2*3*IIID* mutation showed a further drop in the numbers of spores ($10^5$ spores $ml^{-1}$ culture at T20) as compared with the 0A3*, 0A1*3*, and 0A2*3* mutant strains ($10^6$ spores $ml^{-1}$ culture at T20) (Figure IV-2). We found that lesser numbers of spores were formed in the 0A1*2* and 0A3*IIID* strains ($10^7$ spores $ml^{-1}$ culture) than in the wild type strain ($10^8$ spores $ml^{-1}$culture) at T6, while sporulation in these mutants was restored to approximately the wild type levels at T20 ($10^8$ spores $ml^{-1}$ culture) (Figure IV-2). In the strain harboring the *spoIID* deletion (MF7436 *ΔspoIID*), no spores were detected (<10 spores $ml^{-1}$ culture) (Figure IV-9). These results indicate that the 0A3 box primarily plays an important role in controlling *spoIID* expression, resulting in proper sporulation.

IV.iii.2 Spores in 0A-3 box mutants have abnormal (bulging) phenotype

In the wild type strain, the SpoIID-SpoIIM-SpoIIP complex is required for hydrolysis of the septal peptidoglycan, leading to forespore engulfment (Eichenberger et al., 2001). As previously reported, (Eichenberger et al., 2001; Pogliano et al., 1999) the hydrolysis of the septal peptidoglycan does not extend

to the edges and thus prevents engulfment from proceeding in the *spoIID* mutant. This leads to the bulge formation of the forespore compartment into the mother cell chamber.

Based on these results, I hypothesized that the sporulation-deficient phenotype caused by the 0A3* mutation in the *spoIID* promoter region (Figure IV-2) would be arrested prior to the stage of engulfment, leading to the bulging formation. To test this hypothesis, we constructed a set of strains with reporter genes that are expressed in a stage- and compartment-specific manner. For the event before the completion of engulfment, we constructed a forespore-specific $\sigma^F$-controlled *spoIIQ* promoter fusion to the GFP reporter gene ($P_{spoIIQ}$-*gfp*) (Figure IV-3A). For the event after the completion of engulfment, we constructed a forespore-specific $\sigma^G$-controlled *sspA* promoter fusion to the GFP reporter gene ($P_{sspA}$-*gfp*) (Figure IV-4A). Then, each of these reporter constructs was introduced at the *thrC* locus of the chromosome as a single copy in each of the strains that expresses SpoIID under the control of the *spoIID* promoter containing either single or combinations of the 0A and IIID box mutations.

**Figure IV-3. Effects of 0A box and IIID box mutations in the *spoIID* promoter on $\sigma^F$ activities.**

(A) Schematic diagram depicting the different *spoIID* constructs in which forespore-specific $\sigma^F$ controlled $P_{spoIIQ}$ is fused to *gfp*. (B) Fluorescence microscopy images of the $\sigma^F$ ($P_{spoIIQ}$-*gfp*) reporter constructs with mutated *spoIID* promoters. The mutations in the *spoIID* promoter region are labeled on the left. The sampling time points are indicated on the top of the images, ranging from T1 (one hour) to T4 (four hours) after the onset of sporulation. The samples were processed for fluorescence microscopy as mentioned in Materials and Methods. The white arrowheads highlight the abnormal (bulging) phenotypes. Scale bar is 2 µm.

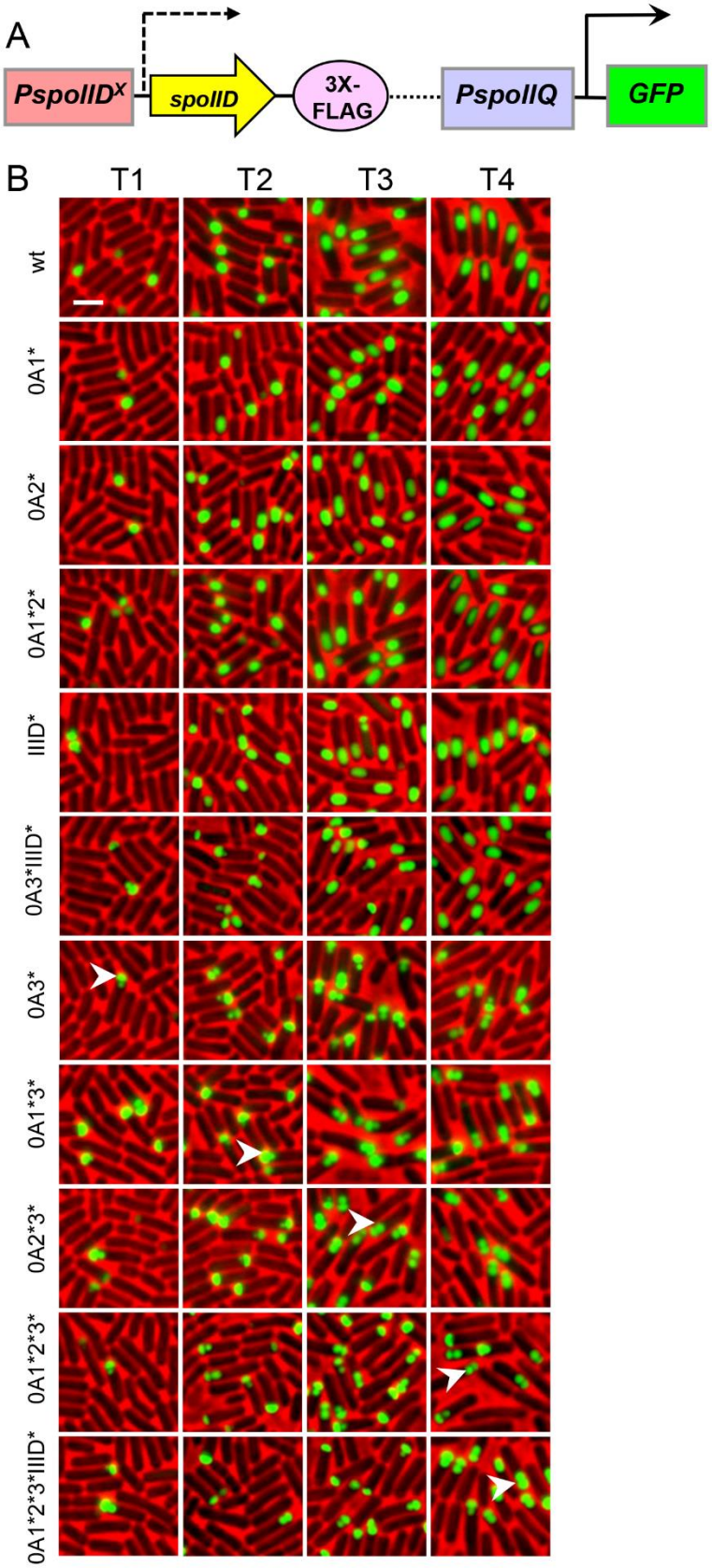
A
PspoIIDX
spoIID
3X-FLAG
PspoIIQ
GFP
B
T1
T2
T3
T4
wt
0A1*
0A2*
0A1*2*
IIID*
0A3*IIID*
0A3*
0A1*3*
0A2*3*
0A1*2*3*
0A1*2*3*IIID*

**Figure IV-4. Effects of 0A box and IIID box mutations in the *spoIID* promoter on $\sigma^G$ activities.**

(A) Schematic diagram depicting the different *spoIID* constructs in which forespore-specific $\sigma^G$ controlled $P_{sspA}$ is fused to *gfp*. (B) Fluorescence microscopy images of the $\sigma^G$ ($P_{sspA}$-*gfp*) reporter constructs with mutated *spoIID* promoters. The mutations in the *spoIID* promoter region are labeled on the left. The sampling time points are indicated on the top of the images, ranging from T2 (two hours) to T6 (four hours) after the onset of sporulation. The samples were processed for fluorescence microscopy as mentioned in Materials and Methods. The white arrowheads highlight the abnormal (bulging) phenotypes. Scale bar is 2 µm.

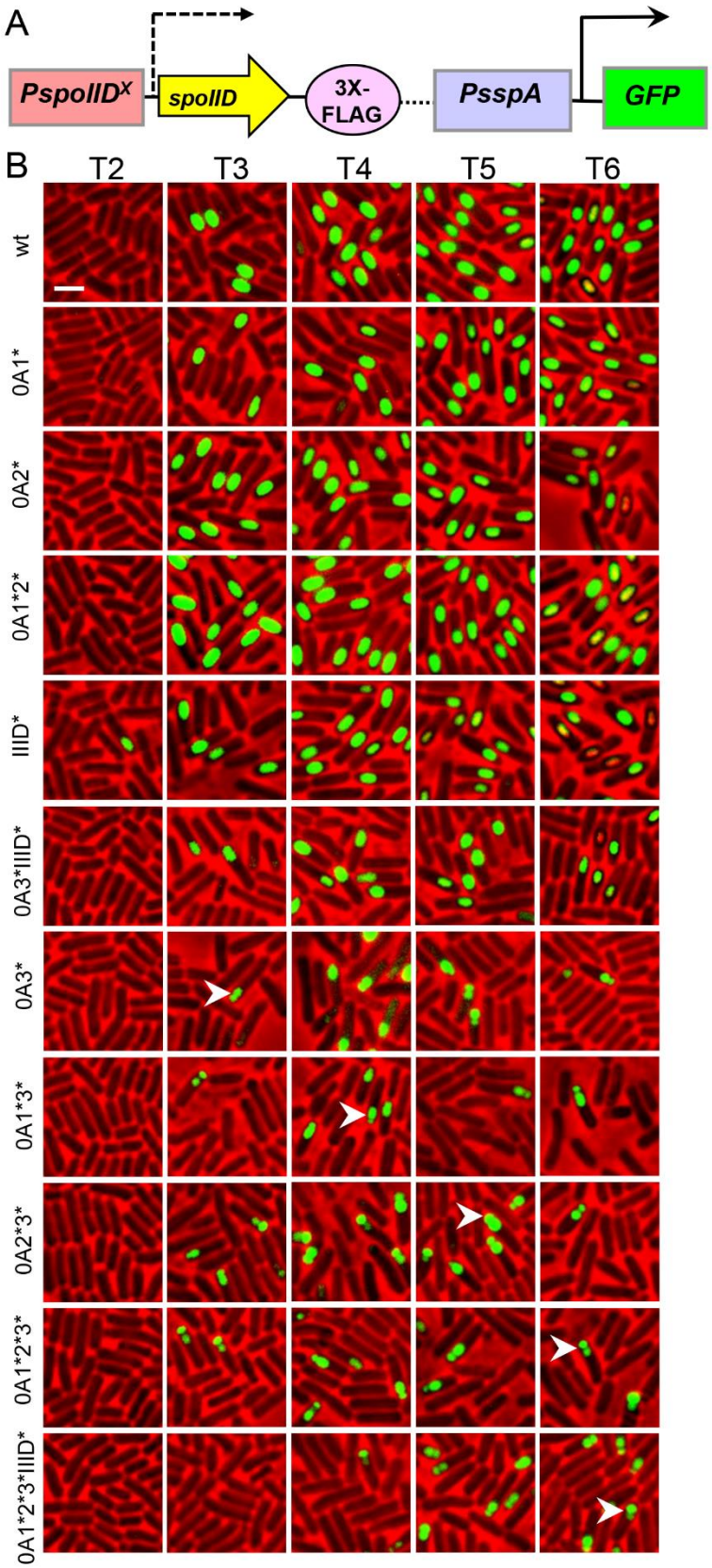
A
PspoIIDX
spoIID
3X-FLAG
PsspA
GFP
B
T2
T3
T4
T5
T6
wt
0A1*
0A2*
0A1*2*
IIID*
0A3*IIID*
0A3*
0A1*3*
0A2*3*
0A1*2*3*
0A1*2*3*IIID*

**Table IV-5. Fluorescence signal counts in $P_{spoIIQ}$-*gfp* reporter constructs**

| $P_{spoIIQ}$-*gfp* at T2 | | | | | | |
|---|---|---|---|---|---|---|
| **Mutations in the *spoIID* promoter region** | **Total spores** | **Normal spores** | **Abnormal spores** | **% Normal spores** | **% Abnormal spores** | **Total cells scored** |
| WT | 183 | 183 | 0 | 100.0 | 0.0 | 1795 |
| 0A1* | 155 | 155 | 0 | 100.0 | 0.0 | 1794 |
| 0A2* | 358 | 358 | 0 | 100.0 | 0.0 | 1555 |
| 0A1*2* | 234 | 234 | 0 | 100.0 | 0.0 | 1572 |
| IIID* | 397 | 397 | 0 | 100.0 | 0.0 | 1736 |
| 0A3*+IIID* | 337 | 297 | 40 | 88.1 | 11.9 | 1734 |
| 0A3* | 233 | 191 | 42 | 82.0 | 18.0 | 1726 |
| 0A1*3* | 214 | 194 | 20 | 90.7 | 9.3 | 1820 |
| 0A2*3* | 249 | 219 | 30 | 88.0 | 12.0 | 1305 |
| 0A1*2*3* | 373 | 313 | 60 | 83.9 | 16.1 | 1628 |
| 0A 1*2*3*IIID* | 154 | 130 | 24 | 84.4 | 15.6 | 1654 |

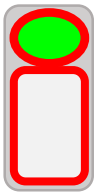

(a)

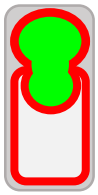

(b)

(a) Illustration of Normal spores and (b) Abnormal spores observed during $P_{spoIIQ}$-*gfp* microscopy

**Table IV-6. Fluorescence signal counts in $P_{sspA}$-*gfp* reporter constructs**

| ***$P_{sspA}$-gfp* at T6** | | | | | | |
|---|---|---|---|---|---|---|
| **Mutations in the *spoIID* promoter region** | **total spores** | **normal spores** | **abnormal spores** | **% normal spores** | **% abnormal spores** | **total cells scored** |
| WT | 801 | 801 | 0 | 100.0 | 0.0 | 1228 |
| 0A1* | 574 | 574 | 0 | 100.0 | 0.0 | 1119 |
| 0A2* | 187 | 187 | 0 | 100.0 | 0.0 | 333 |
| 0A1*2* | 703 | 703 | 0 | 100.0 | 0.0 | 1379 |
| IIID* | 310 | 310 | 0 | 100.0 | 0.0 | 797 |
| 0A3*+IIID* | 331 | 321 | 10 | 97.0 | 3.0 | 1576 |
| 0A3* | 29 | 6 | 23 | 20.7 | 79.3 | 1670 |
| 0A1*3* | 23 | 10 | 13 | 43.5 | 56.5 | 1426 |
| 0A2*3* | 6 | 0 | 6 | 0.0 | 100.0 | 833 |
| 0A1*2*3* | 64 | 8 | 56 | 12.5 | 87.5 | 1443 |
| 0A1*2*3*IIID* | 236 | 15 | 221 | 6.4 | 93.6 | 1573 |

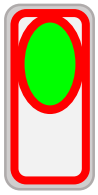

(c)

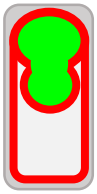

(d)

(c) Illustration of Normal spores and (d) Abnormal spores observed during $P_{sspA}$-*gfp* microscopy

As shown in Table IV-5, Similar numbers of GFP signals from the forespore-specific $\sigma^F$ controlled $P_{spoIIQ}$-*gfp* were observed in the 0A box mutants and the wild type cells (Figure IV-3B and Table IV-5). These results suggest that all strains efficiently entered sporulation by activating $\sigma^F$. In contrast, the number of GFP signals from the forespore-specific $\sigma^G$ controlled $P_{sspA}$-*gfp* diverged in several mutants. In the strains having the 0A3* mutation with the $P_{sspA}$-*gfp* reporter, including 0A3*, 0A1*3*, 0A2*3*, 0A1*2*3*, and 0A1*2*3*IIID*, we found decreasing number of GFP expressing cells (Figure IV-4B and Table IV-6).

These results suggest that the 0A3* mutation causes a defect in the engulfment of sporulating cells, leading to a decreased number of spores. All the other mutant strains 0A1*, 0A2*, 0A1*2*, and IIID* with the $P_{spoIIQ}$-*gfp* reporter (Figure IV-3B and Table IV-5) and $P_{sspA}$-*gfp* reporter (Figure IV-4B and Table IV-6) exhibited a normal sporulation phenotype, similar to the wild type strain. When the 0A3* mutation was combined with the IIID* mutation, the resulting strain (0A3*IIID*) restored sporulation at nearly similar levels to the wild type strain in both the reporter constructs (Tables IV-5 and IV-6).

I further found that a certain number of cells with the 0A3* mutation (including 0A3*, 0A1*3*, 0A2*3*, 0A1*2*3*, 0A1*2*3*IIID* and 0A3*IIID*) showed a bulging forespore phenotype, which is visualized in both the reporters, the $\sigma^F$ controlled $P_{spoIIQ}$-*gfp* and the $\sigma^G$-controlled $P_{sspA}$-*gfp* reporter. The percentage of cells showing the bulging phenotype is smaller in the $\sigma^F$ controlled $P_{spoIIQ}$-*gfp* reporter (Table IV-5) as compared to the percentage of cells in the $\sigma^G$-controlled $P_{sspA}$-*gfp* reporter (Table IV-6).

A similar bulging phenotype has been previously reported (Eichenberger et al., 2001; Pogliano et al., 1999) in the Δ*spoIID* mutant. These results suggest the importance of the 0A3 box for the proper completion of the engulfment process necessary for the progression of sporulation.

Normally, $\sigma^G$ becomes active in the forespore upon completion of engulfment (Harwood & Cutting, 1990). Therefore, the smaller number of $P_{sspA}$-*gfp* expressing cells with 0A3* mutations suggests that these cells are able to activate $\sigma^G$ in the bulging forespore.

IV.iii.3 Time-Lapse Microscopy reveals that strains with a mutated 0A3 box do not produce phase bright spores

For observing the completion of sporulation by the 0A3* mutants, I did a prolonged time course (T3-T46) microscopy experiment, comparing the wild type and 0A3* mutants expressing GFP from the $P_{sspA}$-*gfp* reporter. Representative time points from this experiment are shown below in Figure IV-5. As expected, wild type cells progressed through sporulation normally. In the wild type cells, GFP signals faded away gradually and the number of phase-bright spores increased T12 onwards (Figure IV-5). In contrast, 0A3* mutants exhibited lower and abnormal (bulging) GFP signals and significantly reduced the number of phase bright spores throughout the course of the experiment.

Interestingly, some of the abnormal (bulging) signals faded gradually in these mutants. A time-lapse microscopy experiment was performed, in order to observe the cell fate of the 0A3* mutants producing bulging phenotypes (Figure IV-6)

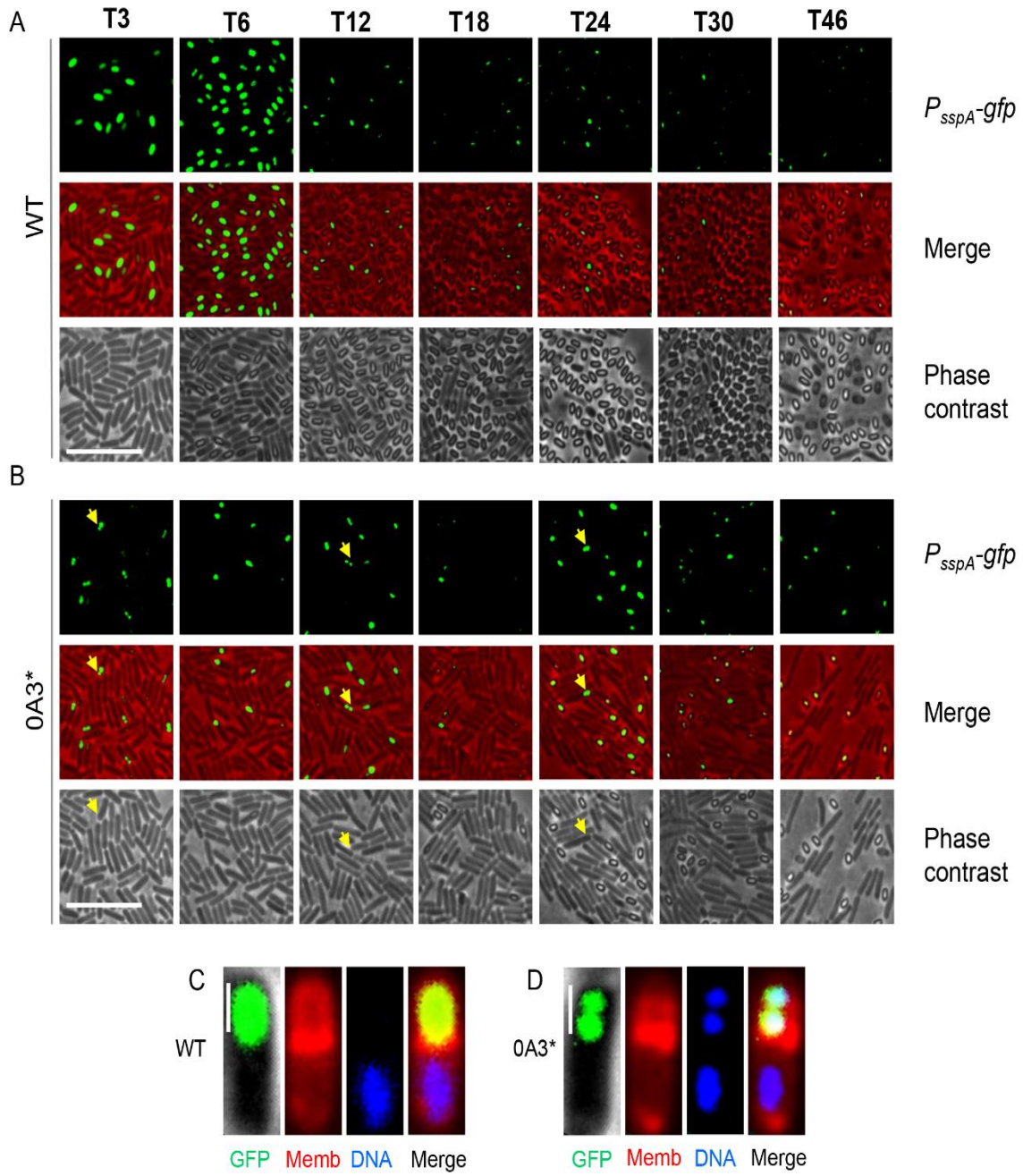


**Figure IV-5. Prolonged time course microscopy of wild type and 0A3* mutant expressing forespore specific $\sigma^G$ controlled *$P_{sspA}$-gfp*.**
All cells were grown in DSM and imaged at the indicated time points, relative to the onset of sporulation, which is defined as T0. A) Wild type images are shown in the top three panels. B) 0A3* images are shown in the bottom three panels. Yellow arrows point toward the abnormal (bulging) signals in the 0A3* mutant observed throughout the experiment. Scale bar for A and B is 10 µm. Enlarged representative examples of WT (C) and 0A3* (D) membrane staining images are shown. GFP, membrane, and DNA images are shown in green, red, and blue respectively. Scale bar for C and D is 1 µm.

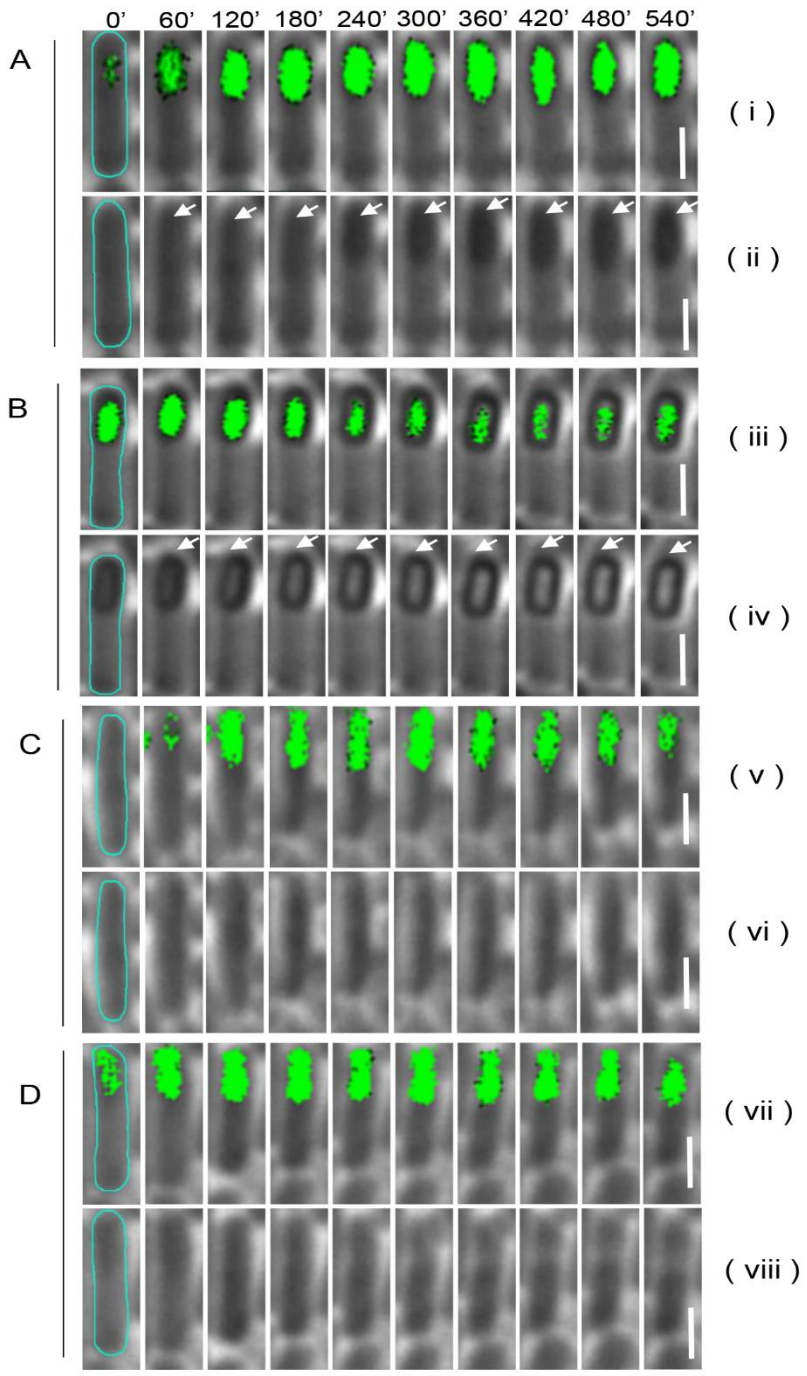


**Figure IV-6. Time-lapse microscopy of wild type and 0A3* mutant expressing forespore specific $\sigma^G$ controlled *$P_{sspA}$-gfp*.**

Time-lapse images of the wild type strains (panels AB) and the 0A3* mutant strains (panels CD) were captured up to 9 hours (540 min) to show the normal and bulging spore shapes. The choice of time zero in each panel is arbitrary in a continuous incubation of the cells on the agarose pad with MSgg + 0.005% glutamate medium. Cell periphery was outlined in each of the panels on the left-hand side. White arrows in panels A-ii and B-iv show the forespore and phase bright spore development, respectively. Scale bar, 2 µm.

Sporulation cultures are heterogeneous, where not all the cells start differentiation programs at the same time (Narula et al., 2016; Veening, Smits, Hamoen, Jongbloed, & Kuipers, 2004) and therefore, I could capture wild type cells in early and later stages of sporulation during the time-lapse microscopy. The images in panel A of Figure IV-6, show a wild type cell in the early stages of sporulation. The $P_{sspA}$-*gfp* signals increased gradually in this cell over time (Panel A-i), and so did the development of forespore (Panel A-ii). Another wild type cell in the later stages of sporulation was captured in panel B. In this cell, the gradual fading of the $P_{sspA}$-*gfp* signals (Panel B-iii), as well as the development of a phase bright spore was noticed (Panel B-iv).

Similarly, two cells of 0A3* mutants are shown in Figure IV-6 (Panels C & D). In both the 0A3* mutant cells, a common trend was observed. The $P_{sspA}$-*gfp* signals were abnormal and they faded gradually (Panels C-v and D-vii), without any visible forespore or phase bright spore development (Panel C-vi and D-viii). These results indicate that a certain number of cells harboring the 0A3* mutation are able to activate $\sigma^G$, but the majority of those cells fail to complete sporulation.

Altogether, these results suggest that binding of 0A~P to 0A3 is indispensable for the proper *spoIID* expression, leading to proper forespore engulfment and sporulation.

IV.iii.4 Strains containing 0A3 box mutation have altered SpoIID expression patterns

Understanding the mechanisms underlying the effects of 0A box mutations on sporulation is important. Our hypothesis is that the 0A3* box mutation alters the expression level and/or timing of SpoIID, leading to sporulation defect. To test this hypothesis, we directly measured SpoIID expression levels in each of the mutant strains cultured under sporulation conditions using immunoblot analysis.

As shown in Figure IV-7, cells of these strains were cultured in DSM, harvested every hour from one hour (T1) to five hours (T5) after the onset of sporulation (T0), and analyzed SpoIID expression levels with immunoblotting using anti-FLAG (Sigma-Aldrich) and also anti-SpoIID antibodies (Doan & Rudner, 2007). To normalize for loading variations, $\sigma^A$, a constitutively expressed house-keeping σ factor, was immunodetected with anti-$\sigma^A$ antibodies and used to adjust the total amount of proteins in each sample (Fujita, 2000).

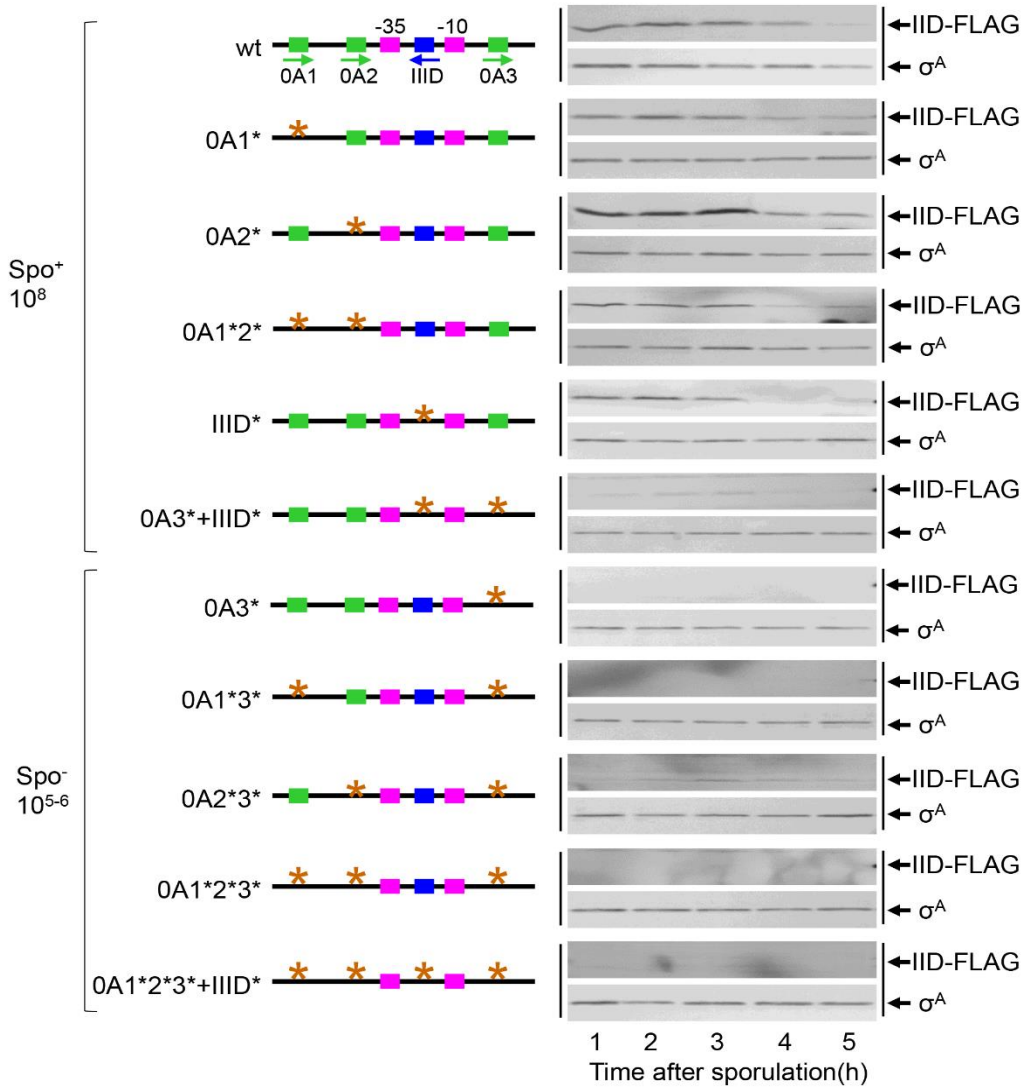


**Figure IV-7. Individual immunoblots of wild type and *spoIID* promoter mutants as detected by IID-FLAG antibodies.**

SpoIID protein levels were determined in a series of strains that express SpoIID-FLAG under the control of the *spoIID* promoter containing either single or combinations of the mutated 0A1*, 0A2*, 0A3*, and IIID* boxes. Cells of the strains expressing SpoIID-FLAG from the wild type and mutant promoters of *spoIID* were cultured in DSM and samples were taken every one hour between T1 and T5. Total cell extracts (10 μg) were prepared, separated by SDS-PAGE, and subjected to immunoblotting with anti-Flag monoclonal antibody (Sigma). Constitutively expressed $\sigma^A$ subunit of RNAP from the total cell extracts (2 μg) was detected by $\sigma^A$ antibodies and used as a loading control. Schematic positions of the wild-type and mutated 0A- and IIID-boxes (*indicates the mutated box) relative to the -35 and -10 elements of $\sigma^E$ promoter are shown on the left side of each gel panel. Approximate numbers of spores per ml culture based on the data from Figure IV-2 are indicated on the left.

**Figure IV-8. Comparison of the SpoIID expression levels expressed in each of the wild type and the box mutant strains at T2.**

A comprehensive comparison of SpoIID expression levels was performed on a series of FLAG-tagged *spoIID* constructs. Total cell extracts (10 µg) from T2 cells were separated by SDS-PAGE and subjected for immunoblot analysis using anti-FLAG monoclonal antibody (Sigma, panels A and D) and anti-SpoIID polyclonal antibodies (gift from Dr. David Rudner, Harvard Medical School, panels B, E, and F). The constitutively expressed $\sigma^A$ subunit of RNAP was detected by $\sigma^A$ antibodies and used as a loading control (panels C and G). Molecular mass markers (Thermo Scientific™ Spectra™ Multicolor Broad Range Protein Ladders) are indicated in kDa on the left. Panels E and F are identical, but the intensities of their bands were enhanced uniformly by auto-contrast in Adobe Photoshop. Strains harboring the FLAG-tagged *spoIID* construct are indicated on the top of each panel. Arrows in the gel denote the positions of SpoIID and SpoIID-FLAG proteins.

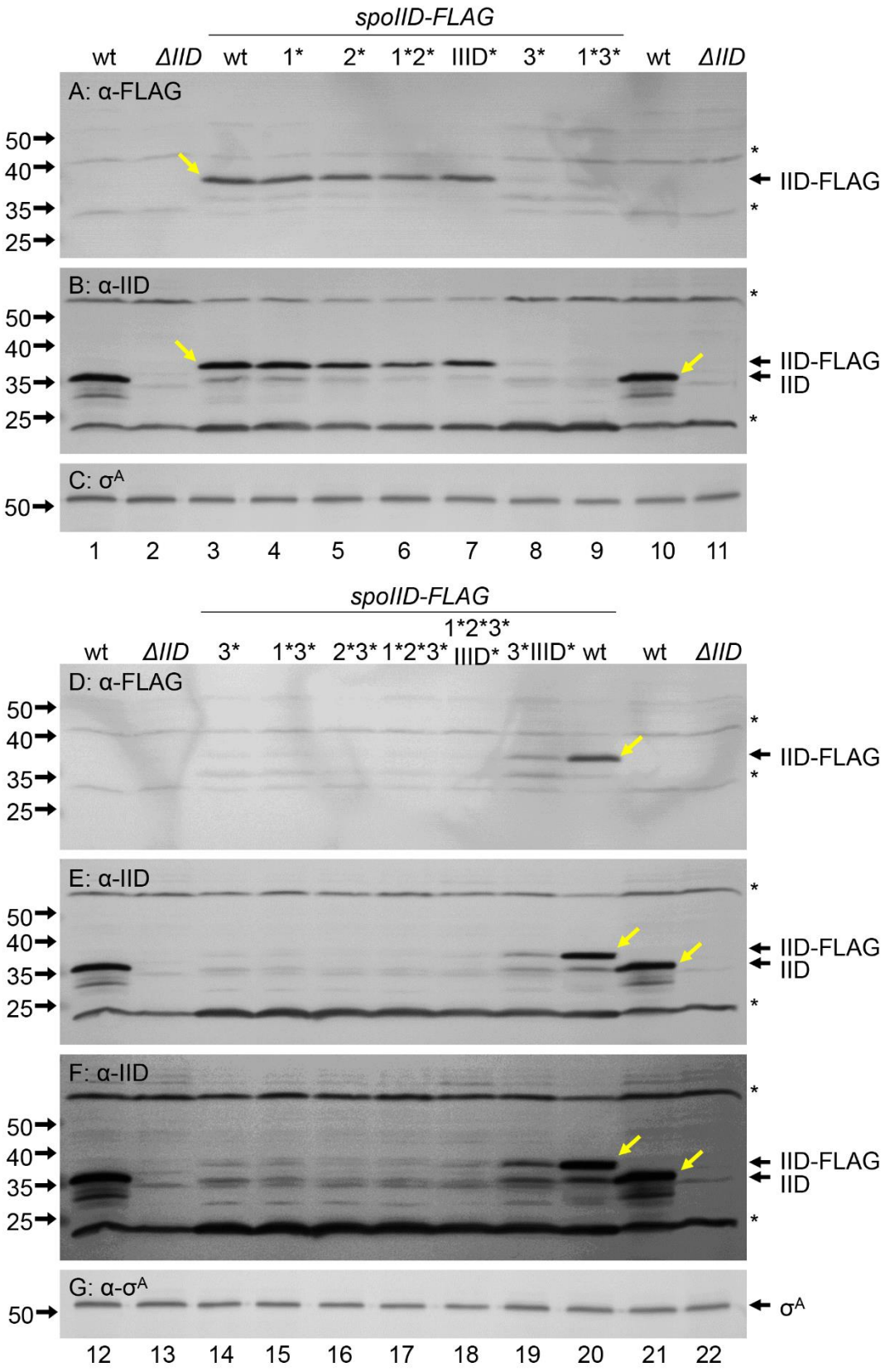
spoIID-FLAG
wt
ΔIID
wt
1*
2*
1*2*
IIID*
3*
1*3*
wt
ΔIID
A: α-FLAG
50
40
35
25
IID-FLAG
B: α-IID
IID-FLAG
IID
C: σA
50
1 2 3 4 5 6 7 8 9 10 11
spoIID-FLAG
wt
ΔIID
3*
1*3*
2*3*
1*2*3*
1*2*3* IIID*
3*IIID*
wt
wt
ΔIID
D: α-FLAG
IID-FLAG
E: α-IID
IID-FLAG
IID
F: α-IID
IID-FLAG
IID
G: α-σA
σA
12 13 14 15 16 17 18 19 20 21 22

The results indicate that similar levels of SpoIID were detected in the 0A1*, 0A2*, IIID*, and wild type strains, while the levels were slightly lower in the 0A1*2* strain (Figure IV-7 and IV-8A). All these mutants produce a similar number of spores as compared to the wild type strain ($10^8$ spores $ml^{-1}$ of culture) as seen before in Figure IV-2. Thus, it is clear that strains with intact (unimpaired) sporulation also exhibit normal SpoIID expression levels.

In contrast, in the 0A3*, 0A1*3*, 0A2*3*, 0A1*2*3*, and 0A1*2*3*IIID* strains, SpoIID expression levels significantly decreased (Figure IV-7). Even though the SpoIID expression levels are significantly decreased in these mutants (Figure IV-7), they are not completely abolished (Figure IV-8DE). The decreased protein was detected (as faint bands) only when the images were enhanced uniformly by auto-contrast in Adobe Photoshop (Figure IV-8F).

When the 0A3* mutation was combined with the IIID* mutation in the 0A3*IIID* strain (Figure IV-8DEF, lane 19), SpoIID expression levels increased than in the strain harboring the 0A3* mutation alone (Figure IV-8DEF, lane 14). These results suggest that the 0A3 box plays a key role in maintaining sufficient expression levels of SpoIID, thus facilitating sporulation. In contrast, 0A1, 0A2, and IIID boxes appear to be required for modulation or fine-tuning of SpoIID expression timing and level. Interestingly, the *lacZ* reporter activities showed higher levels in the 0A3* mutant than in the wild-type strain, while the SpoIID protein levels were lower in the 0A3* mutant strain than in the wild type strain. These results suggest that SpoIID is unstable when expressed in an inappropriate manner, although the mechanism(s) of instability or degradation of SpoIID remains unclear.

IV.iii.5 Overexpression of SpoIID induces normal sporulation

Next, we determined whether *spoIID* expression is strictly controlled by 0A~P, SpoIID, and $\sigma^E$-RNAP in a triple-input AND gate manner. To this end, the *spoIID* promoter was replaced with an IPTG inducible promoter repressed by LacI and recognized by the housekeeping sigma factor $\sigma^A$ (Britton et al., 2002). Previously, it was reported that the formation of the sporulation septum is inhibited by premature and simultaneous expression of SpoIID, SpoIIM, and SpoIIP under the control of the $\sigma^H$-dependent *spoVG* promoter ($P_{spoVG}$), leading to a slight decrease in sporulation ($10^7$ spores $ml^{-1}$), as compared with the wild type strain ($10^8$ spores $ml^{-1}$) (Eichenberger et al., 2001). However, when SpoIID is solely and prematurely expressed under the control of the $P_{spoVG}$ promoter, sporulation is restored to the wild type levels ($10^8$ spores $ml^{-1}$) (Eichenberger et al., 2001). It was also reported that the onset of engulfment occurs when SpoIID, SpoIIM, and SpoIIP are simultaneously over-expressed under the control of the IPTG-inducible promoter in the *sigE* null mutant (Rodrigues, Marquis, Meisner, & Rudner, 2013). However, in those prior studies, there were no demonstrations of the correlation between the SpoIID expression levels and sporulation (Eichenberger et al., 2001) (Rodrigues et al., 2013). Therefore, we altered the timing and levels of SpoIID-FLAG expression using the IPTG-inducible strain by adding varying concentrations of IPTG to the DSM culture. As a control, cells expressing SpoIID-FLAG under the control of the native *spoIID* promoter were cultured in DSM in parallel. Cells were harvested at 2 h of sporulation (T2), a time at which expression of SpoIID in the wild type strain had reached its maximum in DSM (Doan & Rudner, 2007). Then,

crude cell extracts were prepared and processed for immunoblot analysis by using anti-FLAG antibodies. Results indicated that sporulation in the IPTG-inducible SpoIID strain was fully restored similar to the wild type levels ($10^8$ spores $ml^{-1}$) in the presence of 10 μM IPTG (Figure IV-9). The levels of the SpoIID induced by 10 μM IPTG were approximately half of those in the wild type, but sufficient to restore sporulation (Figure IV-9). We observed normal sporulation in the cells cultured in the presence of up to 1 mM IPTG (data not shown). These results indicate that the triple-input AND gate mechanism for *spoIID* expression can be bypassed when the SpoIID expression levels reach a certain level in the IPTG-inducible system. Thus, these results suggest that the expression level of SpoIID is more important than the expression timing for engulfment.

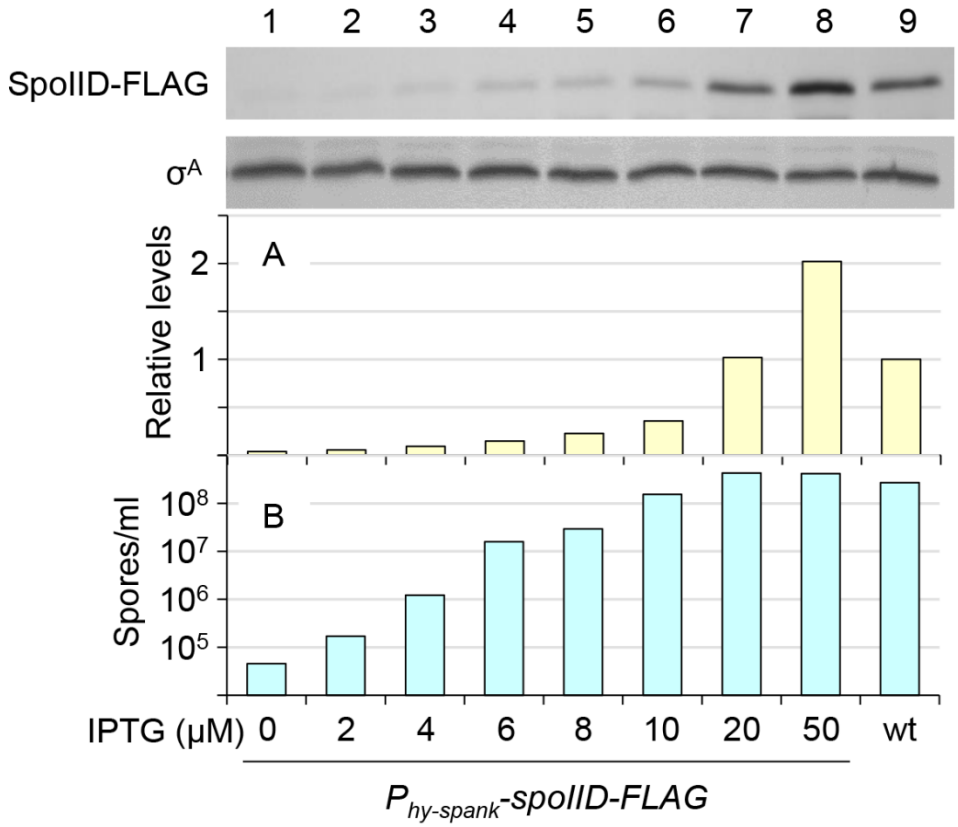


**Figure IV-9. Restoration of normal sporulation by overexpression of SpoIID.**
The upper panels show immunoblots of extracts from cells in which *spoIID-FLAG* was under the control of the IPTG-inducible promoter $P_{hy\text{-}spank}$ and the wild type promoter (used as a control). Synthesis of SpoIID was induced in the IPTG inducible strain by the addition of the indicated concentrations of IPTG at the start of cell culture in DSM. Extracts were prepared from cells collected at T2, the time at which the steady-state levels of SpoIID were reached, separated by SDS-PAGE, and subjected to immunoblotting with anti-FLAG antibodies and anti-$\sigma^A$ antibodies. The lower panel shows the corresponding levels of SpoIID (A) and sporulation (B) at the indicated concentrations of IPTG. SpoIID levels from the immunoblot analysis were quantified and normalized to the levels of $\sigma^A$ and then normalized to the wild type control strain. The spores per ml of culture at T20 was measured by the number of heat-resistant (80 °C for 15 min) CFU on DSM agar plates.

IV.iii.6 At the peak of its expression, 12,000 SpoIID molecules are present per cell.

The number of SpoIID molecules per cell of the wild type strain was determined by quantitative immunoblot analysis. For this purpose, we calculated expression levels of SpoIID in the cell extracts prepared from known numbers of cells using a known amount of the purified protein as a standard. First, we cultured cells expressing SpoIID-FLAG under the wild type *spoIID* promoter in DSM, harvested cells at T2, and prepared crude cell extracts. We used colony-forming assay to evaluate the numbers of viable cells in the harvested culture samples. As a normalization control, we used the commercially available carboxy-terminal FLAG-BAP™ Fusion Protein (FLAG fusion to the Bacterial Alkaline Phosphatase protein, Sigma-Aldrich) (Figure IV-10). In brief, serially diluted crude cell extracts containing SpoIID-FLAG and the purified FLAG-BAP™ Fusion Protein were processed for immunoblot using anti-FLAG antibody. Then, the SpoIID-FLAG protein levels were determined with the standard curve by using a serially diluted FLAG-BAP™ Fusion Protein (Figure IV-10). Results indicated that 12,000 molecules of SpoIID present per cell, harvested at T2 in DSM. If the DMP subunit stoichiometry is 1:1:1, SpoIIM and SpoIIP would be present similar levels to SpoIID.

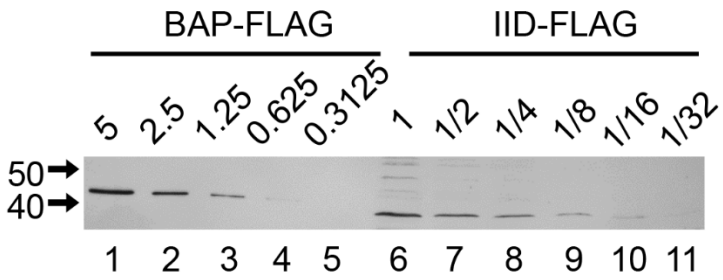


**Figure IV-10. Assessment of SpoIID molecules per cell by use of FLAG-BAP™ fusion protein.**
Cells expressing SpoIID-FLAG under the control of the wild type *spoIID* promoter were cultured in DSM and harvested at T2, the time at which the steady-state levels of SpoIID were reached. The numbers of cells were determined by plating serially diluted aliquots of culture at T2. Total cell extracts were serially diluted from 0 to 1:32 (lanes 6 - 11) and subjected for immunoblot analysis using an anti-FLAG monoclonal antibody. As a standard for FLAG protein calibration, the absolute quantities of BAP-FLAG (bacterial alkaline phosphatase-FLAG, Sigma) were analyzed together with SpoIID-FLAG on the same gel by immunoblot analysis using anti-FLAG monoclonal antibody (lanes 1 - 5). The intensity values of the bands were determined by FluorChem™ densitometry (Alpha Innotech Corporation).

IV.iii.7 Homology search shows that *spoIID* promoter organization is conserved among *Bacillus* species

Next, I investigated whether the mother cell-specific Spo0A-controlled mechanism of *spoIID* expression is conserved across spore-forming organisms. To examine this, I searched for homologous sequences in the *spoIID* coding region and a 100 bp DNA fragment of the promoter region of *spoIID* in *B. subtilis* through BLAST. The results revealed that the nucleotide sequences of the upstream region of *spoIID,* including the 0A boxes, the IIID box, and the $\sigma^E$ promoter are completely conserved across several *Bacillus* species, including *B. vallismortis*, *B. cereus*, *B. gibsonii*, and *B. halotolerans* (Table IV-7).

**Table IV-7. Sequence homology for the upstream and coding region of *spoIID***

| | | Identity to *spoIID* in *B. subtilis* 168 | | | | | |
|---|---|---|---|---|---|---|---|
| | | Nucleotides | | | | | Amino acids |
| ***Bacillus* species** | **Accession number** | **0A boxes[1]** | **IIID box[2]** | **$\sigma^{E3}$** | **Upstream region[5]** | **Coding region[6]** | **Coding region[7]** |
| *Bacillus sp. KBS0812* | CP041757.1 | 100% | 100% | 100% | 100% | 100% | 100% |
| *Bacillus vallismortis strain DSM 11031* | CP026362.1 | 100% | 100% | 100% | 100% | 91% | 97% |
| *Bacillus cereus MBGJa3* | CP026523.1 | 100% | 100% | 100% | 100% | 91% | 97% |
| *Bacillus gibsonii FJAT-10019* | CP017070.1 | 100% | 100% | 100% | 100% | 99% | 99% |
| *Bacillus subtilis subsp. natto strain CGMCC 2108* | CP014471.1 | 100% | 100% | 100% | 100% | 100% | 100% |
| *Bacillus subtilis subsp. inaquosorum strain DE11* | CP013984.1 | 100% | 100% | 100% | 100% | 93% | 97% |
| *Bacillus sp. BSn5* | CP002468.1 | 100% | 100% | 100% | 100% | 99% | 99% |
| *Bacillus halotolerans strain F41-3* | CP041357.1 | 100% | 100% | 100% | 100% | 88% | 96% |
| *Bacillus halotolerans strain ZB201702* | CP029364.1 | 100% | 100% | 100% | 100% | 88% | 96% |
| *Bacillus subtilis subsp. spizizenii SW83* | CP030925.1 | 100% | 100% | 100% | 100% | 99% | 99% |
| **Pathogenic spore formers** | **Accession number** | **0A boxes** | **IIID box** | **$\sigma^{E4}$** | **Upstream region** | **Coding region** | **Coding region** |
| *Bacillus licheniformis ATCC 14580* | CP000002.3 | Not found | 100% | Found | 67% | 71% | 83% |
| *Bacillus cytotoxicus NVH 391-98* | CP000764.1 | Not found | Not found | Found | 52% | 59% | 67% |
| *Bacillus anthracis str. Ames* | AE016879.1 | Not found | Not found | Found | 43% | 59% | 67% |
| *Bacillus thuringiensis serovar. Konkukian str. 97-27* | AE017355.1 | Not found | Not found | Found | 43% | 61% | 68% |
| *Clostridioides difficile 630* | CP010905.2 | Not found | Not found | Found | 51% | 44% | 52% |
| *Clostridium botulinum BKT015925* | CP002410.1 | Not found | Not found | Found | 48% | 50% | 54% |
| *Clostridium perfringens ATCC 13124* | CP000246.1 | Not found | Not found | Found | 45% | 51% | 59% |

0A boxes[1], 0A1: ATGACAAA, 0A2: CTGTCCAA, 0A3: GAGTCGAA

IIID box[2], GGACAA A

$\sigma^{E3}$, in *Bs*, TCAT (-35) - 17 bp space - CATA (-10)

$\sigma^{E4}$, in *Clostridium*, ATA (-35) - 19 bp space - ATA (-10)

Upstream region[5], 100 bp from the start codon ATG

SpoIID coding region[6], 1032 bp in Bs

SpoIID coding region[7], 343 aa in Bs

**Table IV-8. Conservation of the amino acid residues important for SpoIID activity**

| **Important residues (E88, R106, K203, D210, H297, Y323, and Y324) in SpoIID*** | |
|---|---|
| ***Bacillus* species** | **Conserved residues** |
| *Bacillus sp. KBS0812* | all |
| *Bacillus vallismortis strain DSM 11031* | all |
| *Bacillus cereus MBGJa3* | all |
| *Bacillus gibsonii FJAT-10019* | all |
| *Bacillus subtilis subsp. natto strain CGMCC 2108* | all |
| *Bacillus subtilis subsp. Inaquosorum strain DE11* | all |
| *Bacillus sp. BSn5* | all |
| *Bacillus halotolerans strain F41-3* | all |
| *Bacillus halotolerans strain ZB201702* | all |
| *Bacillus subtilis subsp. spizizenii SW83* | all |
| **Pathogenic spore formers** | **Conserved residues** |
| *Bacillus licheniformis ATCC 14580* | all |
| *Bacillus cytotoxicus NVH 391-98* | all |
| *Bacillus anthracis str. Ames* | all |
| *Bacillus thuringiensis serovar. Konkukian str. 97-27* | all |
| *Clostridioides difficile 630* | all |
| *Clostridium botulinum BKT015925* | All except D210 |
| *Clostridium perfringens ATCC 13124* | All except D210, Y324 |

* E88, R106, H297, Y323, and Y324 are reported to be essential for SpoIID activity (Morlot et al., 2010).
E88, R106, K203, and D210 are reported to be important for SpoIID activity (Gutierrez et al., 2010)

The observed sequence changes in the SpoIID coding region were not at the catalytic or active residues of the enzyme (Table IV-8). These results suggest that the Spo0A-controlled mechanism for *spoIID* expression is widely conserved across several *Bacillus* species. However, in the pathogenic spore-forming species, including *Clostridium spp.* and *B. anthracis*, the upstream regions showed no DNA homology to the 0A and the IIID boxes (Figure IV-10, Table IV-7), while the catalytic or active residues of the *spoIID* coding region were highly conserved (Table 3).

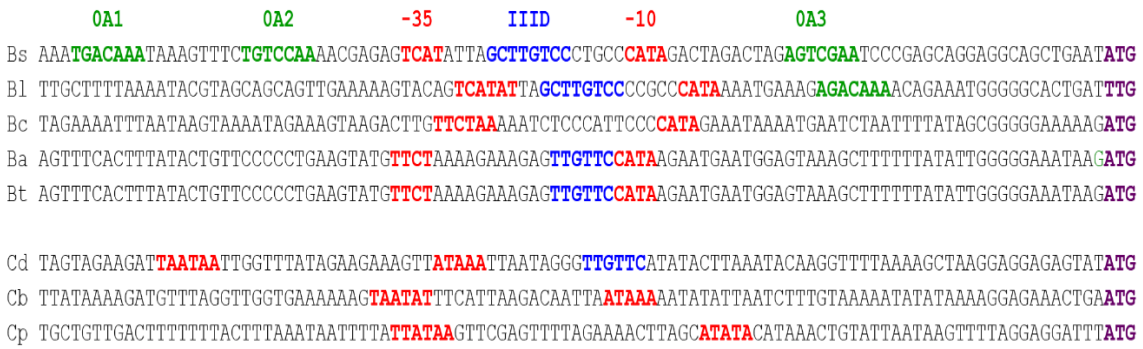


**Figure IV-11. Sequence alignment for the *spoIID* upstream region in the pathogenic spore-formers.**
0A and IIID boxes are highlighted in green and blue, respectively. The consensus promoter for $\sigma^E$-RNAP in *B. subtilis* is TCAT in the -35 element and CATA in the -10 element with 17 bp spacing between these two elements. The consensus promoter for $\sigma^E$-RNAP in *Clostridium* species is ATA in the -35 element and ATA in the -10 element with 19 bp spacing between these two elements. Bs, *B. subtilis*; Bl, *Bacillus licheniformis* ATCC 14580; Bc, *Bacillus cytotoxicus* NVH 391-98, Ba, *Bacillus anthracis* str. Ames; Bt, *Bacillus thuringiensis serovar. Konkukian str. 97-27*; Cd, *Clostridioides difficile* 630; Cb, *Clostridium botulinum* BKT015925; Cp, *Clostridium perfringens* ATCC 13124.

Although the 0A and IIID boxes are not conserved in the *spoIID* upstream regions of those pathogenic spore-forming species, we found short stretches of DNA that are similar to the $\sigma^E$ promoter consensus sequence in those species (Figure IV-11) (Johnson et al., 2008; Sauer et al., 1995). As shown in Figure IV-12, the $\sigma^E$ factor 2.4 and 4.2 regions known to directly interact with the −10 and −35 elements are highly conserved in all those pathogenic and non-pathogenic spore formers (Haldenwang, 1995) (Rice, Longden, & Bleasby, 2000), while the target promoter consensus sequences at -10 and -35 are different between *Bacillus* and *Clostridium* species (Eichenberger et al., 2004) (Johnson et al., 2008) (Saujet et al., 2013). Nevertheless, these results suggest that pathogenic and non-pathogenic spore-forming bacterial species have differently evolved the mother

cell-specific Spo0A-controlled mechanism of *spoIID* expression to adapt to environments with varying levels of nutrients.

```
Bs        LATYASRCIENEILMYLRRNNKIRSEVSFYEPLNIDWDGNELLLSDVLGTDDDIITKDIE        169
Bsk       LATYASRCIENEILMYLRRNNKIRSEVSFDEPLNIDWDGNELLLSDVLGTDDDIITKDIE        169
Bv        LATYASRCIENEILMYLRRNNKIRSEVSFDEPLNIDWDGNELLLSDVLGTDDDIITKDIE        169
Bcm       LATYASRCIENEILMYLRRNNKIRSEVSFDEPLNIDWDGNELLLSDVLGTDDDIITKDIE        169
Bg        LATYASRCIENEILMYLRRNNKIRSEVSFDEPLNIDWDGNELLLSDVLGTDDDIITKDIE        169
Bsn       LATYASRCIENEILMYLRRNNKIRSEVSFDEPLNIDWDGNELLLSDVLGTDDDIITKDIE        169
Bsi       LATYASRCIENEILMYLRRNNKIRSEVSFDEPLNIDWDGNELLLSDVLGTDDDIITKDIE        169
Bsb       LATYASRCIENEILMYLRRNNKIRSEVSFDEPLNIDWDGNELLLSDVLGTDDDIITKDIE        169
Bhf       LATYASRCIENEILMYLRRNNKIRSEVSFDEPLNIDWDGNELLLSDVLGTDDDIITKDIE        169
Bhz       LATYASRCIENEILMYLRRNNKIRSEVSFDEPLNIDWDGNELLLSDVLGTDDDIITKDIE        169
Bss       LATYASRCIENEILMYLRRNNKIRSEVSFDEPLNIDWDGNELLLSDVLGTDDDIITKDIE        169
Bl        LATYASRCIENEILMYLRRNNKIRSEVSFDEPLNIDWDGNELLLSDVLGTENDIITKDIE        169
Bcy       LATYASRCIENEILMHLRRNNKNRSEVSFDEPLNIDWDGNELLLSDVLGTDDDIITKDLE        169
Ba        LATYASRCIENEILMHLRRNNKNRSEVSFDEPLNIDWDGNELLLSDVLGTDDDIITKDLE        169
Bt        LATYASRCIENEILMHLRRNNKNRSEVSFDEPLNIDWDGNELLLSDVLGTDDDIITKDLE        169
Cd        LATYASRCIENEILMYLRKNNKKKTEVSFDEPLNIDLDGNELLLSDVLGTENDEIYKIIE        169
Cb        LATYASRCIENEILMYLRRNNKVKAEISFYEPLNTDWDGNKLLLSDILGTENDMVYNLIE        179
Cp        LATYASRCIENEILMYLRRNSKVKAEISFYEPLNIDWDGNELLLSDILGTDDDIVYNLIE        165
          ****.**********:**:*.* ::*:** **** * ***:*****:***::* : : :*

Bs        ANVDKKLLKKALEQLNEREKQIMELRFGLVGEE-EKTQKDVADMMGISQSYISRLEKRII        228
Bsk       ANVDKKLLKKALEQLNEREKQIMELRFGLVGEE-EKTQKDVADMMGISQSYISRLEKRII        228
Bv        ANVDKKLLKKALEQLNEREKQIMELRFGLVGEE-EKTQKDVADMMGISQSYISRLEKRII        228
Bcm       ANVDKKLLKKALEQLNEREKQIMELRFGLVGEE-EKTQKDVADMMGISQSYISRLEKRII        228
Bg        ANVDKKLLKKALEQLNEREKQIMELRFGLVGEE-EKTQKDVADMMGISQSYISRLEKRII        228
Bsn       ANVDKKLLKKALEQLNEREKQIMELRFGLVGEE-EKTQKDVADMMGISQSYISRLEKRII        228
Bsi       ANVDKKLLKKALEQLNEREKQIMELRFGLVGEE-EKTQKDVADMMGISQSYISRLEKRII        228
Bsb       ANVDKKLLKKALEQLNEREKQIMELRFGLVGEE-EKTQKDVADMMGISQSYISRLEKRII        228
Bhf       ANVDKKLLKKALEQLNEREKQIMELRFGLVGEE-EKTQKDVADMMGISQSYISRLEKRII        228
Bhz       ANVDKKLLKKALEQLNEREKQIMELRFGLVGEE-EKTQKDVADMMGISQSYISRLEKRII        228
Bss       ANVDKKLLKKALEQLNEREKQIMELRFGLVGEE-EKTQKDVADMMGISQSYISRLEKRII        228
Bl        ANVDKKLLKKALEQLNDREKQIMELRFGLVGGE-EKTQKDVADMLGISQSYISRLEKRII        228
Bcy       ANVDRYLLMKALHQLNDREKQIMELRFGLAGGE-EKTQKDVADMLGISQSYISRLEKRII        228
Ba        ATVDRHLLMKALHQLNDREKQIMELRFGLAGGE-EKTQKDVADMLGISQSYISRLEKRII        228
Bt        ATVDRHLLMKALHQLNDREKQIMELRFGLAGGE-EKTQKDVADMLGISQSYISRLEKRII        228
Cd        EEIDRDLLVMALDRLSDREKQIMELRFGLIDKGIEKTQKEVAGMLGISQSYISRLEKKII        229
Cb        DEVDKQLLFIAMRKLSEREKEIIKLRFGLTGKG-EKTQKQVADLLGISQSYISRLEKRII        238
Cp        DEVDKELLFTAMKNLSNREKEIVELRFGLCGYK-EKTQKEVADMLGISQSYISRLEKKII        224
            :*: **  *: .*.:***.*::**:** .   *****:**.::************:**

Bs        KRLRKEFNKMV          239
Bsk       KRLRKEFNKMV          239
Bv        KRLRKEFNKMV          239
Bcm       KRLRKEFNKMV          239
Bg        KRLRKEFNKMV          239
Bsn       KRLRKEFNKMV          239
Bsi       KRLRKEFNKMV          239
Bsb       KRLRKEFNKMV          239
Bhf       KRLRKEFNKMV          239
Bhz       KRLRKEFNKMV          239
Bss       KRLRKEFNKMV          239
Bl        KRLRKEFNKMV          239
Bcy       KRLRKEFNKMV          239
Ba        KRLRKEFNKMV          239
Bt        KRLRKEFNKMV          239
Cd        SRLQKEMKKFV          240
Cb        KRLKKEINKMV          249
Cp        KRLKKEINKMI          235
          .**:**::*::
```

**Figure IV-12. Alignment of the promoter-recognition regions (2.4 and 4.2) of $\sigma^E$ in *Bacillus* and *Clostridium* species.**
Regions 2.4 and 4.2 of *B. subtilis* $\sigma^E$ are highlighted in blue**.** The strains shown here are the same as in Table IV-7. An asterisk (*) indicates a conserved residue, a colon (:) indicates a conserved substitution, and a period (.) indicates a semi-conserved substitution.

## IV.iv Discussion

In this Chapter, I constructed SpoIID-FLAG strains fused to mutated and non-mutated (wild type) *spoIID* promoters, in order to understand the role of Spo0A regulation in forespore engulfment. The spore count assays revealed that mutations in the 0A3 box make the cells sporulation defective ($10^5$spores $ml^{-1}$ of culture in 0A3* mutant as compared to $10^8$spores $ml^{-1}$ of culture in wild type) (Figure IV-2). To further investigate this interesting evidence microscopy analysis was performed.

For the microscopy studies, two stage- and compartment-specific reporters ($P_{spoIIQ}$-*gfp* and $P_{sspA}$-*gfp*) were inserted at the non-essential thrC locus. Abnormal (bulging) spore signal was observed in these sporulation defective 0A3* mutants, during microscopic studies. Such abnormal (bulging)spore signals have previously been reported in a *spoIID* deletion mutant due to block in the engulfment process (Eichenberger et al., 2001; Pogliano et al., 1999). These results suggest that 0A~P regulation at the 0A3 box of *spoIID* promoter is crucial for proper engulfment. To further study the cell fate of the mutants with improper engulfment, we did a time-lapse experiment which showed that *gfp* signal in the 0A3* mutant fades away without forespore or phase bright spore development. Thus it was clear that cells with a mutation in the 0A3 box produce bulging spore signals which might be due to improper engulfment and further impair the ability to sporulate.

Immunoblot studies, carried out to examine the SpoIID expression levels further divulged that the SpoIID levels were altered in all the 0A3* mutants. Since lower expression of SpoIID in 0A3* mutants causes improper engulfment and

sporulation defects, we decided to study whether over-expression of SpoIID restores normal sporulation. For this purpose, *spoIID-FLAG* strain under the control of an IPTG inducible promoter ($P_{hy\text{-}spank}$) was constructed. Previous studies report that a simultaneous overproduction of SpoIID, SpoIIM, and SpoIIP under the control of an IPTG inducible promoter in the *sigE* null strain is able to artificially induce the onset of engulfment while no data indicating frequencies of engulfment are provided (Rodrigues et al., 2013; Rodrigues et al., 2016). We note that, in those prior studies, IPTG was used at 1 mM concentration at which the protein is generally overproduced, although the authors argue that the expression levels are similar to those in the wild type (Rodrigues et al., 2013; Rodrigues et al., 2016).

In our tested conditions using the IPTG-inducible SpoIID system here, the addition of IPTG (10 - 1,000 µM) to cells during growth was shown to induce normal sporulation. Since IPTG is not metabolized, SpoIID is assumed to be continuously and constantly synthesized in the presence of IPTG, until later stages after asymmetric division, at least as long as the $\sigma^A$-RNAP activity continues. These results indicate that cells are able to undergo sporulation, at least when the SpoIID expression levels are reached to certain levels under the control of the IPTG-inducible promoter. In support of this view, cells harboring the 0A3* mutation expressed lower levels of SpoIID than the wild type cells, leading to incomplete forespore engulfment.

As discussed earlier in the result section, the transcription level from the 0A3* promoter is stronger than that from the wild-type promoter. However, the expression level of SpoIID in the 0A3* mutant becomes lower than in the wild type

strain. These results suggest that, when SpoIID is expressed too fast and high levels from the mutated 0A box promoter, the protein is degraded, and thus DMP complex is not formed at sufficient levels for engulfment. We are not sure why SpoIID is functional when overexpressed from the IPTG-inducible $\sigma^A$ promoter but not from the mutated 0A box promoter. The IPTG-inducible $\sigma^A$ promoter can be expressed in the presence of IPTG during growth, before and after asymmetric division, while the $\sigma^E$ promoter is active only in the mother cell after asymmetric division. Therefore, the transcription kinetics of these two promoters might be important to determine the timing, compartment specificity, and levels of the protein expression.

According to the homology search (Table IV-7), *spoIID* promoter organization is conserved only among the *B. subtilis* and its closely related species, but not in the pathogenic spore-formers. It might be interesting to speculate why these regulations are different between pathogenic- and non-pathogenic-spore forming bacteria. The pathogenic spore-forming bacteria may generally absorb nutrients from a host organism under the relatively stable conditions with constant levels of nutrients, while the non-pathogenic environmental spore-forming bacteria need to survive under the harsh conditions. Therefore, more sophisticated gene regulatory systems might be required for the non-pathogenic spore-forming bacteria than for the pathogenic ones. Nevertheless, these results suggest that pathogenic and non-pathogenic spore-forming bacterial species have distinctly evolved the mother cell-specific Spo0A-controlled mechanism of *spoIID* expression to adapt to environments with varying levels of nutrients.

The DMP complex which carries out the first step in engulfment, peptidoglycan hydrolysis consists of three proteins (SpoIID, SpoIIM and SpoIIP) with different activities. SpoIID is a membrane-anchored cell wall hydrolase (lytic transglycosylase) that hydrolyzes the glycan strands of the peptidoglycan after the stem peptides have been removed by SpoIIP, an amidase, and endopeptidase(Gutierrez et al., 2010). These two proteins are held in place by a scaffolding protein SpoIIM. Together, this DMP complex is localized to the polar septal membrane(Morlot et al., 2010). Studies have revealed that premature and simultaneous expression of all three components (DMP) interfere with sporulation(Eichenberger et al., 2001). DMP activity is known to be a rate-limiting step for membrane migration during engulfment (Abanes-De Mello et al., 2002; Meyer et al., 2010). These results suggest that the timing and levels of DMP complex formation are important for engulfment.

Based on the results presented in this Chapter, I propose that a certain portion of the total amount of SpoIID molecule synthesized under the control of 0A~P is assembled with the existing SpoIIP and SpoIIM to form a functional IID–IIP–IIM complex. Thus, all these results suggest that the timing and levels of DMP complex formation are important for engulfment. Among three factors, SpoIID would be the key determinant of the functional DMP complex formation required for proper engulfment and sporulation.

Figure IV-13 gives the model for *spoIID* regulation by 0A~P along with $\sigma^E$-RNAP and SpoIIID. In summary, Spo0A, previously known as a master regulator for asymmetric division, a hallmark of entry into sporulation, also acts as a mother

cell-specific transcription factor required for the proper expression of *spoIID* gene that controls the engulfment of forespore by mother cell. Thus *spoIID* gene expression is regulated by a triple AND gate which involves 0A~P, along with $\sigma^E$-RNAP and SpoIIID.

We have proposed that the phosphorelay plays a role in the gradual increase in protein and activity levels of Spo0A and this gradual increase in 0A~P levels is required for entry into sporulation. As a result, genes that respond to a low level of 0A~P are switched on or off prior to genes that respond to a high level of 0A~P. Now we provide new insight into the additional role of Spo0A beyond asymmetric division.

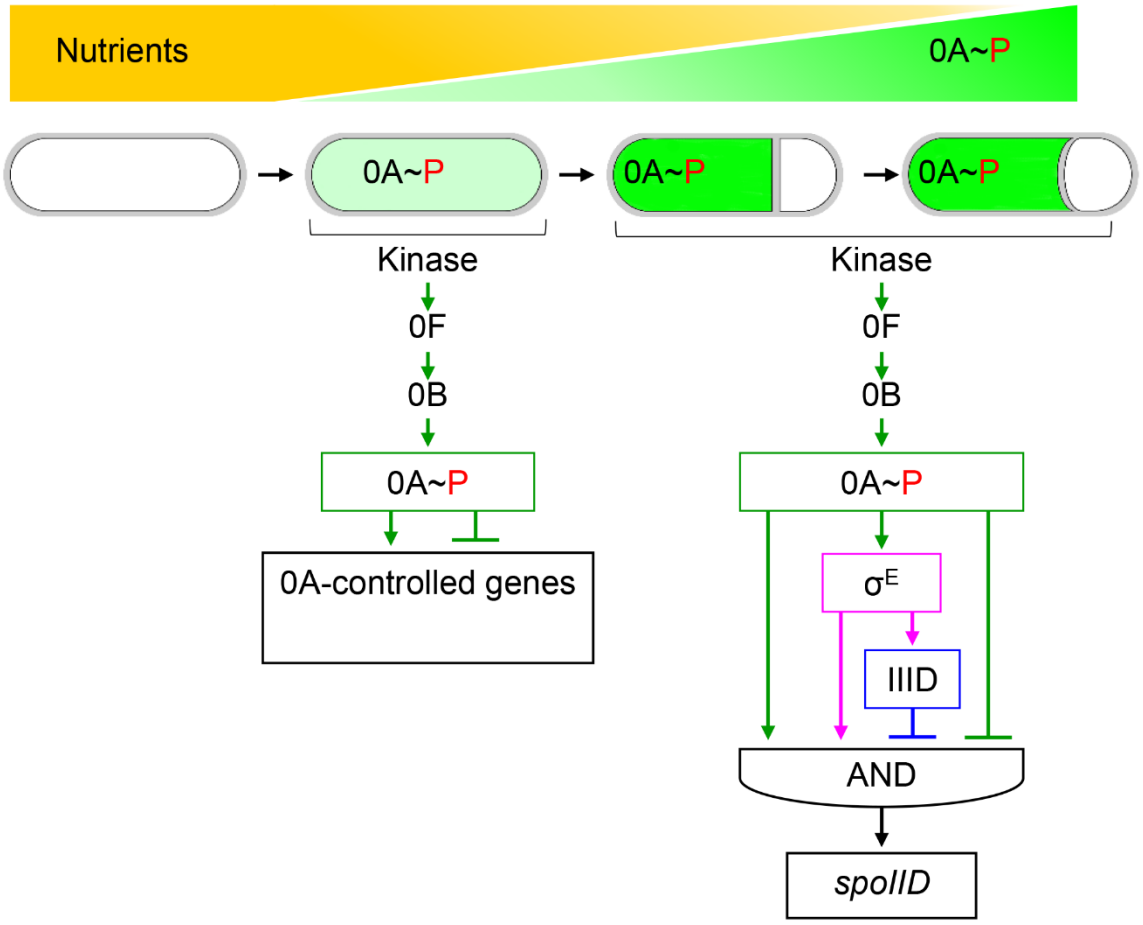


**Figure IV-13. Model for *spoIID* expression regulation via a triple AND gate comprising of 0A~P, $\sigma^E$-RNAP, and SpoIIID.**
Upon nutrient depletion, the 0A~P level increases gradually through a four component phosphorelay. 0A~P reaches a threshold level, which leads to asymmetric division. Further activity of 0A~P occurs only in the mother cell and is required for proper *spoIID* expression, a gene encoding cell wall hydrolase enzyme. Proper expression of *spoIID* ensures completion of engulfment and is crucial for sporulation. Pointed arrows indicate positive regulation and flat arrows indicate negative regulation.

# Chapter V: Conclusive remarks and Future perspectives

Within the ambit of this dissertation, I have investigated the transcriptional control of the *spo0A* and the role of this master regulator protein after asymmetric septation in the starving *Bacillus subtilis*. My work here provides an insight into the *spo0A* transcriptional control and the role of three regulatory 0A boxes. I have further elucidated the mother cell-specific function of Spo0A after asymmetric septation in controlling engulfment.

For exploring the *spo0A* transcriptional control, I started by finding out the relative binding affinities of three 0A boxes to 0A~P using electrophoretic mobility shift assays. These experiments contributed a first of its kind direct experimental evidence of 0A~P binding to the three 0A boxes in the upstream *spo0A* region with different binding affinity. Later on, we constructed 0A box mutants and fused them transcriptionally to *lacZ*. I assayed the transcriptional activities of mutated and non-mutated promoter fusion strains. In order to compare the contribution of two kinases; KinA and KinC during the *spo0A* transcription, I studied them in the *kinA*/*kinC* knockout strains. These data in Chapter II, have enabled me to present a detailed model highlighting the role of 0A boxes in the *spo0A* transcriptional control.

In order to investigate the mechanism of 0A regulation in a mother cell-specific gene, I studied Spo0A regulated *spoIID* expression in Chapter III. Here, I have presented key evidence for the existence of two previously unidentified regulatory 0A boxes in the upstream region of *spoIID*, a mother cell-specific gene encoding a lytic transglycosylase enzyme important for engulfment process during

sporulation. The transcriptional data elucidated the regulatory roles of each of the three 0A boxes in *spoIID* expression.

In chapter IV, I inspected the importance of mother cell-specific 0A activity during sporulation. For this purpose, SpoIID expression levels were examined using a SpoIID-FLAG construct. In this study, the FLAG tag was chosen in place of GFP or other fluorescent reporters because C-terminal GFP fusion to SpoIID is not stable or functional. FLAG tag is smaller in size than GFP and hence doesn't jeopardize the stability of the SpoIID. The microscopy and immunoblot data from chapter IV provides crucial evidence that the regulation of *spoIID* by 0A~P is important for the completion of engulfment and progression of sporulation. The collective experiments in Chapter III and IV have facilitated in deciphering the role of Spo0A in transcriptional regulation of *spoIID*, and revise the model for *spoIID* transcriptional regulation, mediated by a triple-input AND gate consisting of $\sigma^E$-RNA polymerase, SpoIIID, and Spo0A~P.

Few interesting pursuits are beyond the scope of this dissertation and could be followed in the future to expand and complete our understanding of these regulatory pathways. Some of these interesting questions that arose during this study have been mentioned below.

**V.i Investigation into the role of the 0A4 box in transcriptional control of *spo0A***

The upstream promoter region of *spo0A* consists of four 0A boxes for 0A~P binding, but previous studies have speculated no role for the 0A4 box in the *spo0A* transcription (Chastanet & Losick, 2011) (Chibazakura et al., 1991). This 0A4 box

overlaps the -10 region of the $P_S$ promoter recognition element (Figure V-1A). Our transcriptional assay data indicates that the promoter activity decreases at later time points, which can be explained as feedback regulation by 0A~P. However, the actual mechanism is unknown, one possible explanation might be the role of 0A4 in this regulation. Since 0A4 box is positioned such that it overlaps with the -10 region of the $P_S$ promoter recognition element, 0A~P binding to this 0A4 can interfere with the $P_S$ promoter activity leading to reduced or no *spo0A* transcription from the $P_S$ promoter. In order to verify this possible role of 0A4, EMSA (Electrophoretic mobility shift assay) must be repeated as the first step. Transcriptional study on the 0A4 mutated *spo0A* promoter will also prove to be essential. The binding to 0A4 might be the least out of all 0A boxes, otherwise, it can hinder the *spo0A* transcription from $P_S$ promoter very early on in the starvation, which doesn't seem to be the case.

The previous experiments conducted on the 0A4 box included replacing the entire $P_S$ promoter region (-35 and -10 recognition sites including the 0A4 box) with another $\sigma^H$-controlled promoter, $P_{spoVG}$. The data showed no significant difference in the promoter activity of the replaced promoter which led the authors to conclude that 0A4 does not play an important role in promoter switching between $P_V$ and $P_S$ (Chastanet & Losick, 2011). One important point to note here is that the sampling time points for these experiments were very early during the starvation phase. According to our hypothesis, the 0A4 box might play a role in regulating the $P_S$ promoter activity during the later stages of starvation. Hence it would be interesting

to mutate the 0A4 box and assay the mutants as well as find the 0A~P binding affinity to that region.

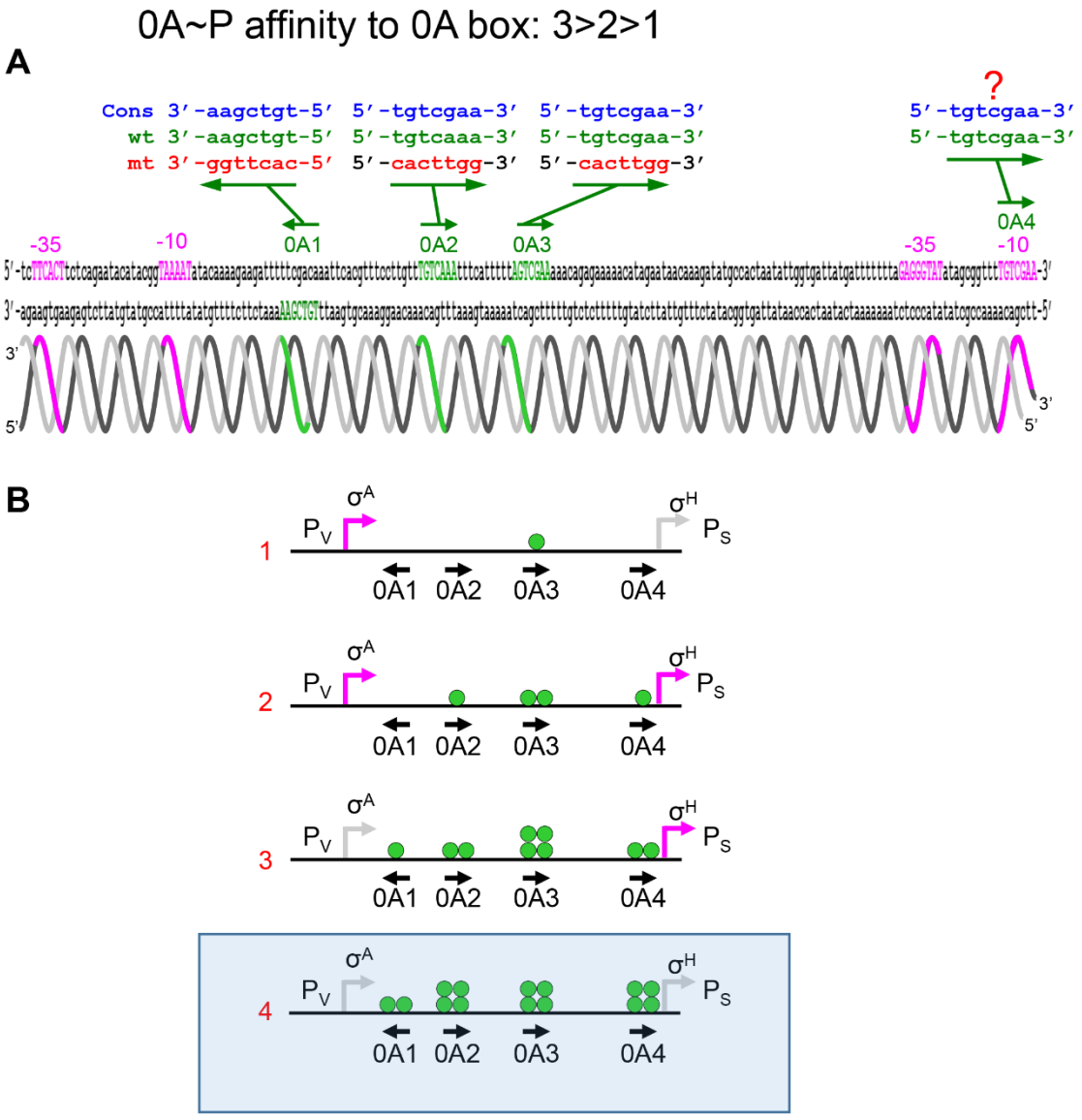


**Figure V-1. *spo0A* transcription model with a possible role for the 0A4 box.**
(A) Schematic representation of the *spo0A* promoter region, $P_V$, and $P_S$ promoter recognition elements are highlighted in pink and the four 0A boxes are highlighted in green. The role of 0A4 needs to be studied experimentally.
(B) Schematic representation of the *spo0A* transcriptional control and the regulatory functions of 0A boxes. Our speculation is that binding to 0A4 in the later stages of starvation might repress *spo0A* transcription from the $P_S$ promoter as shown in the highlighted box in 4B.

## V.ii Studies determining the effects of phosphorelay on the regulation of mother cell-specific *spoIID* expression

The transcriptional assays described in Chapter III, suggest that phosphorelay is active in the mother cell after asymmetric septation. Upon comparing the reporter activities of 0A3*IIID* mutant and 0A1*2*3*IIID* mutant, it is clear that the reporter activities gradually increase over time more significantly in the 0A3*IIID* mutant than in the 0A1*2*3*IIID* mutant, during 2 - 3 hrs. after the onset of sporulation (Figure III-5D). In the 0A3*IIID* mutant, 0A~P binds to the 0A1 and 0A2 boxes and stimulates transcription from the $\sigma^E$-RNAP dependent promoter. In contrast, transcription from the 0A1*2*3*IIID* promoter is solely dependent on $\sigma^E$-RNAP, but not 0A~P. Thus, we speculate that the gradual increase in the reporter activities in the 0A3*IIID* mutant may arise from an increase in 0A~P levels due to de novo activation of phosphorelay in a mother cell-specific manner. In order to study the effect of phosphorelay, it is essential to decouple the 0A~P signaling from the $\sigma^E$-RNAP signaling. To make this signaling possible, we have designed and constructed a unique “rewired” system that expresses the *spoIIG* operon under the control of a constitutively transcribed promoter ($\sigma^A$-dependent $P_{spac}$) that is independent of 0A~P (0A-independent $\sigma^E$) (Figure V-2B). Thus in this “rewired” system, *spoIID* expression is controlled both by 0A~P and $\sigma^E$-RNAP in a parallel but mutually independent manner. Experiments will be designed to measure the true increase in the mother cell-specific 0A~P levels, with the help of this system.

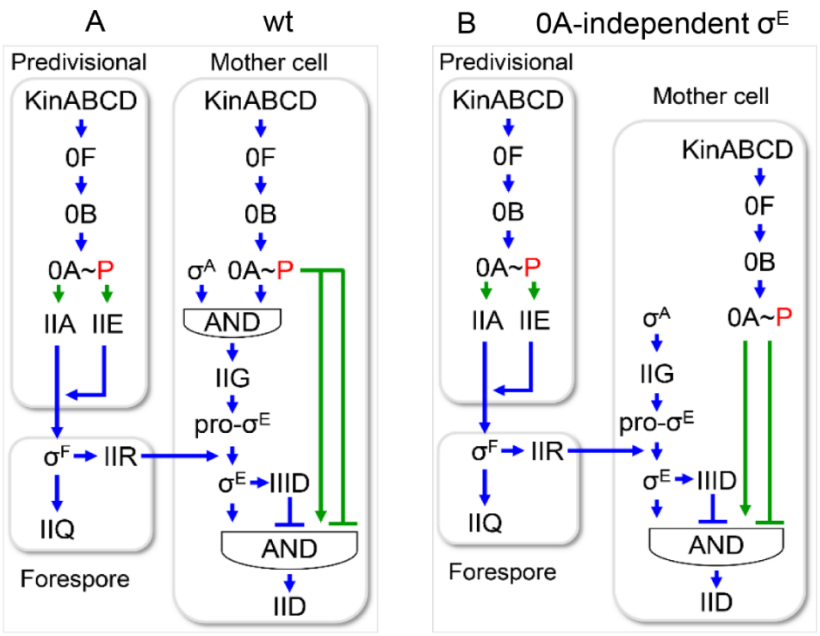


**Figure V-2. Schematic representation of the wild type and "rewired" system.**
(A) Wild type gene network. (B) Unique "rewired" system expressing $\sigma^E$ in the 0A independent manner.

## V.iii Elucidation of the major phosphorelay kinase responsible for Spo0A activation in the mother cell compartment

It would be interesting to find out which kinase is required for the mother cell-specific phosphorelay. For this purpose, single kinase mutations or combinations of multiple kinase mutations can be constructed and introduced into the *spoIID* promoter strains used in chapter III and IV. The above mentioned "rewired" system can also be useful in determining the major kinase(s) responsible for activating the Spo0A through phosphorelay. The introduction of single kinase mutations or combinations of multiple kinase mutations can be introduced in this rewired strain background and reporter activities can be determined along with the use of proper controls.

## V.iv Conclusion

Here I have provided fundamental experimental evidence of 0A~P binding to three regulatory 0A boxes in the *spo0A* promoter. My work has advanced the understanding of the mechanism for *spo0A* transcriptional control and revised the existing model for the *spo0A* regulation. Furthermore, I have presented crucial evidence for two additional regulatory 0A boxes in the *spoIID* promoter. My findings indicate that after asymmetric septation, Spo0A acts as a mother cell-specific transcription factor and this activity is essential for proper engulfment, mediated by *spoIID* regulation.

On the whole, the work presented in this dissertation significantly contributes to our understanding of the regulatory pathways involved in making the cell fate decision in *Bacillus subtilis*. Thus with the help of this work we have moved one step forward in bridging our knowledge gaps pertaining to the regulation of cellular differentiation processes in bacteria.

# BIBLIOGRAPHY


Abanes-De Mello, A., Sun, Y. L., Aung, S., & Pogliano, K. (2002). A cytoskeleton-like role for the bacterial cell wall during engulfment of the *Bacillus subtilis* forespore. *Genes Dev, 16*(24), 3253-3264.

Aguilar, C., Vlamakis, H., Losick, R., & Kolter, R. (2007). Thinking about *Bacillus subtilis* as a multicellular organism. *Curr Opin Microbiol, 10*(6), 638-643.

Atrih, A., & Foster, S. J. (2001). In vivo roles of the germination-specific lytic enzymes of *Bacillus subtilis* 168. *Microbiology, 147*(Pt 11), 2925-2932.

Banse, A. V., Chastanet, A., Rahn-Lee, L., Hobbs, E. C., & Losick, R. (2008). Parallel pathways of repression and antirepression governing the transition to stationary phase in *Bacillus subtilis*. *Proc Natl Acad Sci U S A, 105*(40), 15547-15552.

Beauregard, P. B., Chai, Y., Vlamakis, H., Losick, R., & Kolter, R. (2013). *Bacillus subtilis* biofilm induction by plant polysaccharides. *Proc Natl Acad Sci U S A, 110*(17), E1621-1630.

Blaylock, B., Jiang, X., Rubio, A., Moran, C. P., Jr., & Pogliano, K. (2004). Zipper-like interaction between proteins in adjacent daughter cells mediates protein localization. *Genes Dev, 18*(23), 2916-2928.

Boonstra, M., de Jong, I. G., Scholefield, G., Murray, H., Kuipers, O. P., & Veening, J. W. (2013). Spo0A regulates chromosome copy number during sporulation by directly binding to the origin of replication in *Bacillus subtilis*. *Mol Microbiol, 87*(4), 925-938.

Branda, S. S., Chu, F., Kearns, D. B., Losick, R., & Kolter, R. (2006). A major protein component of the *Bacillus subtilis* biofilm matrix. *Mol Microbiol, 59*(4), 1229-1238.

Britton, R. A., Eichenberger, P., Gonzalez-Pastor, J. E., Fawcett, P., Monson, R., Losick, R., & Grossman, A. D. (2002). Genome-wide analysis of the stationary-phase sigma factor (sigma-H) regulon of *Bacillus subtilis*. *J Bacteriol, 184*(17), 4881-4890.

Brock, T. (1961). Milestones in Microbiology. *London : Prentice Hall International*.

Brown, D. P., Ganova-Raeva, L., Green, B. D., Wilkinson, S. R., Young, M., & Youngman, P. (1994). Characterization of *spo0A* homologues in diverse

*Bacillus* and *Clostridium* species identifies a probable DNA-binding domain. *Mol Microbiol, 14*(3), 411-426.

Bryers, J. D. (2008). Medical biofilms. *Biotechnol Bioeng, 100*(1), 1-18.

Burbulys, D., Trach, K. A., & Hoch, J. A. (1991). Initiation of sporulation in *B. subtilis* is controlled by a multicomponent phosphorelay. *Cell, 64*(3), 545-552.

Cairns, L. S., Hobley, L., & Stanley-Wall, N. R. (2014). Biofilm formation by *Bacillus subtilis*: new insights into regulatory strategies and assembly mechanisms. *Mol Microbiol, 93*(4), 587-598.

Chai, Y., Chu, F., Kolter, R., & Losick, R. (2008). Bistability and biofilm formation in *Bacillus subtilis*. *Mol Microbiol, 67*(2), 254-263.

Chastanet, A., & Losick, R. (2011). Just-in-time control of Spo0A synthesis in *Bacillus subtilis* by multiple regulatory mechanisms. *J Bacteriol, 193*(22), 6366-6374.

Chastanet, A., Vitkup, D., Yuan, G. C., Norman, T. M., Liu, J. S., & Losick, R. M. (2010). Broadly heterogeneous activation of the master regulator for sporulation in *Bacillus subtilis*. *Proc Natl Acad Sci U S A, 107*(18), 8486-8491.

Chen, Y., Cao, S., Chai, Y., Clardy, J., Kolter, R., Guo, J. H., & Losick, R. (2012). A *Bacillus subtilis* sensor kinase involved in triggering biofilm formation on the roots of tomato plants. *Mol Microbiol, 85*(3), 418-430.

Chibazakura, T., Kawamura, F., & Takahashi, H. (1991). Differential regulation of *spo0A* transcription in *Bacillus subtilis*: glucose represses promoter switching at the initiation of sporulation. *J Bacteriol, 173*(8), 2625-2632.

Chumsakul, O., Takahashi, H., Oshima, T., Hishimoto, T., Kanaya, S., Ogasawara, N., & Ishikawa, S. (2011). Genome-wide binding profiles of the *Bacillus subtilis* transition state regulator AbrB and its homolog Abh reveals their interactive role in transcriptional regulation. *Nucleic Acids Res, 39*(2), 414-428.

Claverys, J. P., & Havarstein, L. S. (2007). Cannibalism and fratricide: mechanisms and raisons d'etre. *Nat Rev Microbiol, 5*(3), 219-229.

Cohn, H. J. (1930). The identity of *Bacillus subtilis*. *the Journal of Infectious Diseases, 46*(4), 341-350.

Cutting, S., Roels, S., & Losick, R. (1991). Sporulation operon *spoIVF* and the characterization of mutations that uncouple mother-cell from forespore gene expression in *Bacillus subtilis*. *J Mol Biol, 221*(4), 1237-1256.

Daelman, J., Sharma, A., Vermeulen, A., Uyttendaele, M., Devlieghere, F., & Membre, J. M. (2013). Development of a time-to-detect growth model for heat-treated *Bacillus cereus* spores. *Int J Food Microbiol, 165*(3), 231-240.

Decatur, A. L., & Losick, R. (1996). Three sites of contact between the *Bacillus subtilis* transcription factor sigmaF and its antisigma factor SpoIIAB. *Genes Dev, 10*(18), 2348-2358.

Devi, S. N., Vishnoi, M., Kiehler, B., Haggett, L., & Fujita, M. (2015). In vivo functional characterization of the transmembrane histidine kinase KinC in *Bacillus subtilis*. *Microbiology, 161*(Pt 5), 1092-1104.

Doan, T., & Rudner, D. Z. (2007). Perturbations to engulfment trigger a degradative response that prevents cell-cell signalling during sporulation in *Bacillus subtilis*. *Mol Microbiol, 64*(2), 500-511.

Dubnau, D. (1991). Genetic competence in *Bacillus subtilis*. *Microbiol Rev, 55*(3), 395-424.

Eichenberger, Fawcett, & Losick. (2001). A three-protein inhibitor of polar septation during sporulation in *Bacillus subtilis*. *Mol Microbiol, 42*(5), 1147-1162.

Eichenberger, Fujita, Jensen, Conlon, & Rudner. (2004). The program of gene transcription for a dingle differentiating cell type during sporulation in *Bacillus subtilis*. *PloS Biol, 2*(10), 1664-1683.

Eichenberger, Jensen, S. T., Conlon, E. M., van Ooij, C., Silvaggi, J., González-Pastor, J.-E., . . . Losick, R. (2003). The σE regulon and the identification of additional sporulation genes in *Bacillus subtilis*. *J Mol Biol, 327*(5), 945-972.

Eswaramoorthy, P., Dravis, A., Devi, S. N., Vishnoi, M., Dao, H. A., & Fujita, M. (2011). Expression level of a chimeric kinase governs entry into sporulation in *Bacillus subtilis*. *J Bacteriol, 193*, 6113-6122.

Eswaramoorthy, P., Duan, D., Dinh, J., Dravis, A., Devi, S. N., & Fujita, M. (2010). The threshold level of the sensor histidine kinase KinA governs entry into sporulation in *Bacillus subtilis*. *J Bacteriol, 192*(15), 3870-3882.

Eswaramoorthy, P., Guo, T., & Fujita, M. (2009). In vivo domain-based functional analysis of the major sporulation sensor kinase, KinA, in *Bacillus subtilis*. *J Bacteriol, 191*(17), 5358-5368.

Ferrari, F. A., Trach, K., LeCoq, D., Spence, J., Ferrari, E., & Hoch, J. A. (1985). Characterization of the *spo0A* locus and its deduced product. *Proc Natl Acad Sci U S A, 82*(9), 2647-2651.

Frandsen, N., & Stragier, P. (1995). Identification and characterization of the *Bacillus subtilis spoIIP* locus. *J Bacteriol, 177*(3), 716-722.

Fredlund, J., Broder, D., Fleming, T., Claussin, C., & Pogliano, K. (2013). The SpoIIQ landmark protein has different requirements for septal localization and immobilization. *Mol Microbiol, 89*(6), 1053-1068.

Fujita, M. (2000). Temporal and selective association of multiple sigma factors with RNA polymerase during sporulation in *Bacillus subtilis*. *Genes. Cells., 5*(2), 79-88.

Fujita, M., Gonzalez-Pastor, J. E., & Losick, R. (2005). High- and low-threshold genes in the Spo0A regulon of *Bacillus subtilis*. *J Bacteriol, 187*(4), 1357-1368.

Fujita, M., & Losick, R. (2002). An investigation into the compartmentalization of the sporulation transcription Factor sigE in *Bacillus subtilis*. *Mol Microbiol, 43*(1), 27-38.

Fujita, M., & Losick, R. (2003). The master regulator for entry into sporulation in *Bacillus subtilis* becomes a cell-specific transcription factor after asymmetric division. *Genes Dev, 17*(9), 1166-1174.

Fujita, M., & Losick, R. (2005). Evidence that entry into sporulation in *Bacillus subtilis* is governed by a gradual increase in the level and activity of the master regulator Spo0A. *Genes Dev, 19*(18), 2236-2244.

Fujita, M., & Sadaie, Y. (1998). Feedback loops involving Spo0A and AbrB in in vitro transcription of the genes involved in the initiation of sporulation in *Bacillus subtilis*. *J Biochem, 124*(1), 98-104.

Gober, J. W., & Marques, M. V. (1995). Regulation of cellular differentiation in *Caulobacter crescentus*. *Microbiol Rev, 59*(1), 31-47.

Golden, J. W., & Yoon, H. S. (1998). Heterocyst formation in *Anabaena*. *Curr Opin Microbiol, 1*(6), 623-629.

Gonzalez-Pastor, J. E. (2011). Cannibalism: a social behavior in sporulating *Bacillus subtilis*. *FEMS Microbiol Rev, 35*(3), 415-424.

Grimshaw, C. E., Huang, S., Hanstein, C. G., Strauch, M. A., Burbulys, D., Wang, L., . . . Whiteley, J. M. (1998). Synergistic kinetic interactions between components of the phosphorelay controlling sporulation in *Bacillus subtilis*. *Biochemistry, 37*(5), 1365-1375.

Grossman, A. D. (1995). Genetic networks controlling the initiation of sporulation and the development of genetic competence in *Bacillus subtilis*. *Annu. Rev. Genet., 29*, 477-508.

Guerout-Fleury, A. M., Frandsen, N., & Stragier, P. (1996). Plasmids for ectopic integration in *Bacillus subtilis*. *Gene, 180*(1-2), 57-61.

Gutierrez, J., Smith, R., & Pogliano, K. (2010). SpoIID-mediated peptidoglycan degradation is required throughout engulfment during *Bacillus subtilis* sporulation. *J Bacteriol, 192*(12), 3174-3186.

Haldenwang. (1995). The Sigma Factors of *Bacillus subtilis*. *Microbiological Reviews, 59*(1), 1-30.

Hamon, M. A., Stanley, N. R., Britton, R. A., Grossman, A. D., & Lazazzera, B. A. (2004). Identification of AbrB-regulated genes involved in biofilm formation by *Bacillus subtilis*. *Mol Microbiol, 52*(3), 847-860.

Harwood, C. R., & Cutting, S. M. (1990). Molecular biological methods for *Bacillus*. Chichester, New York: Wiley URL

Hoch, J. A. (1993). Regulation of the phosphorelay and the initiation of sporulation in *Bacillus subtilis*. *Annu Rev Microbiol, 47*, 441-465.

Holscher, T., Bartels, B., Lin, Y. C., Gallegos-Monterrosa, R., Price-Whelan, A., Kolter, R., . . . Kovacs, A. T. (2015). Motility, chemotaxis and aerotaxis contribute to competitiveness during bacterial pellicle biofilm development. *J Mol Biol, 427*(23), 3695-3708.

Horneck, G., Bucker, H., & Reitz, G. (1994). Long-term survival of bacterial spores in space. *Adv Space Res, 14*(10), 41-45.

Jakimowicz, D., & van Wezel, G. P. (2012). Cell division and DNA segregation in *Streptomyces*: how to build a septum in the middle of nowhere? *Mol Microbiol, 85*(3), 393-404.

Jiang, M., Shao, W., Perego, M., & Hoch, J. A. (2000). Multiple histidine kinases regulate entry into stationary phase and sporulation in *Bacillus subtilis*. *Mol Microbiol, 38*(3), 535-542.

Johnson, M., Zaretskaya, I., Raytselis, Y., Merezhuk, Y., McGinnis, S., & Madden, T. L. (2008). NCBI BLAST: a better web interface. *Nucleic Acids Res, 36*(Web Server issue), W5-9.

Ju, J., & Haldenwang, W. G. (1999). The "pro" sequence of the sporulation-specific sigma transcription factor sigma(E) directs it to the mother cell side of the sporulation septum. *J Bacteriol, 181*(19), 6171-6175.

Kalamara, M., Spacapan, M., Mandic-Mulec, I., & Stanley-Wall, N. R. (2018). Social behaviours by *Bacillus subtilis*: quorum sensing, kin discrimination and beyond. *Mol Microbiol, 110*(6), 863-878.

Karow, M. L., Glaser, P., & Piggot, P. J. (1995). Identification of a gene, *spoIIR*, that links the activation of sigma E to the transcriptional activity of sigma F during sporulation in *Bacillus subtilis*. *Proc Natl Acad Sci U S A, 92*(6), 2012-2016.

Kearns, D. B., Chu, F., Branda, S. S., Kolter, R., & Losick, R. (2005). A master regulator for biofilm formation by *Bacillus subtilis*. *Mol Microbiol, 55*(3), 739-749.

Kellner, E. M., Decatur, A., & Moran, C. P., Jr. (1996). Two-stage regulation of an anti-sigma factor determines developmental fate during bacterial endospore formation. *Mol Microbiol, 21*(5), 913-924.

Khanna, K., Lopez-Garrido, J., Zhao, Z., Watanabe, R., Yuan, Y., Sugie, J., . . . Villa, E. (2019). The molecular architecture of engulfment during *Bacillus subtilis* sporulation. *Elife, 8*.

Kiehler, B., Haggett, L., & Fujita, M. (2017). The PAS domains of the major sporulation kinase in *Bacillus subtilis* play a role in tetramer formation that is essential for the autokinase activity. *Microbiologyopen, 6*(4).

Konkol, M. A., Blair, K. M., & Kearns, D. B. (2013). Plasmid-encoded ComI inhibits competence in the ancestral 3610 strain of *Bacillus subtilis*. *J Bacteriol, 195*(18), 4085-4093.

Koo, B. M., Kritikos, G., Farelli, J. D., Todor, H., Tong, K., Kimsey, H., . . . Gross, C. A. (2017). Construction and analysis of two genome-scale deletion libraries for *Bacillus subtilis*. *Cell Syst, 4*(3), 291-305.

Kroos, L., Kuspa, A., & Kaiser, D. (1986). A global analysis of developmentally regulated genes in *Myxococcus xanthus*. *Dev Biol, 117*(1), 252-266.

Kroos, L., Zhang, B., Ichikawa, H., & Yu, Y. T. (1999). Control of sigma factor activity during *Bacillus subtilis* sporulation. *Mol Microbiol, 31*(5), 1285-1294.

Kunst, F., Ogasawara, N., Moszer, I., Albertini, A. M., Alloni, G., Azevedo, V., . . . Danchin, A. (1997). The complete genome sequence of the gram-positive bacterium *Bacillus subtilis*. *NATURE, 390*(6657), 249-256.

LaBell, T. L., Trempy, J. E., & Haldenwang, W. G. (1987). Sporulation-specific sigma factor sigma 29 of *Bacillus subtilis* is synthesized from a precursor protein, P31. *Proc Natl Acad Sci U S A, 84*(7), 1784-1788.

LeDeaux, J. R., Yu, N., & Grossman, A. D. (1995). Different roles for KinA, KinB, and KinC in the initiation of sporulation in *Bacillus subtilis*. *J Bacteriol, 177*(3), 861-863.

Lewis, R. J., Scott, D. J., Brannigan, J. A., Ladds, J. C., Cervin, M. A., Spiegelman, G. B., . . . Wilkinson, A. J. (2002). Dimer formation and transcription activation in the sporulation response regulator Spo0A. *J Mol Biol, 316*(2), 235-245.

Lin, D., Qu, L. J., Gu, H., & Chen, Z. (2001). A 3.1-kb genomic fragment of *Bacillus subtilis* encodes the protein inhibiting growth of *Xanthomonas oryzae pv. oryzae*. *J Appl Microbiol, 91*(6), 1044-1050.

Liu, W. T., Yang, Y. L., Xu, Y., Lamsa, A., Haste, N. M., Yang, J. Y., . . . Dorrestein, P. C. (2010). Imaging mass spectrometry of intraspecies metabolic exchange revealed the cannibalistic factors of *Bacillus subtilis*. *Proc Natl Acad Sci U S A, 107*(37), 16286-16290.

Londono-Vallejo, J. A., & Stragier, P. (1995). Cell-cell signaling pathway activating a developmental transcription factor in *Bacillus subtilis*. *Genes Dev, 9*(4), 503-508.

Lonetto, M., Gribskov, M., & Gross, C. A. (1992). The sigma 70 family: sequence conservation and evolutionary relationships. *J Bacteriol, 174*(12), 3843-3849.

Lopez, D., & Kolter, R. (2010). Functional microdomains in bacterial membranes. *Genes Dev, 24*(17), 1893-1902.

Lopez, D., Vlamakis, H., Losick, R., & Kolter, R. (2009). Cannibalism enhances biofilm development in *Bacillus subtilis*. *Mol Microbiol, 74*(3), 609-618.

Losick, R., & Stragier, P. (1992). Crisscross Regulation of Cell Type Specific Gene Expression During Development in *B. subtilis*. *NATURE, 355*, 601-604.

Madeira, F., Madhusoodanan, N., Lee, J., Tivey, A. R. N., & Lopez, R. (2019). Using EMBL-EBI Services via Web Interface and Programmatically via Web Services. *Curr Protoc Bioinformatics, 66*(1), e74.

Madeira, F., Park, Y. M., Lee, J., Buso, N., Gur, T., Madhusoodanan, N., . . . Lopez, R. (2019). The EMBL-EBI search and sequence analysis tools APIs in 2019. *Nucleic Acids Res, 47*(W1), W636-W641.

McLoon, A. L., Guttenplan, S. B., Kearns, D. B., Kolter, R., & Losick, R. (2011). Tracing the domestication of a biofilm-forming bacterium. *J Bacteriol, 193*(8), 2027-2034.

Meyer, P., Gutierrez, J., Pogliano, K., & Dworkin, J. (2010). Cell wall synthesis is necessary for membrane dynamics during sporulation of *Bacillus subtilis*. *Mol Microbiol, 76*(4), 956-970.

Molle, V., Fujita, M., Jensen, S. T., Eichenberger, P., Gonzalez-Pastor, J. E., Liu, J. S., & Losick, R. (2003). The Spo0A regulon of *Bacillus subtilis*. *Mol Microbiol, 50*(5), 1683-1701.

Morikawa, M. (2006). Beneficial biofilm formation by industrial bacteria *Bacillus subtilis* and related species. *J Biosci Bioeng, 101*(1), 1-8.

Morlot, C., Uehara, T., Marquis, K. A., Bernhardt, T. G., & Rudner, D. Z. (2010). A highly coordinated cell wall degradation machine governs spore morphogenesis in *Bacillus subtilis*. *Genes Dev, 24*(4), 411-422.

Narula, J., Fujita, M., & Igoshin, O. A. (2016). Functional requirements of cellular differentiation: lessons from *Bacillus subtilis*. *Curr Opin Microbiol, 34*, 38-46.

Narula, J., Kuchina, A., Lee, D. D., Fujita, M., Suel, G. M., & Igoshin, O. A. (2015). Chromosomal arrangement of phosphorelay genes couples sporulation and DNA replication. *Cell, 162*(2), 328-337.

Nicholson, W. L., Munakata, N., Horneck, G., Melosh, H. J., & Setlow, P. (2000). Resistance of *Bacillus* endospores to extreme terrestrial and extraterrestrial environments. *Microbiol Mol Biol Rev, 64*(3), 548-572.

Ohlsen, K. L., Grimsley, J. K., & Hoch, J. A. (1994). Deactivation of the sporulation transcription factor Spo0A by the Spo0E protein phosphatase. *Proc Natl Acad Sci U S A, 91*(5), 1756-1760.

Ojkic, N., Lopez-Garrido, J., Pogliano, K., & Endres, R. G. (2016). Cell-wall remodeling drives engulfment during *Bacillus subtilis* sporulation. *Elife, 5*.

Perego, M. (2001). A new family of aspartyl phosphate phosphatases targeting the sporulation transcription factor Spo0A of *Bacillus subtilis*. *Mol Microbiol, 42*(1), 133-143.

Perego, M., Cole, S. P., Burbulys, D., Trach, K., & Hoch, J. A. (1989). Characterization of the gene for a protein kinase which phosphorylates the sporulation-regulatory proteins Spo0A and Spo0F of *Bacillus subtilis*. *J Bacteriol, 171*(11), 6187-6196.

Perego, M., Glaser, P., & Hoch, J. A. (1996). Aspartyl-phosphate phosphatases deactivate the response regulator components of the sporulation signal transduction system in *Bacillus subtilis*. *Mol Microbiol, 19*(6), 1151-1157.

Perego, M., Spiegelman, G. B., & Hoch, J. A. (1988). Structure of the gene for the transition state regulator, *abrB*: regulator synthesis is controlled by the *spo0A* sporulation gene in *Bacillus subtilis*. *Mol Microbiol, 2*(6), 689-699.

Piggot, P. J., & Hilbert, D. W. (2004). Sporulation of *Bacillus subtilis*. *Curr Opin Microbiol, 7*(6), 579-586.

Pogliano, J., Osborne, N., Sharp, M. D., Abanes-De Mello, A., Perez, A., Sun, Y.-L., & Pogliano, K. (1999). A vital stain for studying membrane dynamics in bacteria: a novel mechanism controlling septation during *Bacillus subtilis* sporulation. *Mol Microbiol, 31*(4), 1149-1159.

Predich, M., Nair, G., & Smith, I. (1992). *Bacillus subtilis* early sporulation genes *kinA*, *spo0F*, and *spo0A* are transcribed by the RNA polymerase containing sigma H. *J Bacteriol, 174*(9), 2771-2778.

Rice, P., Longden, I., & Bleasby, A. (2000). EMBOSS: the European Molecular Biology Open Software Suite. *Trends Genet, 16*(6), 276-277.

Rodrigues, C. D., Marquis, K. A., Meisner, J., & Rudner, D. Z. (2013). Peptidoglycan hydrolysis is required for assembly and activity of the transenvelope secretion complex during sporulation in *Bacillus subtilis*. *Mol Microbiol, 89*(6), 1039-1052.

Rodrigues, C. D., Ramirez-Guadiana, F. H., Meeske, A. J., Wang, X., & Rudner, D. Z. (2016). GerM is required to assemble the basal platform of the SpoIIIA-SpoIIQ transenvelope complex during sporulation in *Bacillus subtilis*. *Mol Microbiol, 102*(2), 260-273.

Rogers, W. J. (2012). Steam and dry heat sterilization of biomaterials and medical devices. 20-55.

Rosales-Mendoza, S., & Angulo, C. (2015). *Bacillus subtilis* comes of age as a vaccine production host and delivery vehicle. *Expert Rev Vaccines, 14*(8), 1135-1148.

Sambrook, J., & Russell, D. (2001). Molecular Cloning: A Laboratory Manual, 3rd edn. Cold Spring Harbor, N.Y.: Cold Spring Harbor Laboratory Press.

Satola, S. W., Baldus, J. M., & Moran, C. P., Jr. (1992). Binding of Spo0A stimulates *spoIIG* promoter activity in *Bacillus subtilis*. *J Bacteriol, 174*(5), 1448-1453.

Sauer, U., Santangelo, J. D., Treuner, A., Buchholz, M., & Durre, P. (1995). Sigma factor and sporulation genes in *Clostridium*. *FEMS Microbiol Rev, 17*(3), 331-340.

Saujet, L., Pereira, F. C., Serrano, M., Soutourina, O., Monot, M., Shelyakin, P. V., . . . Martin-Verstraete, I. (2013). Genome-wide analysis of cell type-specific gene transcription during spore formation in *Clostridium difficile*. *PLoS Genet, 9*(10), e1003756.

Setlow, B., & Setlow, P. (1987). Thymine-containing dimers as well as spore photoproducts are found in ultraviolet-irradiated *Bacillus subtilis* spores that lack small acid-soluble proteins. *Proc Natl Acad Sci U S A, 84*(2), 421-423.

Setlow, B., & Setlow, P. (1993a). Binding of small, acid-soluble spore proteins to DNA plays a significant role in the resistance of *Bacillus subtilis* spores to hydrogen peroxide. *Appl Environ Microbiol, 59*(10), 3418-3423.

Setlow, B., & Setlow, P. (1993b). Dipicolinic acid greatly enhances production of spore photoproduct in bacterial spores upon UV irradiation. *Appl Environ Microbiol, 59*(2), 640-643.

Setlow, P. (2006). Spores of *Bacillus subtilis*: their resistance to and killing by radiation, heat and chemicals. *J Appl Microbiol, 101*(3), 514-525.

Shafikhani, S. H., & Leighton, T. (2004). AbrB and Spo0E control the proper timing of sporulation in *Bacillus subtilis*. *Curr Microbiol, 48*(4), 262-269.

Shahcheraghi, S., Ayatollahi, J., & Lotfi, M. (2015). Applications of *Bacillus subtilis* as an important bacterium in medical sciences and human life. *Tropical Journal of Medical Research, 18*(1), 1.

Shemesh, M., & Chai, Y. (2013). A combination of glycerol and manganese promotes biofilm formation in *Bacillus subtilis* via histidine kinase KinD signalling. *J Bacteriol, 195*(12), 2747-2754.

Smith, K., & Youngman, P. (1993). Evidence that the *spoIIM* gene of *Bacillus subtilis* is transcribed by RNA polymerase associated with sigma E. *J Bacteriol, 175*(11), 3618-3627.

Sonenshein, A. L. (2000). Control of sporulation initiation in *Bacillus subtilis*. *Curr Opin Microbiol, 3*, 561-566.

Soni, A., Oey, I., Silcock, P., & Bremer, P. (2016). *Bacillus* spores in the food industry: A review on resistance and response to novel inactivation technologies. *Comprehensive Reviews in Food Science and Food Safety, 15*(6), 1139-1148.

Stephenson, & Hoch. (2002). Evolution of signalling in the sporulation phosphorelay. *Mol Microbiol, 46*(2), 297-304.

Stragier, P., & Losick, R. (1996). Molecular genetics of sporulation in *Bacillus subtilis*. *Annu Rev Genet, 30*, 297-241.

Strauch, Spiegelman, G. B., Perego, M., Johnson, W. C., Burbulys, D., & Hoch, J. A. (1989). The transition state transcription regulator AbrB of *Bacillus subtilis* is a DNA binding protein. *EMBO J, 8*(5), 1615-1621.

Strauch, Trach, Day, & Hoch. (1992). Spo0A activates and represses its own synthesis by binding at its dual promoters. *Biochimie, 74*(7-8), 619-626.

Strauch, Webb, Spiegelman, & Hoch. (1990). The Spo0A protein of *Bacillus subtilis* is a repressor of the *abrB* gene. *Proc Natl Acad Sci U S A, 87*(5), 1801-1805.

Sun, P., Wang, J. Q., & Zhang, H. T. (2010). Effects of *Bacillus subtilis* natto on performance and immune function of preweaning calves. *J Dairy Sci, 93*(12), 5851-5855.

Tan, I. S., & Ramamurthi, K. S. (2014). Spore formation in *Bacillus subtilis*. *Environ Microbiol Rep, 6*(3), 212-225.

Trach, K., Burbulys, D., Strauch, M., Wu, J. J., Dhillon, N., Jonas, R., . . . et al. (1991). Control of the initiation of sporulation in *Bacillus subtilis* by a phosphorelay. *Res Microbiol, 142*(7-8), 815-823.

Vaseeharan, B., & Ramasamy, P. (2003). Control of pathogenic *Vibrio spp.* by *Bacillus subtilis* BT23, a possible probiotic treatment for black tiger shrimp *Penaeus monodon*. *Lett Appl Microbiol, 36*(2), 83-87.

Veening, J. W., Smits, W. K., Hamoen, L. W., Jongbloed, J. D., & Kuipers, O. P. (2004). Visualization of differential gene expression by improved cyan fluorescent protein and yellow fluorescent protein production in *Bacillus subtilis*. *Appl Environ Microbiol, 70*(11), 6809-6815.

Vishnoi, M., Narula, J., Devi, S. N., Dao, H. A., Igoshin, O. A., & Fujita, M. (2013). Triggering sporulation in *Bacillus subtilis* with artificial two-component systems reveals the importance of proper Spo0A activation dynamics. *Mol Microbiol, 90*(1), 181-194.

Vlamakis, H., Aguilar, C., Losick, R., & Kolter, R. (2008). Control of cell fate by the formation of an architecturally complex bacterial community. *Genes Dev, 22*(7), 945-953.

Vlamakis, H., Chai, Y., Beauregard, P., Losick, R., & Kolter, R. (2013). Sticking together: building a biofilm the *Bacillus subtilis* way. *Nat Rev Microbiol, 11*(3), 157-168.

Yepes, A., Schneider, J., Mielich, B., Koch, G., Garcia-Betancur, J. C., Ramamurthi, K. S., . . . Lopez, D. (2012). The biofilm formation defect of a *Bacillus subtilis* flotillin-defective mutant involves the protease FtsH. *Mol Microbiol, 86*(2), 457-471.

Youngman, P., Perkins, J. B., & Losick, R. (1984). Construction of a cloning site near one end of Tn917 into which foreign DNA may be inserted without affecting transposition in *Bacillus subtilis* or expression of the transposon-borne *erm* gene. *Plasmid, 12*(1), 1-9.

Zeigler, D. R., Pragai, Z., Rodriguez, S., Chevreux, B., Muffler, A., Albert, T., . . . Perkins, J. B. (2008). The origins of 168, W23, and other *Bacillus subtilis* legacy strains. *J Bacteriol, 190*(21), 6983-6995.